Order Number 9417505

The synthesis and nucleic acid interactions of an acridine-porphyrin heterodimer

Scarborough, Alex Laon, Ph.D.

City University of New York, 1994

U·M·I

300 N. Zeeb Rd.
Ann Arbor, MI 48106

The Synthesis and Nucleic Acid Interactions of an Acridine-Porphyrin Heterodimer

by

Alex Laon Scarborough

A dissertation submitted to the Graduate Faculty in Biochemistry in partial fulfillment of the requirements for the degree of Doctor of Philosophy, The City University of New York.

1994

This manuscript has been read and accepted for the Graduate Faculty in Biochemistry in satisfaction of the dissertation requirement for the degree of Doctor of Philosophy.

December 9, 1993
Date

Chair of Examining Committee

August 31, 1993
Date

Executive Officer

Supervisory Committee

The City University of New York

Abstract

The Synthesis and Nucleic Acid Interactions of an Acridine-Porphyrin Heterodimer.

by

Alex Scarborough

Adviser: Prof. David K. Lavallee

Two nucleic acid-interacting compounds were synthesized; binding modes on DNA were evaluated by circular dichroism, UV-visible absorption and fluorescence spectroscopy; equilibrium constants for binding were determined by ethidium bromide competitive binding.

The indicated mode of binding of meso-[tetra(N-[trimethylammoniumethyl]-4-benzamidyl)]porphine (TAP) to poly(dA-dT).(dA-dT) is non-intercalative, external binding. Interaction with poly(dG-dC).(dG-dC) is indicated to be by intercalation. With calf thymus DNA, there is a combination of the two modes.

A molecule with two domains capable of nucleic acid interactions, an acridine-porphyrin heterodimer, 5-[4-(N-[9-acridinyl]-3-aminopropoxy)phenyl]-10,15,20-tri[4-(N-[trimethylammoniumethyl])benzamidyl]porphine (ATB) produces CD, UV-visible and fluorescence emission spectra that are similar.

Equilibrium constants for binding to poly(dA-dT).(dA-dT), poly(dG-dC).(dG-dC) and calf thymus DNA reveal that TAP binds to the nucleic acids with strong affinities, while ATB has much weaker affinities. The data are consistent with a mode of

binding for ATB that is dominated by an intercalated acridine moiety and an externally bound porphyrin macrocycle.

Acknowledgements

I am deeply grateful to my parents, George and Louvina and to my brother, Steve, for their encouragement, support and guidance during the research that made this document possible.

Special thanks goes to Mr. David Gordon for his indefatigable support and backing of this work.

I am also indebted to Ms. Sophie Weintraub, of the Biochemistry Department of the Graduate School and University Center of The City University of New York for her kindly assistance during this course of study.

Table of Contents

List of Tables

List of Illustrations

Figure Page

Chapter One

Introduction

Porphyrins are metal-ion coordinating heterocycles that have many functions in nature; as the oxygen binder in hemoglobin, the prosthetic group heme, Fe(II)-protoporphyrin IX, is crucial for respiration. In plants and in other photosynthetic organisms, the porphyrin chlorophyll is used to harness the energy of light. As part of the cytochrome proteins, heme is necessary for electron transfer in aerobic organisms.

In addition to research designed to understand the mechanisms of action of such prosthetic groups, a class of synthetic porphyrin, the cationic, tetraaryl porphyrins, have generated interest because of their ability to bind to and modify polynucleotides. This property, and their spectroscopic characteristics, has led to their use as probes of nucleic acid conformation in solution: one application has been to estimate the width of the minor groove of DNA in solution (1). These synthetic porphyrins, and the naturally occuring ones, also show great promise as chemotherapeutic and diagnostic agents: haematoporphyrin has already been employed in photodynamic therapy to detect and destroy neoplastic cells (2). Some ^{111}Indium-labelled porphyrins have found use as lymph node imaging reagents (3).

The porphyrins which can bind to and interact with DNA- those with cationic aryl groups in the meso position- have a variety of properties which make them of value in the study of

DNA structure and its modification. Fiel and coworkers (4) reported that meso-[tetra(4-N-methylpyridyl)]porphine (TMPyP, Figure 1-1) can intercalate into calf thymus DNA. The same porphyrin can also intercalate into poly(dG-dC).(dG-dC) or bind externally, by electrostatic interaction, to poly(dA-dT).(dA-dT) (5): the interactions of this porphyrin with the synthetic polynucleotides indicate its mode of binding to GC and AT rich regions in natural DNA. It was also shown in this study that metalloporphyrins with axial ligands, which project outward at an angle perpendicular to the plane of the porphyrin, do not intercalate while those without such ligands do; the bulk of the axial ligands prevents intercalation.

Another property of these porphyrins is their ability to induce DNA strand breakage. The Co(III), Fe(III) and Mn(III) TMPyP complexes have been shown to cleave a 139 base pair restriction fragment of plasmid pBR322 in the presence of the oxidizing agent, oxone, $KHSO_5$; a redox mechanism of action is thought to occur (6,7). The complexes prefer to bind in the minor groove of trinucleotide regions having only adenine and thymine.

Porphyrins can be alkylated at the nitrogen of the pyrrolenine ring by a wide variety of funtional groups e.g. methyl, phenyl or benzyl groups. These N-alkyl porphyrins, when certain metal ions are coordinated at the center of the porphyrin ring, are able to donate the alkyl group to nucleophiles (8-10). Cationic, N-alkylated tetraaryl metalloporphyrins may thus be able to alkylate nucleophilic DNA bases, such as guan-

Figure 1-1: The molecular structure of meso-[tetra(4-N-methylpyridyl)]porphine, showing meso positions (*) and b-pyrrole positions (b).

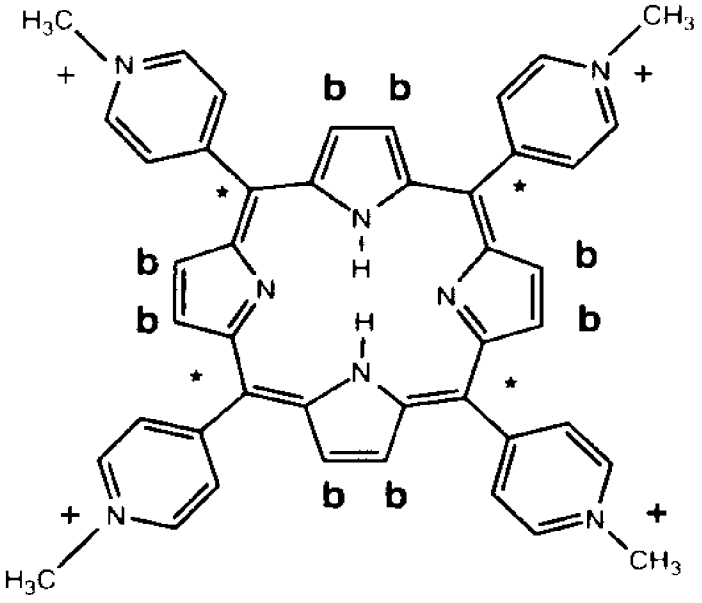
H3C
N
+
CH3
N
+
b b
b
b
N
H
N
H
N
b
b
b b
+
N
H3C
N
+
CH3

ine. A candidate for such studies is the N-alkylated porphyrin N-methyl meso-[tetra(4-aminomethylphenyl)]porphine (NM-TAMPP) (Figure 1-2). NM-TAMPP is able to intercalate into poly(dG-dC)$_2$ (11) and may be able to alkylate GC rich sites at the N-7 atom of guanine when complexed with a metal ion, for example, Pd(II).

The many and diverse spectroscopic properties of these kinds of porphyrin have enabled their nucleic acid interactions to be elucidated. There are distinct changes in the circular dichroism, ultraviolet-visible and fluorescence spectra of these compounds when interaction occurs (5,12).

The ability of these compounds to bind externally to, intercalate into, cut and possibly alkylate nucleic acids has produced interest in the application of these properties in order to probe DNA conformation and DNA-ligand binding. One potential application of the ability of metalloporphyrins to cut DNA is in their use as footprinting reagents to probe DNA-protein and DNA-drug interactions and dynamics. Applications of the alkylation process would be to examine the relaxation of base-pairing in a variety of oligo- and polynucleotides under different conditions of pH, ionic strength and similar variables, as alkylation would proceed more readily when the bases are more available to solution. A fourth, possible use of porphyrin chemistry might be to retard DNA replication in vivo. In any case, the process of porphyrin binding and intercalation must be examined in depth.

There is little doubt that the cationic nature of the

Figure 1-2: The molecular structure of N-methyl meso-[tetra-(aminomethylphenyl])porphine (NM-TAMPP).

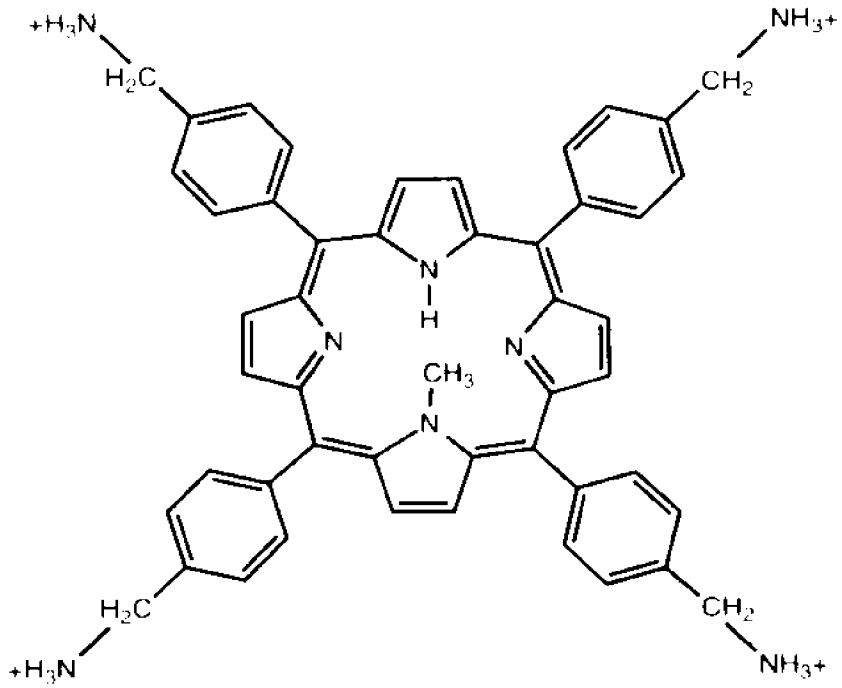
+H3N
H2C
NH3+
CH2
N
H
N
N
CH3
N
H2C
CH2
+H3N
NH3+

aryl groups has an important role in binding. Sari and coworkers (13) as well as Bromley and coworkers (14) examined the effect of total peripheral charge- its number and position- on binding. Sari found that TMPyP analogues with only two and three positive charges could intercalate, but with slightly lower association constants in comparison with that of TMPyP. Bromley assessed binding ability by determining the extent of DNA cleavage. It was found that altering the total charge on the Mn(III) complexes from 3+ to 1+ produced lower affinity constants, as implied by the reduced degree of cutting. When rotation about the bond linking the aryl group to the meso carbon was inhibited by placing bulky groups at the phenyl positions (e.g. Figure 1-3), a series of isomers with four positive charges distributed above and below the flat plane of the central region of the porphyrin macrocycle was obtained. The Mn(III) complexes of these isomers varied, to a lesser degree, in their ability to cut DNA, but in an order consistent with the magnitude of their permanent net dipoles. This shows that electrostatic attraction between cationic porphyrin and the phosphate groups of DNA is important for binding.

In order for intercalation, which is seen mainly in GC rich sites, to occur, there is no doubt that the base pairs of DNA must unstack in the region where the porphyrin will intercalate in order to accomodate such a large molecule; there must also be a modification of porphyrin structure: the 4-N-methylpyridyl groups of TMPyP (Figure 1-1) are normally found perpendicular to the plane of the porphyrin core (15), in or-

Figure 1-3: Analogues of TMPyP differing in position of charge above or below the plane of the porphyrin ring.

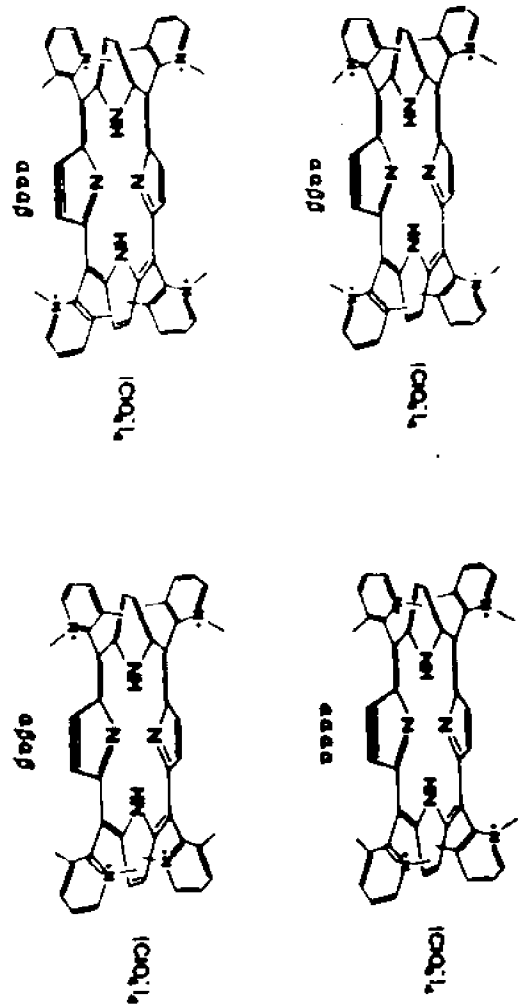
aaab
aabb
abab
abbb

der to expedite intercalation it is necessary for the pyridyl rings to rotate toward a coplanar position. It is expected that a bulky group in the ortho position on the pyridyl rings will hinder rotation and thus intercalation. This is the effect seen when an analogue of TMPyP having 2-N-methylpyridyl groups instead of 4-N-methylpyridyl groups is placed in solution with poly(dG-dC)$_2$. The bulky methyl group is in the ortho position on the pyridyl ring and hinders rotation to give a relatively flat molecule (Figure 1-4). There is no evidence of intercalation (5).

External binding, as opposed to intercalation, is usually associated with AT rich sites and has provided evidence that groove binding may be a major mode (16). Other forms of binding may be a direct interaction between the cationic porphyrin and the anionic phosphate groups and self-stacking along the phosphate backbone.

The size of groups located in a position other than the ortho positions of the aryl groups of porphyrins also plays a role in determining the mode of binding. Meso-[tetra(4-trimethylammoniumbenzyl)]porphine has bulky trimethylammonium groups in the para position of its phenyl ring and forms a complex with DNA in which it is externally bound (17). The non-N-methylated form of NM-TAMPP, which has an aminomethyl group in the para position on the phenyl ring, also binds externally (11).

By synthesizing and using a series of porphyrins which differ by having a variety of DNA intercalators bonded to the

Figure 1-4: (a) The molecular structure of meso-(2-N-methyl-pyridyl)porphine. (b) A schematic diagram showing the orientation of meso-aryl groups (diamonds and thin line) perpendicular to the plane of the porphyrin core (heavy lines).

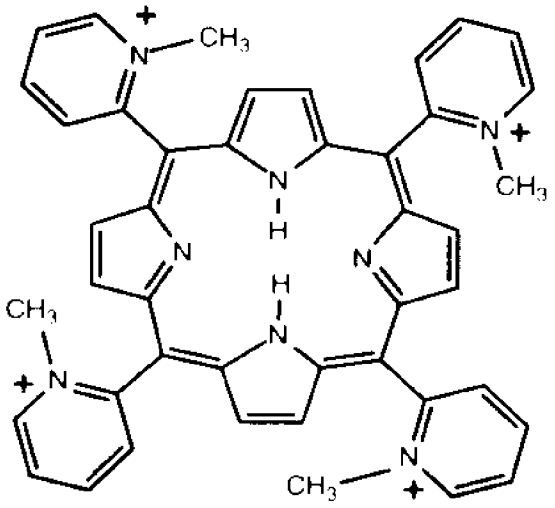

(a)

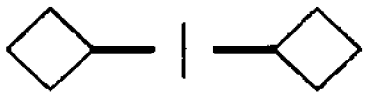

(b)

porphyrin and also by varying the distance between intercalator and porphyrin, we expect to create a new series of footprinting reagents to be used as nucleic acid structural probes these might bind to DNA in a mode similar to that of bleomycin. The DNA intercalator acridine has been well characterized in its synthetic chemistry (18) and modes of DNA interaction (19-21). As a first step, a water-soluble, porphyrin-acridine conjugate was made with the goal of determining the effect of the presence of the acridine on the binding of a cationic tetraarylporphyrin to DNA. This was accomplished by synthesizing both the conjugate and the porphyrin without acridine and then comparing their modes of interaction with calf thymus DNA and the synthetic polynucleotides poly-$(dG\text{-}dC)_2$ and poly$(dA\text{-}dT)_2$. The equilibrium constants derived from these interactions were also determined by a competitive binding method.

Of primary importance was to design a molecule that would be soluble in aqueous buffer at neutral pH. Surprisingly, the ammonium group - bearing porphyrin, meso-[tetra(4-aminomethylphenyl)]porphine (TAMPP) is not soluble at pH 7.0, but only at pH 5.5 or lower (11); meso-[tetra(4-anilino)]porphine is extremely insoluble at neutral pH (12) and there has been no way found to N-alkylate TMPyP, hindering any alkylation studies using this compound. Also of importance was to design a synthetic route to give a tether whose length could be altered in later syntheses.

This work describes the synthesis of a heterodimer with

two nucleic acid - interacting domains, an acridine-porphyrin hybrid, the compound 5-[4-(N-[9-acridinyl]-3-aminopropoxy)-phenyl]-10,15,20-tri[4-(N-[trimethylammoniumethyl])benzamidyl]porphine (ATB) and its analogue (no acridine) meso-[tetra-(4-[N-(trimethylammoniumethyl)]benzamidyl)]porphine (TAP). These reactions are outlined in schemes 1 and 2, respectively. Their modes of interaction with the aforementioned nucleic acids and the equilibrium constants for binding at pH 7.2, and in 0.1 M NaCl, 26 mM phosphate and 1 mM EDTA are reported.

Scheme One: A series of reactions leading to the synthesis of the acridine-porphyrin conjugate.

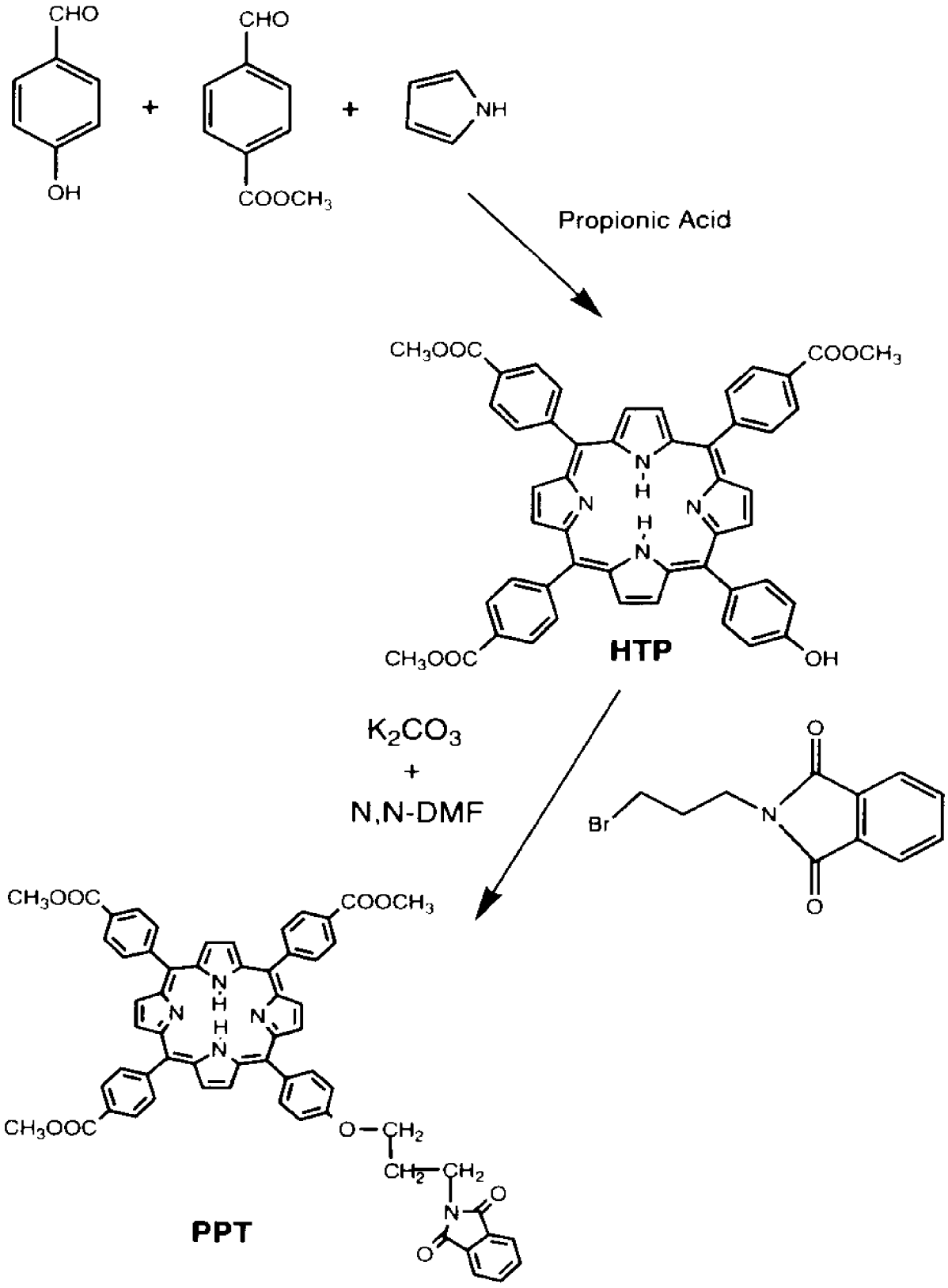
CHO
OH
CHO
COOCH3
NH
Propionic Acid
CH3OOC
COOCH3
CH3OOC
OH
HTP
K2CO3
+
N,N-DMF
Br
O
N
O
CH3OOC
COOCH3
CH3OOC
O—CH2
CH2—CH2
N
O
O
PPT

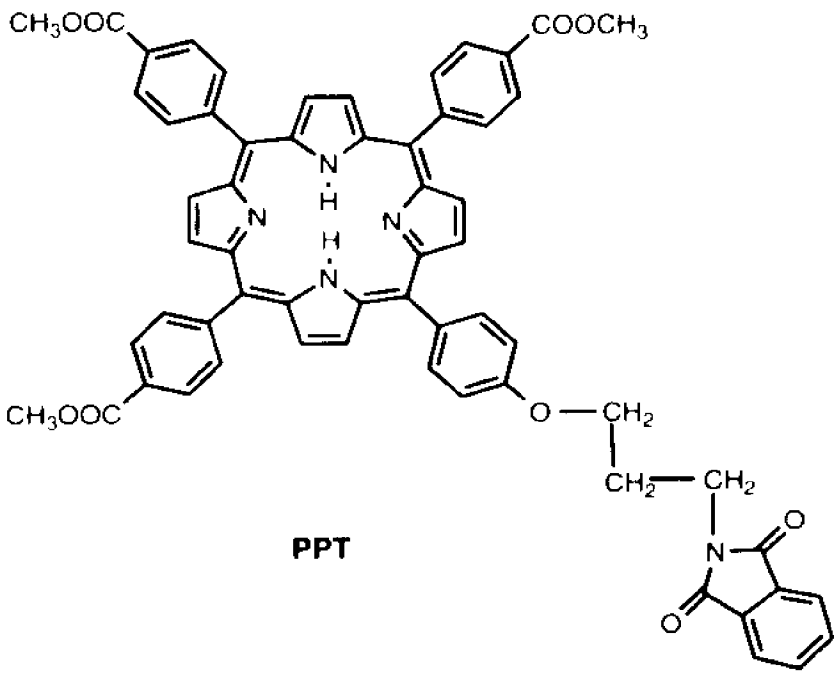
CH3OOC
COOCH3
CH3OOC
O
CH2
CH2
CH2
N
O
O

PPT

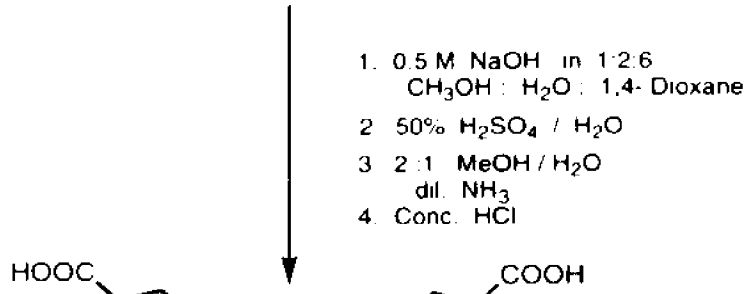
1. 0.5 M NaOH in 1:2:6
CH3OH : H2O : 1,4- Dioxane
2. 50% H2SO4 / H2O
3. 2 :1 MeOH / H2O
dil. NH3
4. Conc. HCl

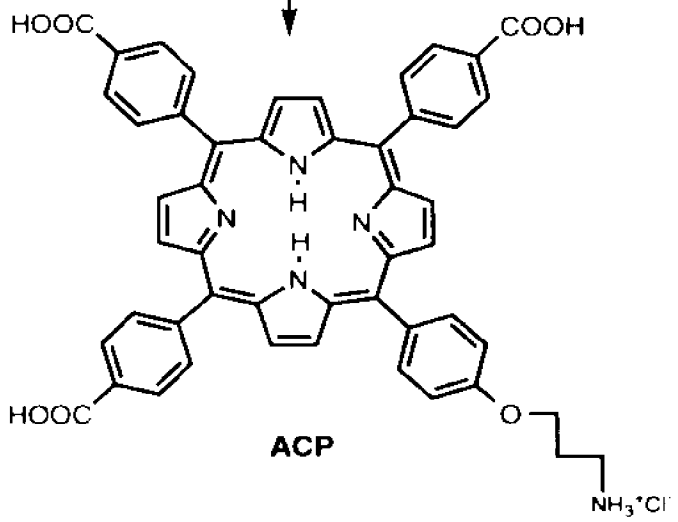
HOOC
COOH
HOOC
O
NH3+Cl-

ACP

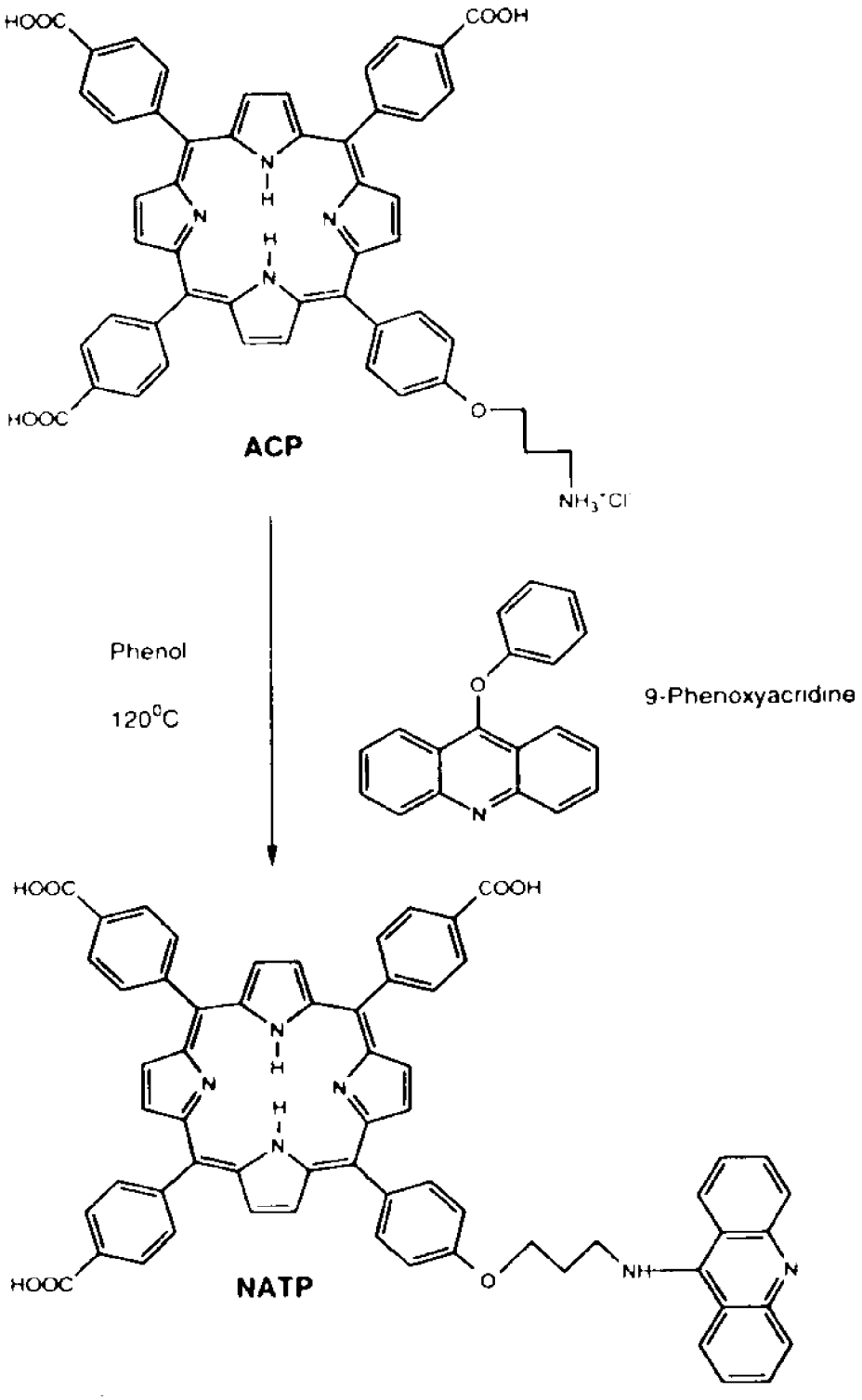
HOOC
COOH
HOOC
O
NH3+Cl-
ACP
Phenol
120°C
O
N
9-Phenoxyacridine
HOOC
COOH
HOOC
O
NH
N
NATP

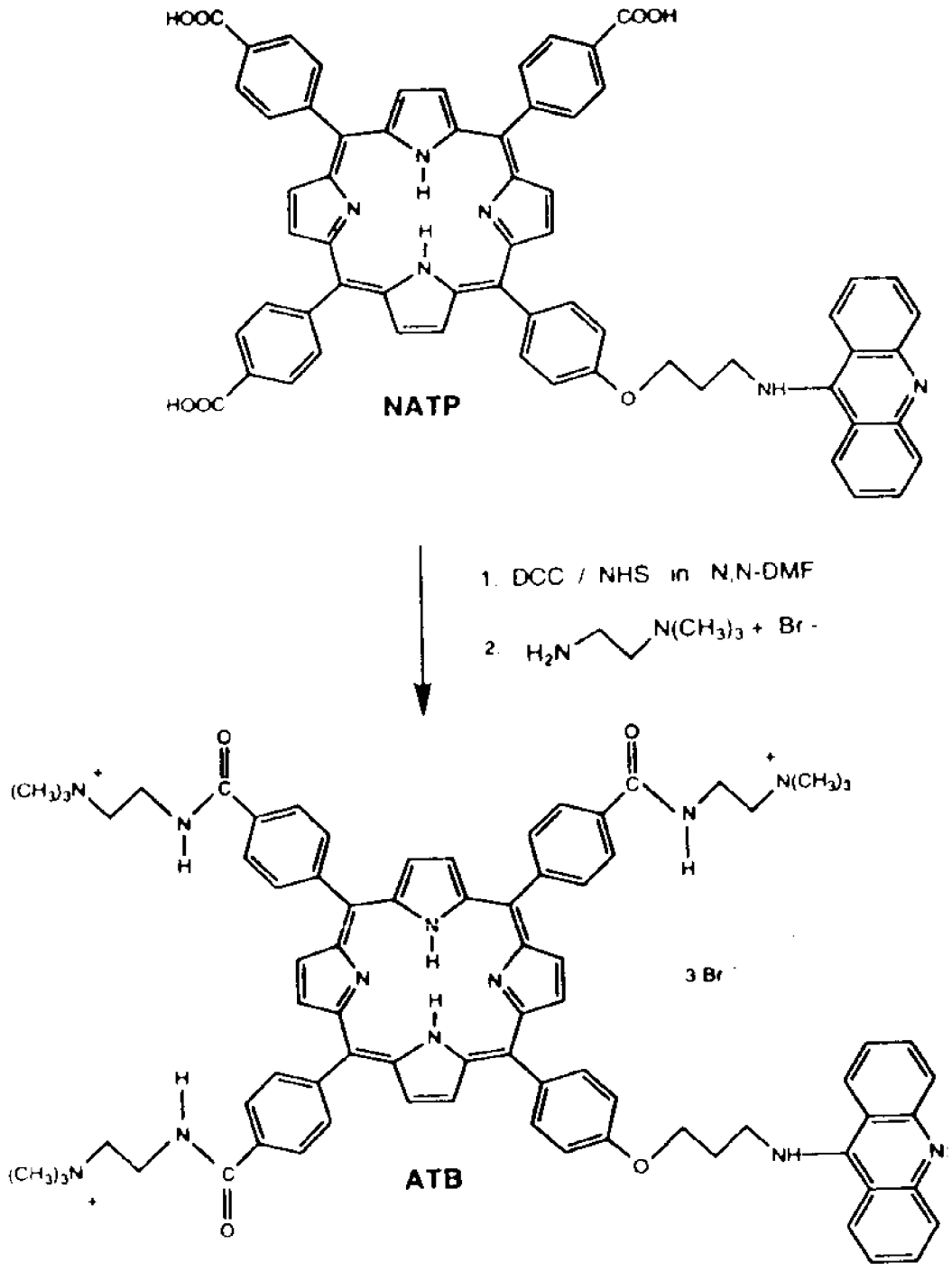
HOOC
COOH
HOOC
NATP
NH
O
N
1. DCC / NHS in N,N-DMF
2. H_2N $N(CH_3)_3$ + Br -
$(CH_3)_3N$
$N(CH_3)_3$
3 Br -
ATB

Scheme 2: Synthesis of meso-[tetra(4-[N-(trimethylammonium-ethyl)]benzamidyl)]porphine (TAP).

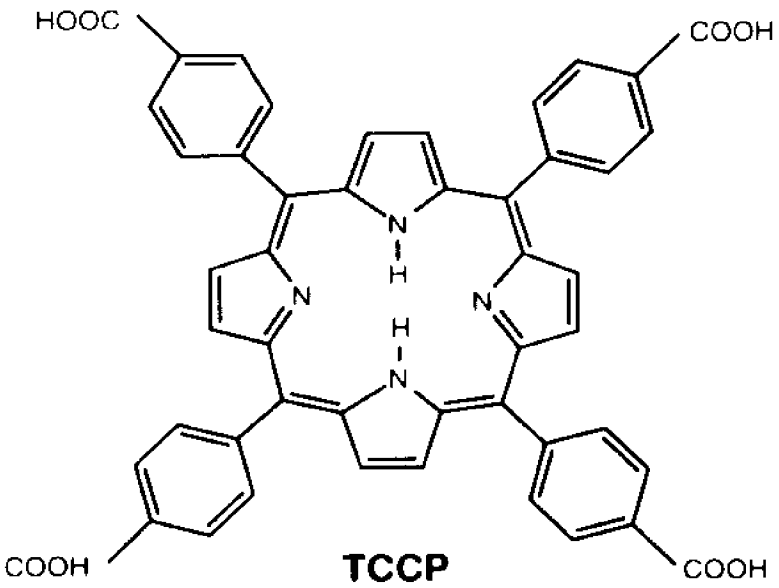
HOOC
COOH
COOH
COOH

TCCP

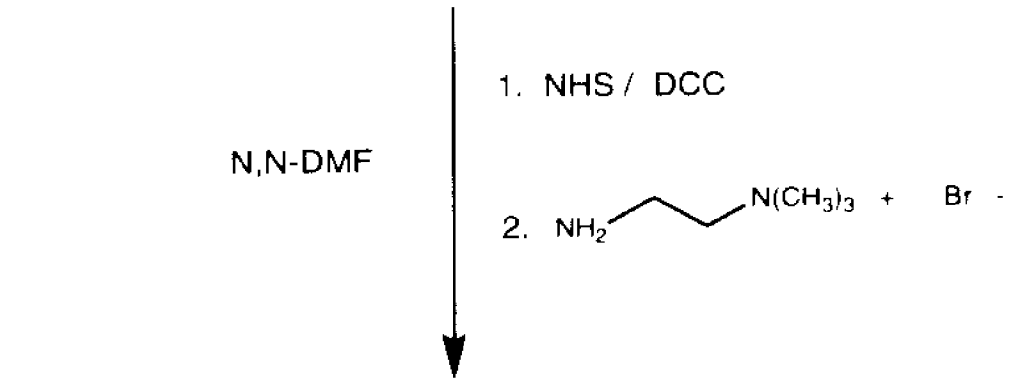
N,N-DMF
1. NHS / DCC
2. NH2
N(CH3)3 + Br -

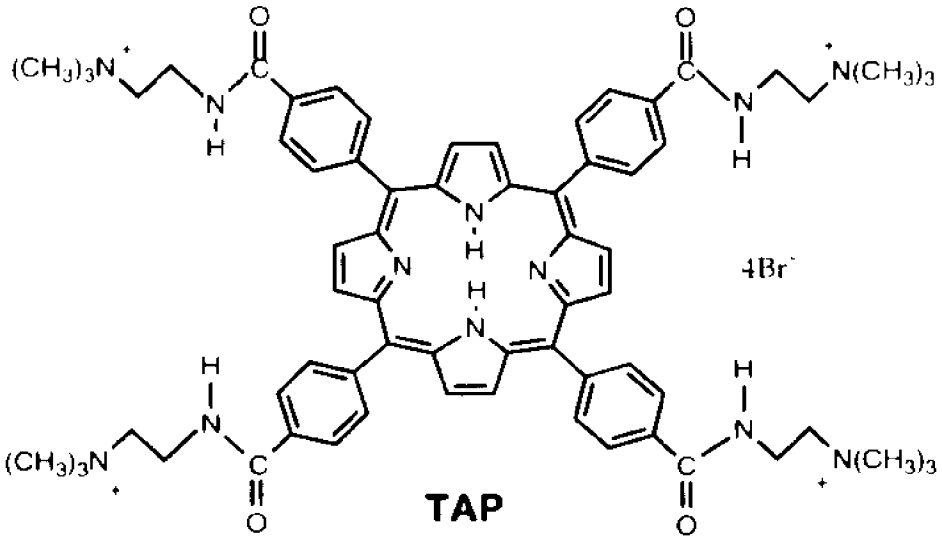
(CH3)3N
N(CH3)3
4Br-
(CH3)3N
N(CH3)3

TAP

Chapter 2

Synthesis of ATB and TAP

2.1 Introduction

The primary difficulty encountered in our attempts to synthesize the tricationic porphyrin-acridine conjugate was, as stated before, related to the need for aqueous solubility. In addition, it was desired at certain stages of the synthetic route to obtain solubility in certain organic solvents. Although the solubility of tetraaryl porphyrins is usually determined by the nature (usually polarity) of the the peripheral aryl groups, any prediction of solubility based on this alone does not always hold true. Therefore, determination of solubility was often a matter of trial and error.

Another requirement was the attachment of the quaternary ammonium groups, which provide solubility, in the presence of acridine. Usually, these groups are produced under harsh conditions that would affect the acridine e.g. by a reaction between alkyl halides functions on the porphyrin and trimethylamine under strongly alkaline conditions (1); the synthesis of alkyl halide functions on porphyrins alone often requires the use of harsh reagents such as thionyl chloride (1) or chlorosulfonic acid (2) which would degrade the acridine moiety. It may be asked why it is not possible to attach acridine after the attachment of the quaternary ammonium groups, but to do

so, it would be necessary to carry out reactions requiring the dissolution of a polycationic species of porphyrin in low-polarity organic solvents. This has been experimentally shown to be not feasible. In addition, alkylating amino functions on the porphyrin could not be undertaken, due to the insolubility of common amino porphyrins in many organic solvents and the likelihood of alkylating the heterocyclic nitrogen of the acridine. Attaching the charges to the precursor of the conjugate was accomplished by using carbodiimide to form amide bonds between carboxyl groups on the porphyrin and a cationic amine. This reaction is a mild process that can be undertaken at neutral pH.

Another one of the important concepts in the synthetic route was the use of an asymmetric porphyrin (all four aryl groups not alike). This allowed easier attachment of the aliphatic tether and of the acridine by providing functional groups that were specific for the reactions involved (Schemes 1 and 2).

A fourth requirement of the synthetic work was the need to use a methodology that would give a tether whose length could be altered in subsequent syntheses. This has been accomplished by using a straight-chain amino-alcohol as precursor; this type of compound is available in different aliphatic carbon chain length e.g. 3-aminopropanol, 6-aminohexanol and 8-aminooctanol.

2.2 Materials and Instruments.

All reagents, except where noted, were used without further purification.

Starting materials for HTP synthesis (refer to scheme 1 for reactions) were pyrrole, 4-formylmethylbenzoate, propionic acid and calcium hydride. All except propionic acid were obtained from Aldrich Chemical Company. Propionic acid was obtained from Fisher Scientific.

Pyrrole was freed from oxidation products and dried by allowing it to be stirred with granulated calcium hydride overnight followed by distillation in an nitrogen atmosphere and under reduced pressure.

For PPT synthesis, phthalic anhydride was purchased from J.T.Baker Chemical Company; 3-aminopropanol and phosphorus tribromide were obtained from Aldrich.

For NATP synthesis, phenol, previously distilled in an all glass apparatus and stored under nitrogen, was used. It was obtained from Aldrich. 9-chloroacridine was also obtained from Aldrich.

In the synthesis of ATB, 2-bromoethylamine hydrobromide, 25% trimethylamine in water (25% wt./vol.), dicyclohexyl-carbodiimide and N-hydroxysuccinimide were purchased from Aldrich.

Spectrapor cellulose dialysis membrane with a molecular weight cut-off of 1000 daltons was obtained from Fisher Scientific.

Tetra(4-carboxyphenyl)porphine (TCPP) for TAP synthesis

(scheme 2) was bought from Midcentury Chemical Company.

All solvents were obtained from Fisher Scientific. N,N-DMF, when used as a solvent for reactions, was dried with 4 Å Davidson-type molecular sieves by gently stirring the solvent and beads for at least three days, the sieves were also obtained from Fisher.

A 300 MHz General Electric QE-300 spectrometer was used for NMR spectroscopy; deuterated solvents were bought from Aldrich. Solutions for NMR spectroscopy were at a concentration of 5 % (weight/volume).

Visible absorption spectra were obtained from a Cary 13 Spectrophotometer.

2.3 Results and discussion

The reactions leading to synthesis of the conjugate are shown in Scheme 1. The first step was the formation of the asymmetric porphyrin 5-(4-hydroxyphenyl)-10,15,20-tri(4-carbomethoxyphenyl)porphine (HTP). The reaction is a modification of the Adler-Longo procedure (4) commonly used to make tetraphenylporphyrins. The modification is the use of two different benzaldehydes instead of one. Figure 2-1 is the proton NMR spectrum of HTP in deuterochloroform ($CDCl_3$). A comparison of this spectrum with that of a symmetric porphyrin such as meso-[tetra(4-carboxyphenyl)]porphine (TCPP, shown in Figure 2-2) shows that the signal from the hydrogen atoms at the beta-pyrrole positions of HTP has been converted from a singlet, such as that seen in the TCPP spectrum at 8.85 ppm, to a doublet and a singlet at 8.90 and 8.78 ppm. This is caused by the asymmetry produced by having three methylbenzoate aryl groups and one phenolic aryl group. This configuration is indicated by the presence of two doublets at 8.44 and 8.29 ppm integrating to twelve hydrogens and representing the aromatic protons of the methyl benzoate aryl groups. Two smaller doublets at 8.06 and 7.22 ppm integrate to four protons and come from the aromatic phenolic protons.

With no nearby protons for spin-spin coupling, the methyl groups of the ester functions of HTP produce a singlet integrating to nine protons in the non-aromatic region of the NMR spectrum at 4.11 ppm.

The next step was the addition of the tether that would

Figure 2-1: The 300 MHz proton NMR spectrum of 5-(4-hydroxyphenyl)-10,15,20-tri(4-carbomethoxyphenyl)porphine (HTP). All NMR solutions were at a 5 % (5 mg/1 mL solvent) concentration; spectra were taken at room temperature.

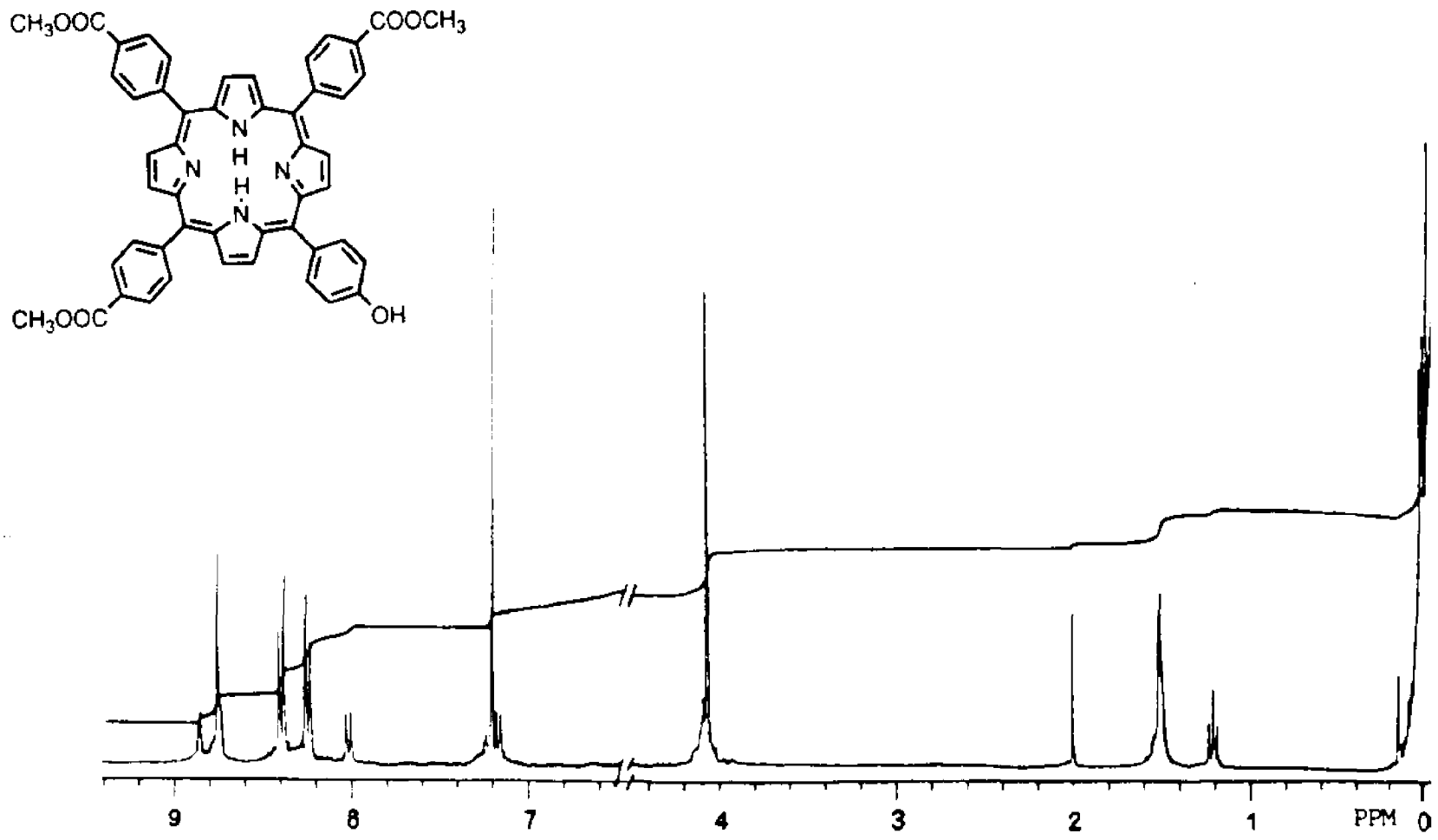
CH3OOC
COOCH3
N
H
H
N
N
N
CH3OOC
OH
9
8
7
4
3
2
1
PPM
0

Figure 2-2: The 300 MHz proton NMR spectrum of meso-[tetra(4-carboxyphenyl)]porphine (TCPP).

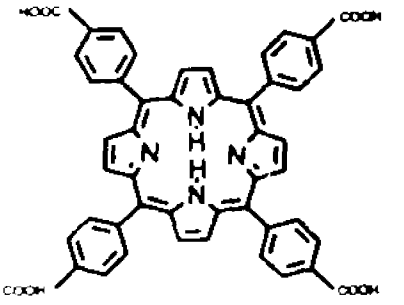
HOOC
COOH
COOH
COOH
N
NH
N
N

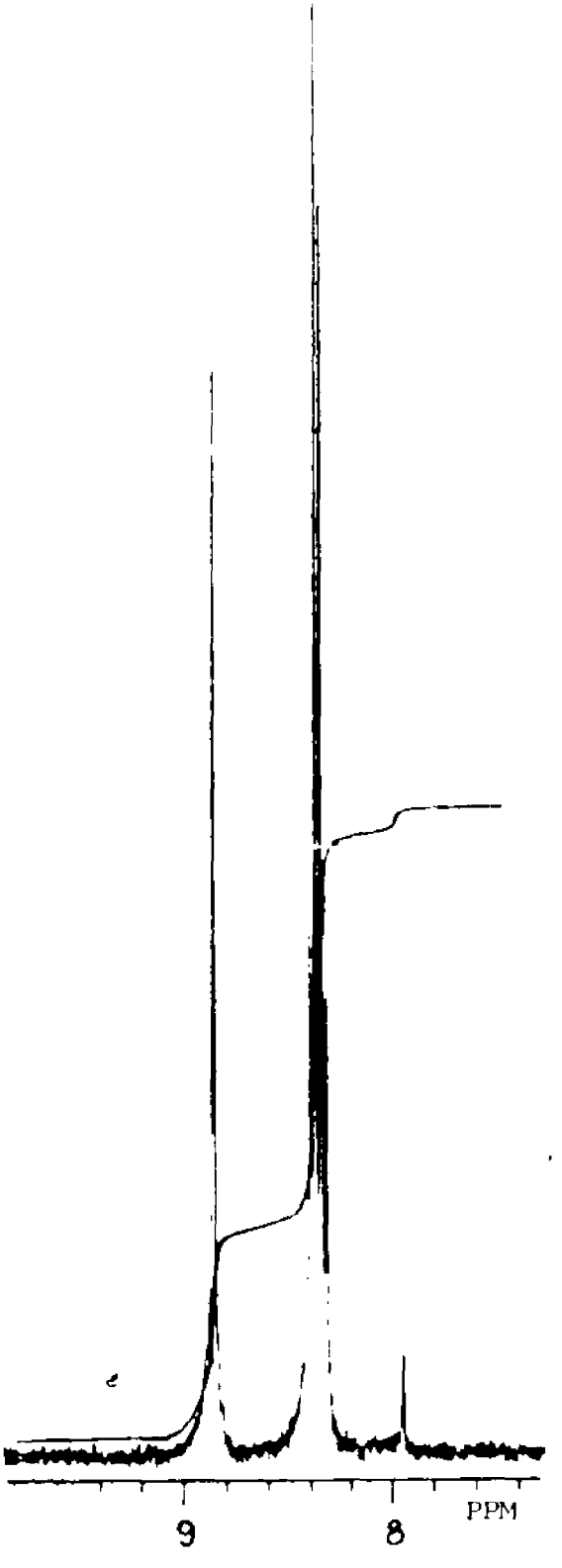
9
8
PPM

link the porphyrin to the acridine molecule; of prime importance was the design of a synthetic route that would enable alteration of the length of this tether in subsequent experiments. N-(3-bromopropyl)phthalimide was made according to a literature method (5). The nucleophilic attack of the phenoxide ion on the carbon bearing the bromine was then employed to form an ether bond between HTP and the propyl group of the phthalimide.

Figure 2-3 is the proton NMR spectrum of the ether derivative of HTP in $CDCl_3$. The linkage of the phthalimide to HTP, forming 5-[4-(3-phthalimidopropoxy)phenyl]-10,15,20-tri[4-carbomethoxyphenylporphine (PPT), can be detected by the presence, in the PPT spectrum, of signals which are similar, in type and location, to those of the bromide. In the spectrum of the bromide (Figure 2-3(a)), a multiplet at 7.70 ppm and an identical one at 7.90 ppm, integrate to four protons and are the standard resonances for phthalimide groups (6); the triplets at 3.80 and 3.35 ppm and the quintuplet at 2.25 ppm integrate to two protons each and come from the propyl group.

Similar resonances are found when the spectrum of PPT is examined: two multiplets, M_1 and M_2, at 7.91 and 7.74 ppm integrate to a total of four protons and come from the phthalimide of PPT. The signals triplet T_1 and quintuplet Q_1, at 4.34 and 2.39 ppm, integrate to two protons each and arise from the methylene group next to oxygen and the methylene group in the center of the chain, respectively. Methyl ester protons give a singlet, S_1, at 4.11 ppm which partially obscures the trip-

Figure 2-3: The 300 MHz proton NMR spectrum of 5-[4-(3-phthal-imidopropoxy)phenyl]-10,15,20-tri[4-carbomethoxyphenyl]-porphine (PPT).

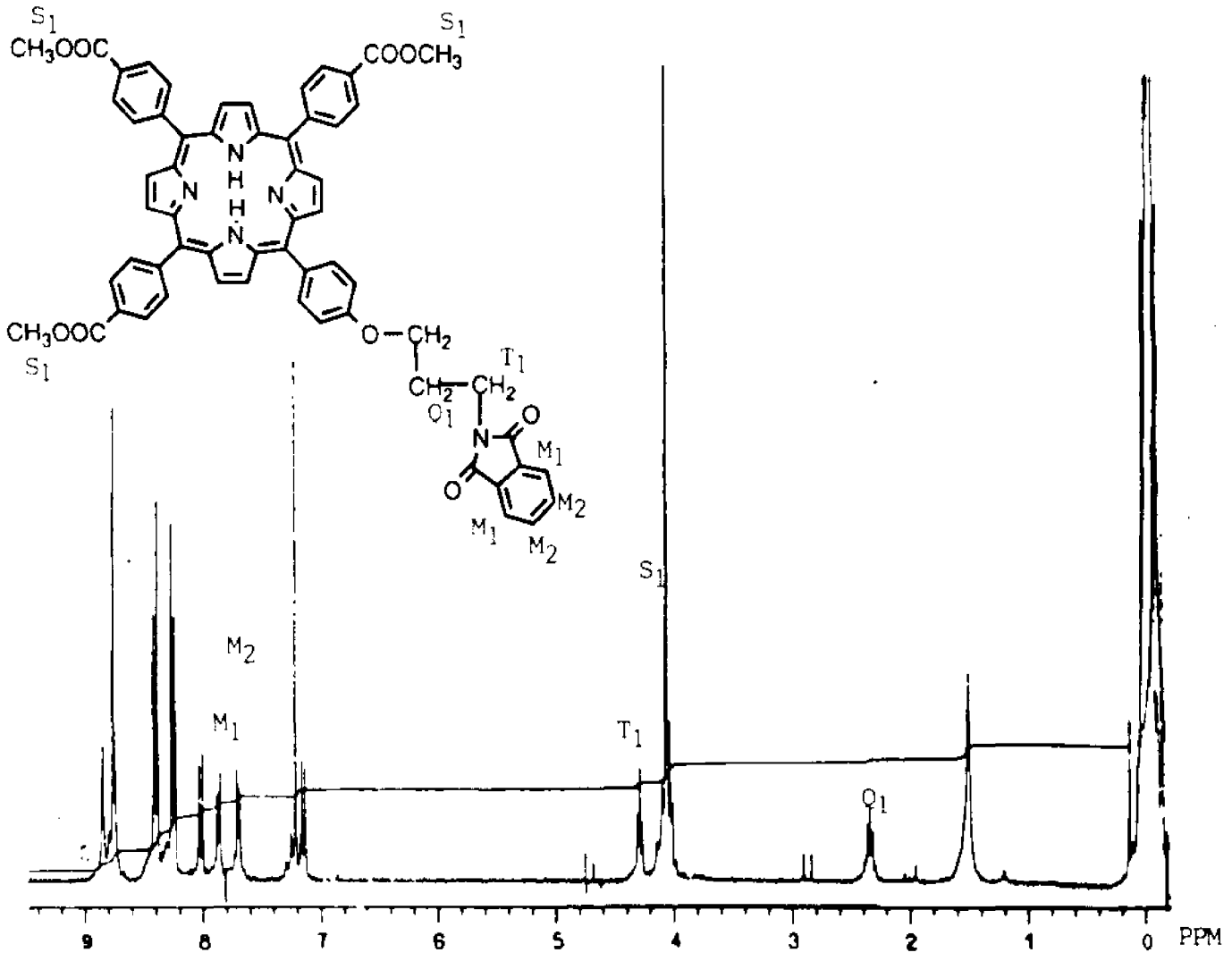
S1
CH3OOC
S1
COOCH3
N
H
H
N
N
N
CH3OOC
S1
O—CH2
T1
CH2—CH2
O1
N
O
O
M1
M2
M1
M2
S1
M2
M1
T1
O1
9
8
7
6
5
4
3
2
1
0
PPM

Figure 2-3(a): The 300 MHz proton NMR spectrum of N-(3-bromo-propyl)phthalimide.

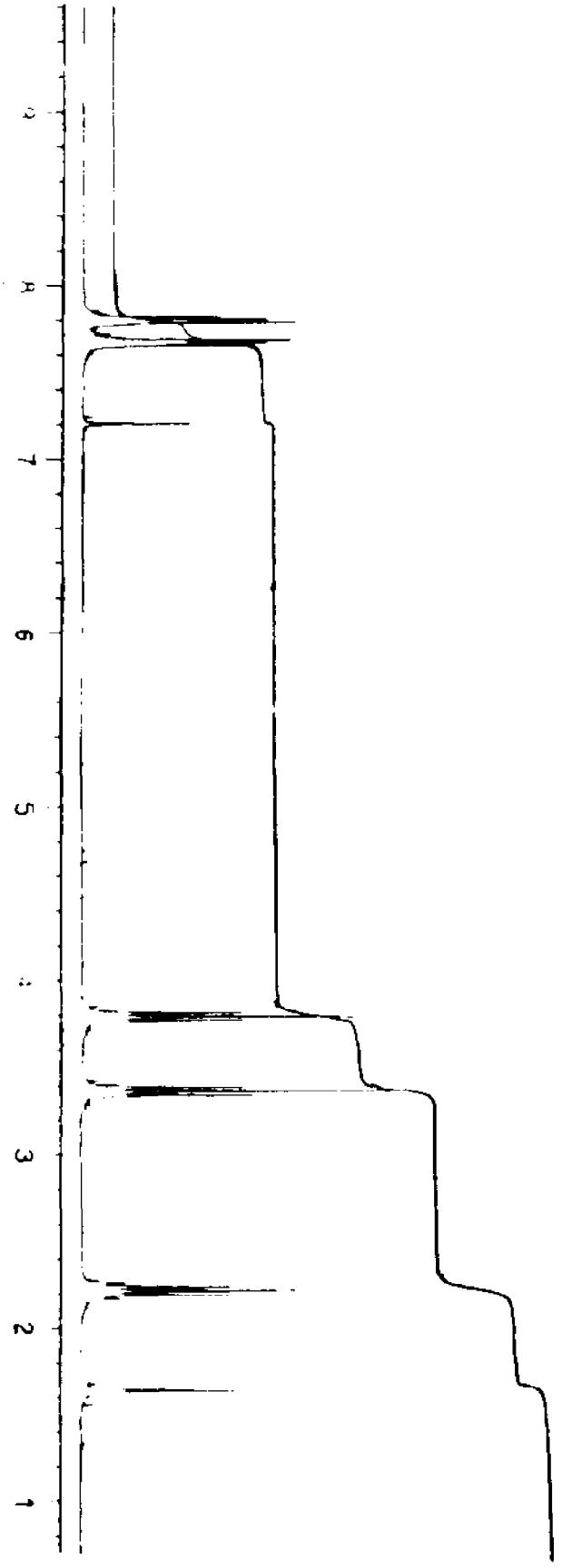
8
7
6
5
4
3
2
1

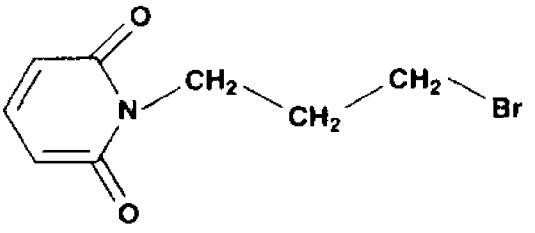
O
N
CH2
CH2
CH2
Br
O

let produced by the third methylene group (adjacent to the nitrogen of the phthalimide group).

The next procedure was the removal of the phthalimide and methyl protecting groups. Basic hydrolysis converted the methyl ester groups to carboxylate salts (7) and the phthalimide groups to the open ring ortho-carboxyl benzamides (8). Hydrolysis under acidic conditions degrades the latter to the corresponding ammonium salt (9). When these reactions were carried out on PPT, 5-[4-(3-aminopropoxy)phenyl]-10,15,20-tri[4-carboxyphenyl]porphine (ACP) was formed.

The proton NMR spectrum of ACP in DMSO-d_6/acetic acid-d_4 (5/1, volume/volume) is given in Fig. 2-4. The multiplets, at 7.91 and 7.74 ppm, of the phthalimide group seen in the PPT spectrum are no longer present in the ACP spectrum. The singlet seen at 4.11 ppm in the PPT spectrum, representing the methyl ester protons of the methyl benzoate groups, is also no longer present in the ACP spectrum.

There are, however, signals in the spectrum of ACP which are similar to signals in the spectrum of the precursor compound, PPT. Triplets T_1 and T_2 , at the chemical shift values of 4.38 and 3.16 ppm and multiplet M_1, at 2.22 ppm, integrate to two protons each and are in the aliphatic region of the spectrum. These are from the propyl section of the tether, which is still present. The signals in the aromatic portion of the spectrum are, as they were in the case of HTP and PPT, from the tetraphenyl macrocycle of the compound.

In order to attach acridine to ACP, the latter was dis-

Figure 2-4: The 300 MHz proton NMR spectrum of 5-[4-(3-amino-propoxy)phenyl]-10,15,20-tri[4-carboxyphenyl]porphine (ACP).

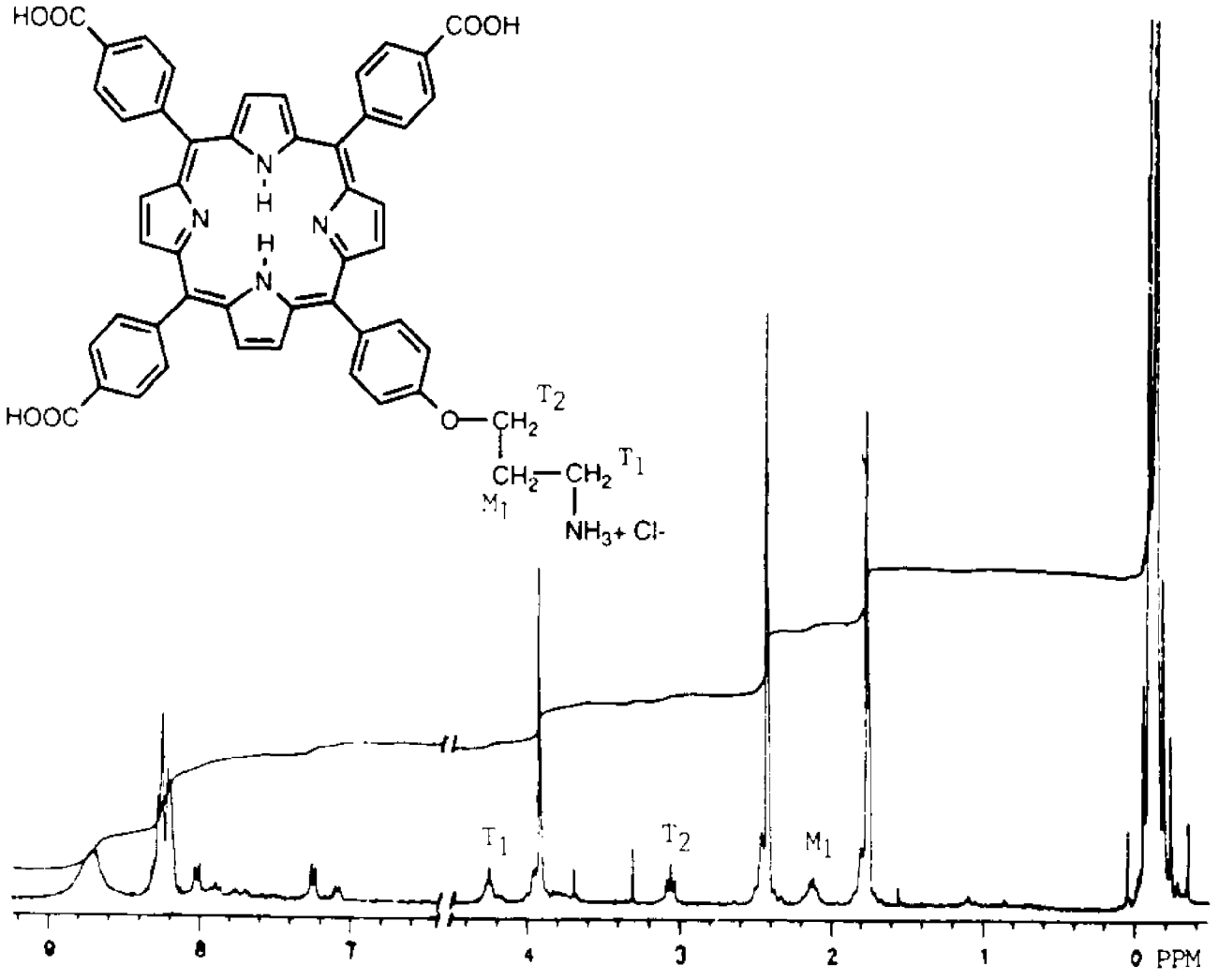
HOOC
COOH
HOOC
N
H
N
H
N
N
O—CH2
T2
CH2—CH2
T1
M1
NH3+ Cl-
T1
T2
M1
9
8
7
4
3
2
1
0 PPM

solved in aqueous, dilute sodium hydroxide solution and then precipitated with concentrated hydrochloric acid. The hydrochloride salt thus obtained was dissolved in phenol and heated with 9-phenoxyacridine prepared from sodium phenoxide and 9-chloro-acridine (10). The subsequent reaction, a nucleophilic substitution of the free amine of ACP for the phenoxide group of 9-phenoxyacridine, resulted in the formation of 5-[4-(N-[9-acridinyl]-3-aminopropoxy)phenyl]-10,15,20-tri[4-carboxyphenyl]porphine (NATP). Figure 2-5 is the proton NMR spectrum of NATP in DMSO-d_6. The outstanding feature of this spectrum is the presence of additional signals in the downfield part of the spectrum in comparison to the spectrum of the precursor ACP. Signals D_1, M_1 and T_1 at 8.61, 7.77 and 7.53 ppm respectively, are due to the presence of newly attached acridine; they integrate to two, four and two protons respectively for a total of eight. Doublet D_1, at greatest chemical shift, arises from those protons nearest the heterocyclic nitrogen (at positions 4- and 5-, see Figure 2-5(a)); they experience the electron-withdrawing effect of the electronegative and electron-delocalizing aromatic nitrogen. The other pair of protons that would give a doublet are some distance from the nitrogen atom attached to the acridine 9- position and, in addition, this nitrogen is not aromatic. Triplet T_1 is at the smallest chemical shift and arises from the protons at the 2- and 7- positions. These protons are two of four whose spin-spin coupling with nearby protons could give a triplet and are the most distant from both nitrogen atoms when compared to the

Figure 2-5: The 300 MHz proton NMR spectrum of 5-[4-(N-[9-acridinyl]-3-aminopropoxy)phenyl]-10,15,20-tri[4-carbomethoxyphenyl]porphine (NATP).

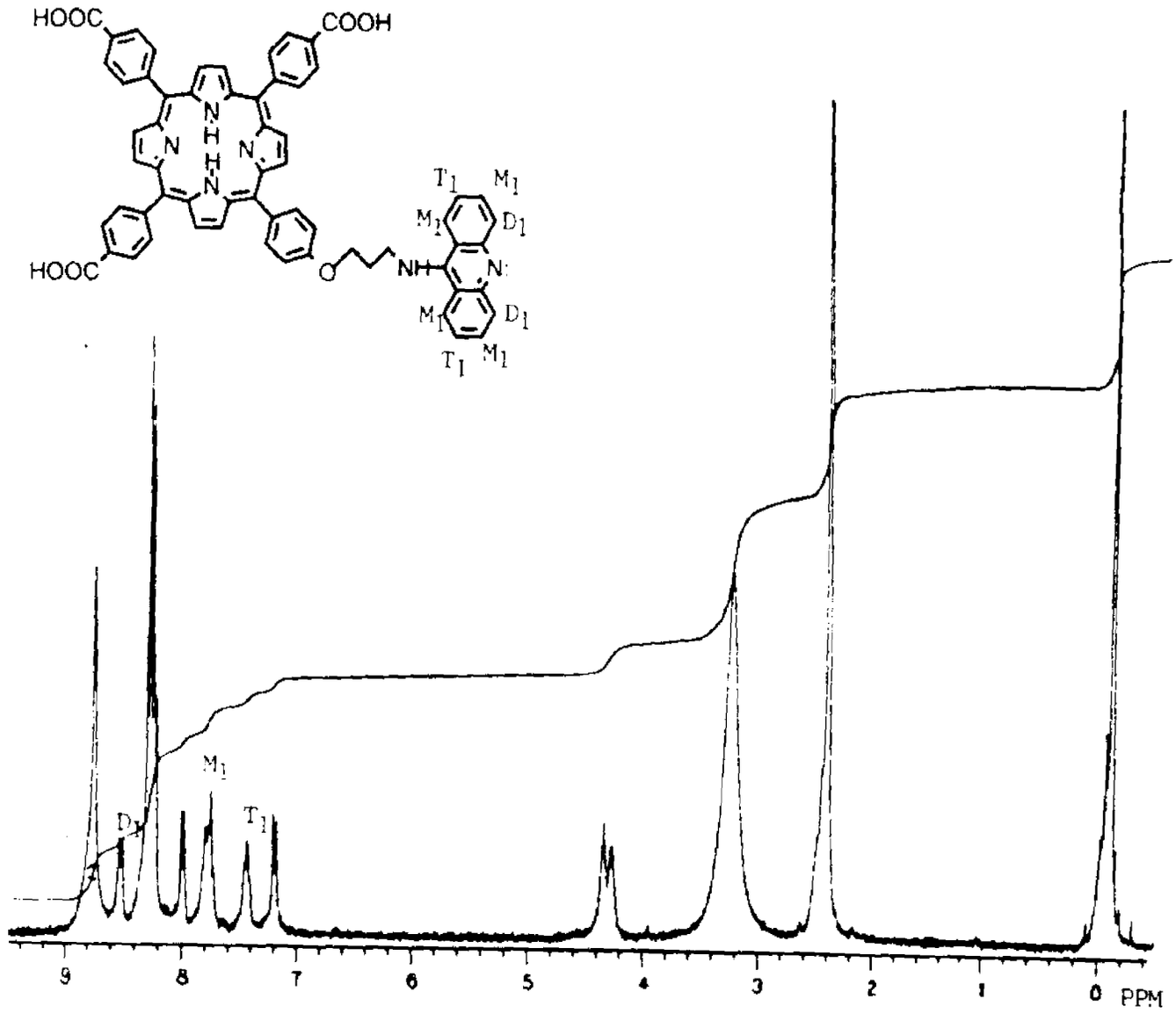
HOOC
COOH
HOOC
N
H
N
H
N
N
O
NH
N
T1
M1
M1
D1
M1
D1
T1
M1
D1
M1
T1
9
8
7
6
5
4
3
2
1
0
PPM

Figure 2-5(a): The numerical system used to specify the position of substituents on the acridine ring.

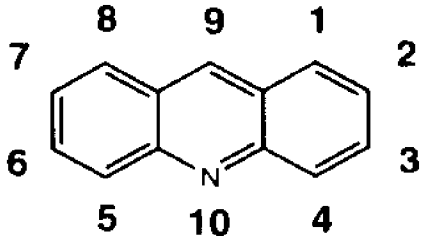
8
9
1
7
2
6
3
N
5
10
4

other acridine protons. Multiplet M_1 is more complex, it is a fusion of two signals, a triplet and a doublet, which are from the protons in the 3-, 6-, 1- and 8- positions . These two pairs of protons are approximately equidistant from the two electronegative nitrogen atoms of the acridine system; thus a triplet and doublet are obtained which are very close in chemical shift and are intermediate, also in terms of shift, between D_1, whose protons are closest to an aromatic nitrogen and are thus most deshielded and T_1, whose protons are farthest away from the two nitrogen atoms and are most shielded.

The resonances from the propyl chain are found at 4.44 and 4.37 ppm in the NATP spectrum; The signal from DMSO-d_6 at 2.49 obscures the resonance given by the central methylene group.

The final reaction was the attachment of the cationic free (unprotonated at basic nitrogen) amine N,N,N-trimethylethylene diamine bromide to each of the three carboxylic groups. A relatively high-energy ester was made first using N-hydroxysuccinimide (NHS) and the dehydrating agent, dicyclohexylcarbodiimide (DCC). Amide bond formation was then carried out by reaction between the charged amine and the labile ester.

The conjugate, ATB, was purified by extensive dialysis using a membrane with a molecular weight cut-off of 1000 daltons. Figure 2-6 illustrates the proton NMR spectrum of ATB in DMSO-d_6/acetic acid-d_4 (5/1, volume/volume). The aromatic portion of the spectrum reveals the presence of the porphyrin

Figure 2-6: The 300 MHz proton NMR spectrum of 5-[4-(N-[9-acridinyl]-3-aminopropoxy)phenyl]-10,15,20-tri[4-(N-[trimethylammoniumethyl])benzamidyl]porphine (ATB).

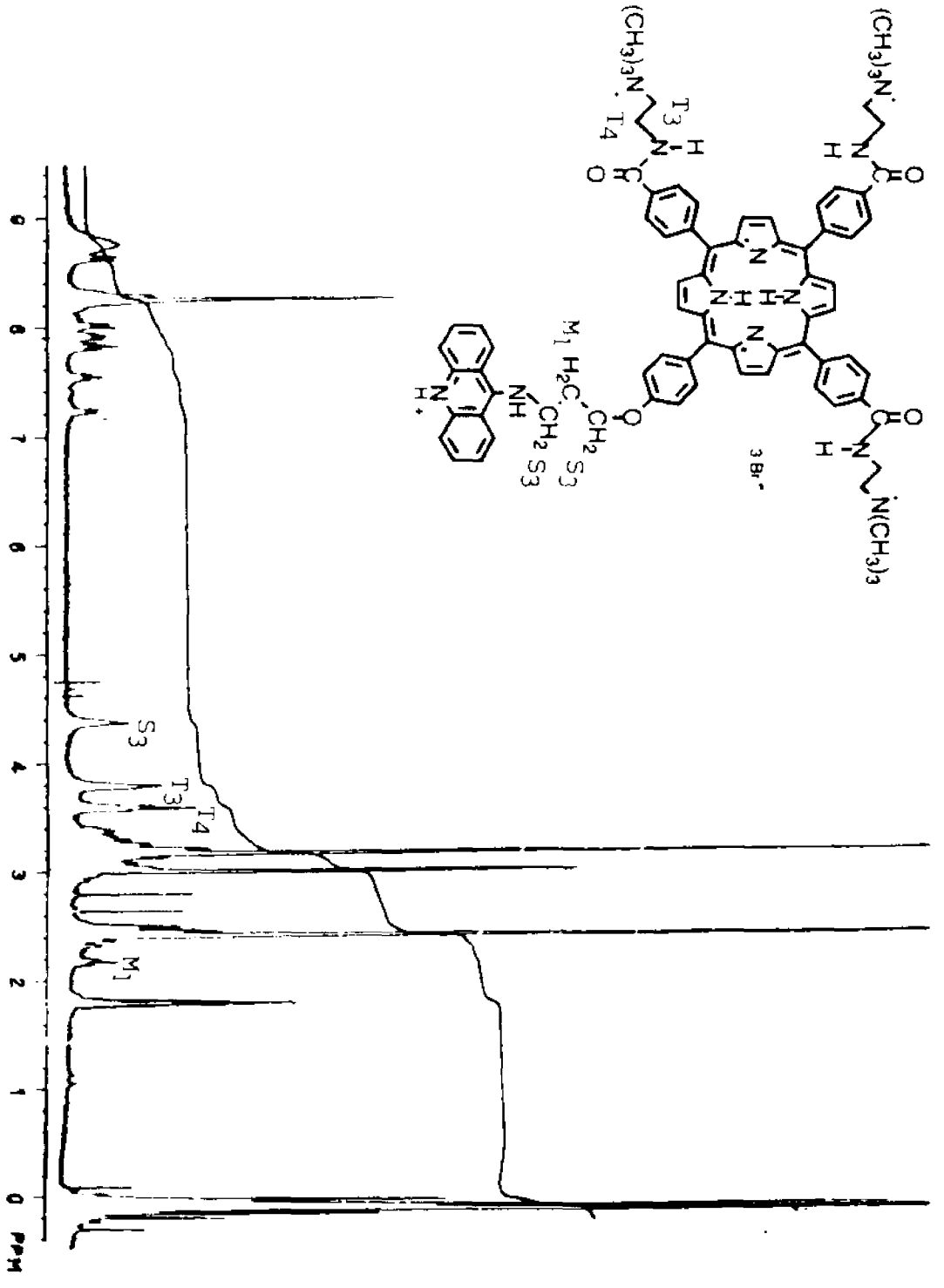
(CH3)3N
T3
T4
M1
H2C
CH2
S3
NH
3Br
S3
T3
T4
M1
PPM

macrocycle as well as the acridine appendage. Figure 2-6(a) is an enlargement of this region. Singlet S_1, eight protons, at 8.87 ppm, comes from the beta-pyrrole hydrogen atoms and is in a position at which resonances for these atoms are usually found (11,12). The large singlet S_2, twelve protons, at 8.37 ppm, represents the protons bound to the three phenyl groups bearing positive charges. It is not a true singlet, but is a union of the two doublets that often arise from these protons; Doublets D_2 and D_4, produced by two protons each, are at 8.11 and 7.32 ppm; they are derived from the phenyl group bearing the ether function and are upfield due to the electron-releasing effect of the ether function; their positions are consistent with those produced by aromatic ethers (13). The amide functions have no such effect.

The other signals in the aromatic region, D_1, D_2, T_1 and T_2, at 8.76, 7.99, 7.91 and 7.63 ppm respectively, integrate to two protons each for a total of eight, and are from the acridine and can be asigned in the same way as with NATP.

The signals in the aliphatic part of the spectrum originate from the propyl and quaternary ammonium groups. Signals S_3 and M_1, at 4.47 and 2.20 ppm, integrate to four and two protons respectively and come from the propyl chain. The signal at 2.20 ppm is in a location typical for the central methylene protons of the propyl chain (14) (e.g. see spectrum of N-(3-bromopropyl)phthalimide). S_3 is from the peripheral methylene groups of the chain and is a union of the two triplets usually seen for these groups and consequently integrates to four pro-

Figure 2-6(a): A magnification of the aromatic portion of the ATB spectrum.

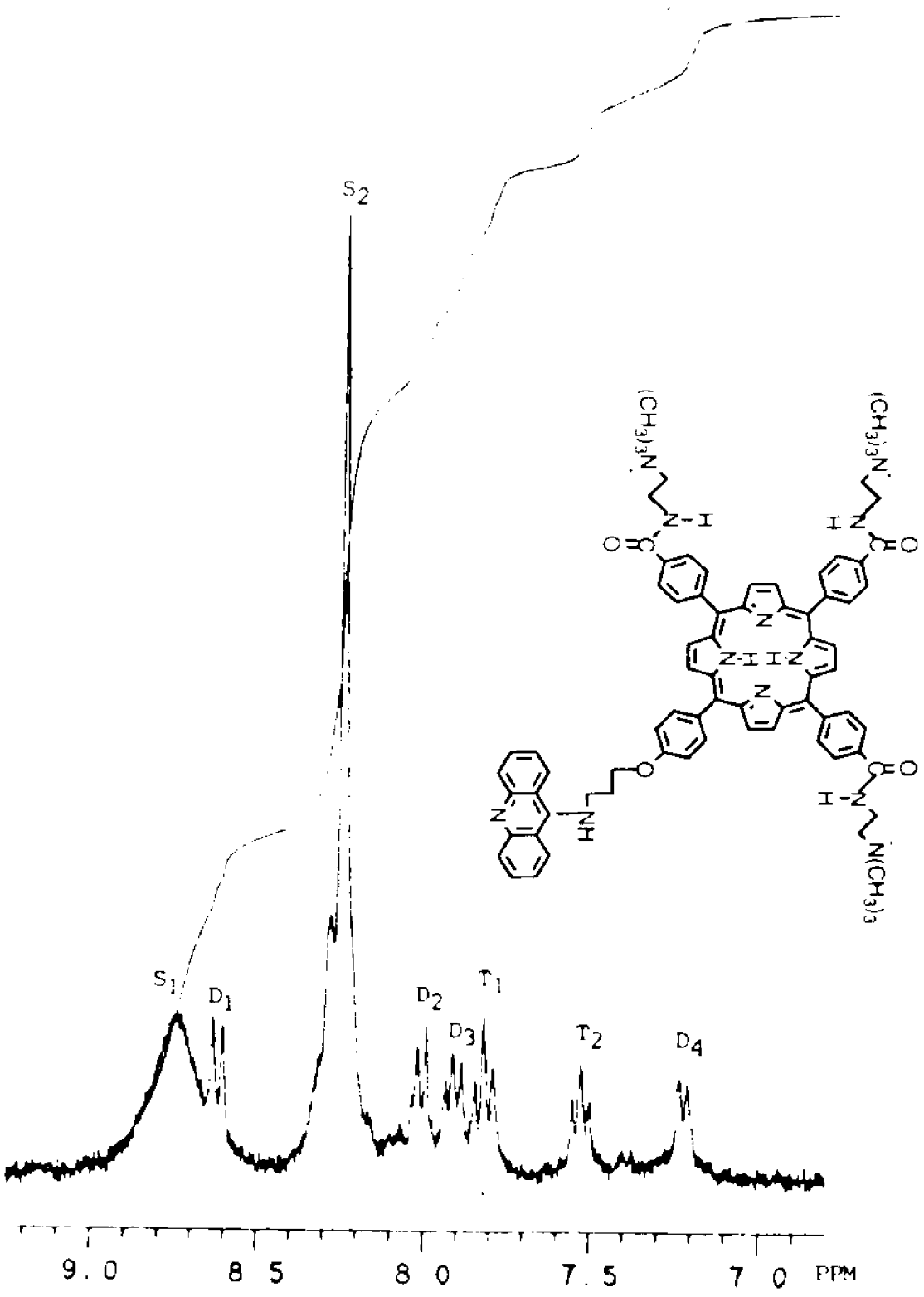
S2
S1
D1
D2
D3
T1
T2
D4
9.0
8.5
8.0
7.5
7.0
PPM
(CH3)3N
(CH3)3N
N(CH3)3

tons. Triplets T_3 and T_4, at 3.89 and 3.69 ppm, integrate to six protons each and are derived from the ethyl group of the quaternary ammonium functions.

N,N,N-trimethylethylene diamine bromide was obtained from 2-bromoethylamine hydrobromide and aqueous trimethylamine; its proton NMR spectrum, taken from D_2O solution, is given in Figure 2-7. Signals from the ethyl group of this compound should integrate to two protons per signal, with a total of two signals. As expected, two multiplets, at 3.69 and 3.54 ppm, are obtained which integrate to two protons each, These chemical shift values for the unattached amine are close to those obtained for the same group in ATB (3.89 and 3.69 ppm). The trimethylammonium protons of the unattached amine are represented by a massive singlet at 3.21 ppm integrating to nine protons. These hydrogen nuclei give rise to a large singlet also, at 3.28 ppm, integrating to twenty-seven protons in the spectrum of the conjugate.

The second cationic porphyrin synthesized, differing from ATB by having no tethered acridine and four positive charges, was made from meso-[tetra(4-carboxyphenyl)]porphine (TCPP) and the charged amine by the same method used to link the amine to NATP. This reaction is shown in Scheme 2.

Figure 2-8 is the proton NMR spectrum of the main reaction product, meso-[tetra(N-[trimethylammoniumethyl]-4-benzamidyl)]porphine (TAP) in DMSO-d_6 solution. This NMR spectrum, like that of ATB, may also be divided into two parts: the resonances in the aromatic section above 7.00 ppm are from pro-

Figure 2-7: The 300 MHz proton NMR spectrum of N,N,N-trimethylethylenediamine bromide.

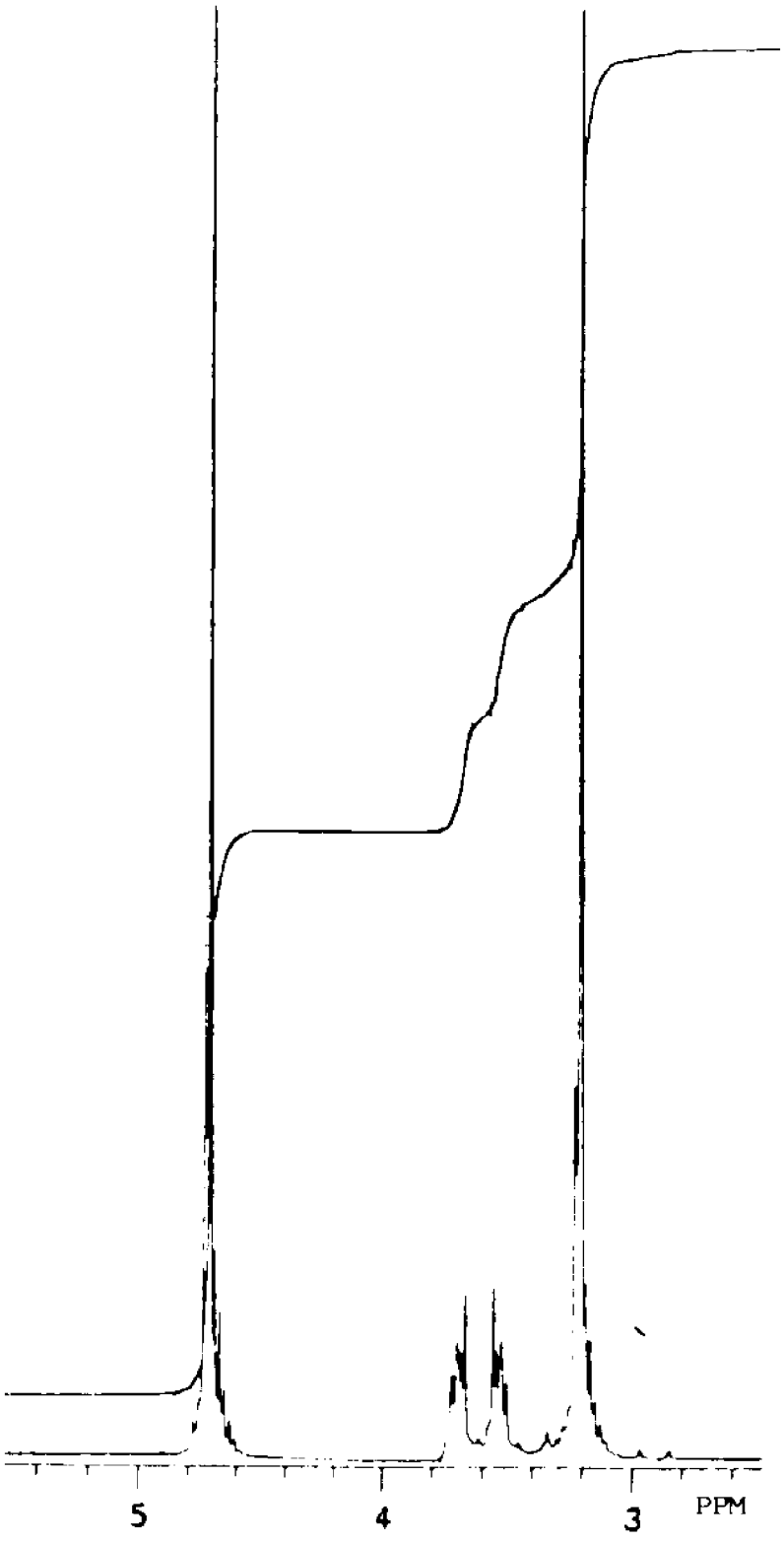
5
4
3
PPM

Figure 2-8: The 300 MHz proton NMR spectrum of meso-[tetra(N-trimethylammoniumethyl]-4-benzamidyl)]porphine (TAP).

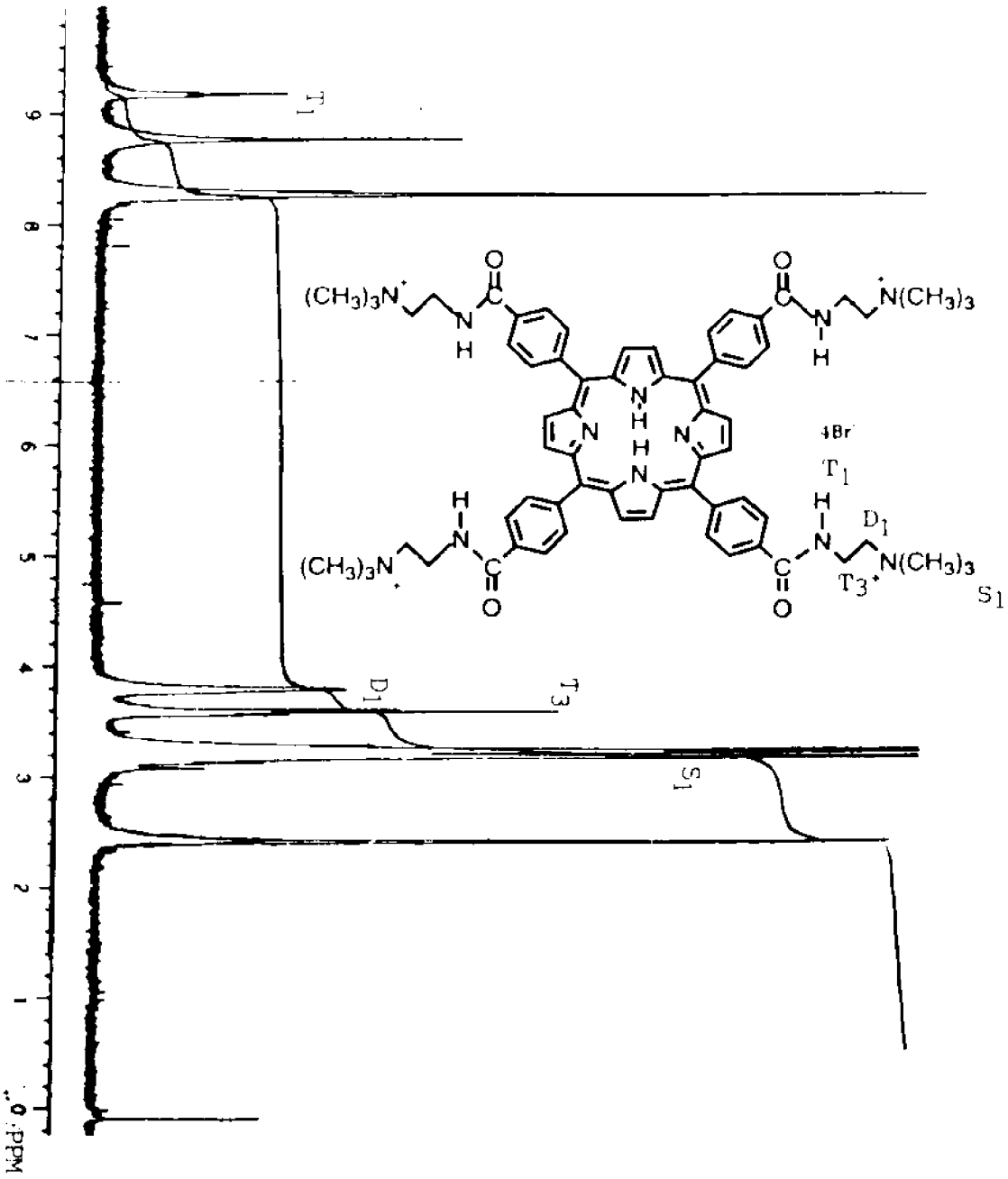
T1
D1
T3
S1
(CH3)3N+
N(CH3)3
4Br-
T1
D1
T3
S1
ppm

tons linked to the tetraphenylporphyrin macrocycle and its amide bonds, while signals in the aromatic region below 7.00 ppm are from protons associated with the quaternary ammonium groups. A comparison with the NMR of the precursor compound TCPP, shown in Figure 2-2, further illustrates this point. There are only two signals obtained from TCPP: a singlet and a large quadruplet at 8.82 and 8.32 ppm integrating to eight and sixteen protons, respectively; these are due to the beta-pyrrole protons and the phenyl protons; there are no signals coming from TCPP in the aliphatic region. TAP has addition resonances in this region however, and these must originate from the quaternary ammonium groups.

The four additional signals are a triplet, T_1, representing four protons, at 9.27 ppm; a doublet, D_1, representing eight protons, at 3.89 ppm; a triplet, T_3, at 3.68 ppm, integrating to eight protons and a large singlet, S_2, representing 36 protons; T_1 lies within the region where amide N-H protons absorb (16); the multiplicity of this signal implies that it couples with two nearby protons, this signal therefore arises from the four N-H protons of the benzamide groups. Amides exhibit slow rates of N-H chemical exchange (17), this is responsible for an observable resonance and its triplet nature. Signals D_1 and T_3, integrating to eight protons each, have chemical shifts of 3.89 and 3.68 ppm respectively, which are not unlike those of the ethyl group of the charged amine (3.69 and 3.54 ppm). Singlet S_2, at 3.27 ppm, integrates to 36 protons and signals the presence of the quaternary methyl groups.

2.4 Experimental Section

Synthesis of 5-[4-(N-[9-acridinyl]3-aminopropoxy)phenyl]-10,15,20-tri[4-(N-[trimethylammoniumethyl])benzamidyl]porphine (ATB).

The procedures for the synthesis of ATB are given in scheme 1.

Synthesis of 5-(4-hydroxyphenyl)-10,15,20-tri(4-carbomethoxyphenyl)porphine: 4-formylmethylbenzoate and 4-hydroxybenzaldehyde at a molar ratio of 3/1 were dissolved in propionic acid (250 mL/0.055 mole of 4-hydroxybenzaldehyde) by vigorous stirring. The stirring acid was brought to 100^{0}C, pyrrole added at a ratio of 4 moles of pyrrole/1 mole of 4-hydroxybenzaldehyde, and the temperature raised to reflux for 0.5 hrs.

The propionic acid solution was allowed to cool to room temperature and as much propionic acid removed as possible, without inducing solidification, by vacuum distillation. The cool propionic acid solution was then poured into methanol to obtain a tarry precipitate. The precipitate was stirred in the methanol, allowed to settle overnight and removed by decantation. The residue was thoroughly dried in a vacuum oven, keeping the temperature at 90^{0}C. A black-purple, brittle solid was obtained.

The crude porphyrin was subjected to silica gel chromatography, using 800 mL of gravity-packed gel per 10 g of impure porphyrin. Methylene chloride was at first used to dissolve

the impure porphyrins and to elute off most of the tar.

Shortwave UV light was used to make porphyrin bands visible; they were eluted with 2 % and then 5 % ethyl acetate in methylene chloride. HTP was the second of three bands of scarlet-colored material. A second chromatography was carried out to further increase the HTP purity, but only 2 % and then 5 % ethyl acetate in methylene chloride were used to elute the desired porphyrin. Yield: 3 %. The proton NMR spectrum of HTP is given in Figure 2-1 and peaks were assigned in the following manner: the doublet and singlet at 8.90 and 8.80 ppm representing eight protons (8H), assigned to the beta-pyrrole protons; two doublets at 8.44 and 8.29 ppm (6H each), assigned to the phenyl protons of the benzoate group; two doublets at 8.06 and 7.22 ppm (2H each), assigned to the phenyl protons of the 4-hydroxyphenyl group; a singlet at 4.11 ppm (9H), assigned to the methyl protons of the methyl benzoate group. The calculated elemental composition of HTP ($C_{50}H_{38}N_4O_7$) is: C, 74.6; H, 4.5; N, 7.0; O, 13.9 %. Elemental Analysis of HTP gave C, 73.9; H, 4.9; N, 6.8; O, 13.7 %.

Synthesis of 5-[4-(3-phthalimidopropoxy)phenyl]-10,15,20-tri[4-carbomethoxyphenyl]porphine from HTP: HTP and N-(3-bromopropyl)phthalimide (synthesized as previously mentioned (7)) in a ratio of 1 mole of HTP/1.4 mole of phthalimide were dissolved in dry N,N-DMF (30 mL/0.5 g HTP). Anhydrous, finely ground potassium carbonate (1.6 g/0.5 g HTP) was then added. The suspension was vigorously stirred for 24 hrs., followed by

heating to 100^{0}C, also with vigorous stirring. The solution was maintained at this temperature for 1 hr to ensure complete reaction. To obtain product, an amount of glacial acetic acid was added that was equimolar to the amount of carbonate used earlier. A few mL of water were added to aid neutralization. The reaction mixture was reduced in volume by evaporation under reduced presure until a volume of N,N-DMF equal to only 15-20 mL remained. Water was added to the residue to precipitate the porphyrin. The PPT was filtered on a glass frit, crushed with a glass rod and washed with water; it was dried by drawing air over it.

Completion of the reaction was checked by silica gel thin-layer chromatography (TLC) using 2 % ethyl acetate in methylene chloride as the solvent. R_f values are: HTP, 0.42; PPT, 0.87. TLC and NMR indicated no further purification was necessary. Yield: 81 %.

The proton NMR spectrum of PPT is shown in Figure 2-3. Signal assignments are as follows: doublet and singlet at 8.90 and 8.80 ppm (8H), from the beta-pyrrole protons; two doublets at 8.44 and 8.30 ppm (6H each), assigned to the phenyl protons of the benzoate groups; doublets at 8.06 and 7.19 ppm (2H each), assigned to the protons of the phenyl ether group; two multiplets at 7.91 and 7.74 ppm (2H each), asigned to the protons of the phthalimide group; triplet at 4.34 ppm (2H), from the methylene group next to oxygen; singlet at 4.11 ppm (9H), from the methyl protons of the methyl benzoate groups; quintuplet at 2.39 ppm (2H), from the central methylene group of

gave the following composition: C, 73.2; H, 4.8; N, 6.9; O, 14.3 %.

Synthesis of 5-[4-(3-aminopropoxyphenyl]-10,15,20-tri[4-carboxyphenyl]porphine (ACP) from PPT: 0.4-0.6 g of PPT was dissolved in 250 mL of 1,4-dioxane. The solution was heated to reflux, after which 84 mL of a 1/1 mixture of methanol and water was slowly added; this was followed by the dropwise addition of 38.5 mL of 5 N NaOH to give a final hydroxide concentration of 0.5 N. The reflux was continued for 1.5 hrs. with vigorous stirring.

The solution was allowed to cool to room temperature before the organic solvent was removed by rotary evaporation. Acidification of the remaining aqueous solution with glacial acetic acid gave a brown precipitate that was filtered on a glass frit, washed with water and heated until just dry in a vacuum oven. The porphyrin was then placed in 100 mL of methanol and dissolved by rapid stirring; 60 mL of water was added followed by the slow, dropwise addition of 40 mL of concentrated sulfuric acid. The green solution was refluxed for at least 16 hrs.

After cooling to room temperature, the solution was chilled by placing the flask in an ice-water bath; a 10 N aqueous sodium hydroxide solution was added dropwise until pH 5.0 was reached, a 1.0 N hydroxide solution was then used until a brown, flocculent precipitate appeared (at pH 5.5 approximately). The precipitate was filtered on a glass frit,

washed with water and dried in a vacuum oven. It was possible to further purify it by dissolving in dilute, aqueous sodium hydroxide and precipitating with glacial acetic acid, but this step, in general, was found to be unnecessary. Yield: 34 %.

The proton NMR spectrum of ACP is shown in Figure 2-5. Signal assignments are as follows: a broad singlet at 8.87 ppm (8H), derived from the beta-pyrrole protons; a quadruplet at 8.38 ppm (12H), derived from the phenyl protons of the 4-carboxyphenyl groups; two small doublets at 8.16 and 7.40 ppm (2H each), derived from the phenyl ether group; a triplet at 4.39 ppm (2H), assigned to the methylene group adjacent to nitrogen; quintuplet at 2.16 ppm (2H), originating from the central methylene group of the propyl chain. The theoretical elemental composition of $Na_3ACP.3H_2O$ ($C_{50}H_{34}O_{10}N_5Na_3$) is C, 63.9; H, 4.26; O, 17.0; N, 7.4; Na, 7.4 %. Analysis gave the following results: C, 64.7; H, 4.3; O, 17.3; N, 6.6; Na, 7.2 %.

Synthesis of 5-[4-(N-[9-acridinyl]-3-aminopropoxy)-phenyl]-10,15,20-tri[4-carboxyphenyl]porphine (NATP) from ACP: 0.2-0.5 g of ACP was dissolved in a mixture of 50 mL of 1 N sodium hydroxide and 100 mL of methanol by stirring for 16 hrs. The methanol was removed by rotoevaporation and 50 mL of concentrated hydrochloric acid added to induce formation and precipitation of the trihydrochloride salt of ACP. The green precipitate was filtered on a frit, washed with water and dried in a vacuum oven.

The ACP trihydrochloride was dissolved in phenol (0.6 g/

12 mL of phenol) by rapid stirring and then heating to 80°C in an oil bath. 9-phenoxyacridine (10) was added at a ratio of 2.8 moles of acridine/1 mole of ACP and the oil bath temperature raised to 120°C, with continued rapid stirring. After 1.5 hrs. the solution was cooled to 40°C it was then poured into anhydrous ethyl ether (200 mL/0.6 g of ACP). The precipitate obtained was collected on a frit and washed with ether.

In order to purify the product, it was dissolved in methanol (50 mL/1 g of product) and dilute ammonia (1 volume conc. ammonia/10 volumes water) added dropwise until the green solution had just turned to a brown-purple color. Water was added slowly to induce precipitation and the precipitate collected on a frit and repetitively washed with cold water. It was then dried in a vacuum oven. Yield: 70 %.

Fig. 2-5 is the proton NMR spectrum of NATP. Signal assignments are as follows: doublet (2H), multiplet (4H) and triplet (2H) at 8.61, 7.77 and 7.53 ppm respectively, assigned to the acridine protons; singlet at 8.84 ppm (8H), assigned to beta-pyrrole protons; large quadruplet at 8.36 ppm (12H), assigned to the phenyl protons of the 4-carboxyphenyl groups; two doublets at 8.08 and 7.20 ppm (2H each), assigned to the protons of the phenyl ether group; triplet at 4.44 ppm (2H), assigned to the protons of the methylene group next to nitrogen; triplet at 4.37 ppm (2H), derived from the protons of the methylene group next to oxygen.

The theoretical elemental composition for NATP dihydrochloride monohydrate ($C_{68}H_{44}N_6O_7.2HCl.H_2O$) is: C, 69.5; H, 4.4;

N, 7.7; O, 11.8; Cl, 6.5 %. Analysis produced the following results: C, 69.4; H, 4.8; N, 7.5; O, 12.0; Cl, 6.3 %.

Synthesis of N,N,N-trimethyl-1,2-diaminoethane bromide (TDB): 2-bromoethylamine hydrobromide and trimethylamine, in a molar ratio of 1/1.25 respectively (trimethylamine in aqueous solution), were dissolved in a 1/1 mixture of methanol and water (50 mL MeOH-water/4.0 g 2-bromoethylamine.HBr). The solution was stirred for 16 hrs at room temperature in a stoppered container.

As much methanol and water as possible were removed by rotoevaporation; further drying was done in a vacuum oven. It was recrystallized from 15 % methanol in 1,4-dioxane; more crystals were obtained by cooling the mother-liquor in an ice-bath. Yield: 42 %.

Fig. 2-7 is the proton NMR spectrum of the quaternary ammonium salt. Signal assignments are: two multiplets at 3.69 and 3.54 ppm (2H each), assigned to the ethyl methylene groups; singlet at 3.21 ppm (9H), assigned to the trimethylammonium protons.

Synthesis of ATB (conjugate) from NATP: N-hydroxysuccinimide and NATP, in a ratio of 5 moles of succinimide/1 mole of NATP, were dissolved in dry N,N-DMF (20 mL N,N-DMF/0.5 g NATP) by stirring, and dicyclohexylcarbodiimide (DCC) added (5 moles of DCC/1 mole of NATP). The mixture was kept free of moisture and stirred at room temperature for 16 hrs. During this time,

TDB hydrobromide was treated with sodium hydroxide (1 mole of the amine/0.7 mole of hydroxide) in 3-5 mL of water. After dissolution, as much water as possible was removed by roto-evaporation and drying in a vacuum oven. After 16 hrs., the N,N-DMF solution was mixed with a quantity of deprotonated amine corresponding to 5 moles of amine/1 mole of NATP. The mixture was vigorously stirred for 2-3 days.

To isolate and purify the ATB, the byproduct, dicyclohexylurea, was removed by filtration through a glass frit and excess N,N-DMF removed by vacuum distillation until only 20 mL of solution was left. Precipitation of crude conjugate was induced by adding dry tetrahydrofuran (100 mL/0.5 g of NATP) with rapid stirring.

Purification of ATB was by extensive dialysis of crude material against water, using an aqueous solution of ATB and a cellulose membrane with a molecular weight cut-off of 1000 daltons. After dialysis, ATB was recovered by lyophilization. Yield: 31 %.

The proton NMR spectrum of ATB is in Figure 2-6. The complete signal assignments for ATB have been previously given in the results and discussion section. The extinction coefficient for ATB in 100 mM NaCl, 26 mM sodium phosphate and 1 mM EDTA, pH 7.2, is 1.05×10^5 M^{-1} cm^{-1} at 421 nm.

The theoretical elemental composition for ATB nonahydrate ($C_{78}H_{83}N_{12}O_4Br_3.9H_2O$) is C, 56.7; H, 6.1; N, 10.2; O, 12.6; Br, 14.4 %. Analysis gave the following results: C, 55.4; H, 6.0; N, 10.6; O, 13.0; Br, 15.0 %.

Synthesis of meso-[tetra(4-[N(trimethylammoniumethyl)]benzamidyl)]porphine (TAP).

The reaction for the synthesis of TAP is given in Scheme 2.

Synthesis of TAP from meso-[Tetra(4-carboxyphenyl)]porphine (TCPP): TCPP was dissolved in dry N,N-DMF by vigorous stirring and at a ratio of 15 mL of N,N-DMF/0.5 g of TCPP. NHS, at a ratio of 3 moles of NHS/0.6 moles of TCPP, was added to the mixture and allowed to dissolve. This was followed by an equimolar amount of DCC. The solution was stirred at room temperature for at least 3.5 hrs.. During this time, N,N,N-trimethyl-1,2-diaminoethane.HBr, at a ratio of 5 moles of the amine/0.6 moles of TCPP, was treated with hydroxide as previously described. At the end of the time alloted for the TCPP-succinimide conjugation, the porphyrin mixture was poured into the flask containing dried deprotonated amine and the suspension was stirred vigorously for two days after dissolution had occurred.

The desired product was obtained by filtering off the urea and obtaining a precipitate by pouring the N,N-DMF solution into methylene chloride once the solution volume was below 20 mL. For larger volumes, the N,N-DMF was first removed by vacuum distillation. The precipitate was allowed to settle and the solution removed by decantation.

The desired product was purified by three recrystallizations from 1 % water in ethanol (volume/volume). Yield:

The proton NMR spectrum of TAP is presented in Figure 2-8. signals are assigned as follows: triplet at 9.27 ppm (4H), derived from the amide N-H protons; singlet at 8.86 ppm (8H), derived from the beta-pyrrole protons; large triplet at 8.36 ppm (16H), assigned to the phenyl protons; a doublet at 3.89 ppm (8H), assigned to the protons of the methylene groups next to the amide functions; a triplet at 3.68 ppm (8H), assigned to the protons of the methylene groups next to quaternary nitrogen; singlet at 3.27 ppm (36H), assigned to the methyl quaternary ammonium protons.

The extinction coefficient of TAP in buffer composed of 0.1 M NaCL, 26 mM sodium phosphate and 1 mM EDTA at pH 7.2 is 2.11×10^5 M^{-1} at 414 nm (the Soret maximum).

Chapter Three

Spectroscopic Studies of the Interactions of ATB and TAP with Nucleic Acids.

3.1 Introduction.

Circular dichroism, UV-visible absorption and fluorescence emission spectra have been used extensively to gather information about the binding sites of cationic porphyrins on nucleic acids. These studies have incontrovertibly shown that binding mode is dependent on the structural geometry of the porphyrin, the ratio of porphyrin molecules to nucleic acid base pairs (the binding ratio, r_o) and on the nucleic acid base sequence and conformation (1-10).

Circular dichroism is based upon the differential absorption of right- and left-handed circularly polarized light by chiral molecules and polymers. Light with its electric field resonating in one plane of space (see Figure 3-1) is composed of right- and left- handed electric field vectors which may be absorbed to different extents by chiral molecules giving rise to a resultant electric field that traces out an ellipse. Although a molecule may be totally achiral in solution alone, it may acquire chirality upon binding in the chiral environment of a macromolecule and thus obtain a circular dichroism spectrum where there was none before, this is termed induced circular dichroism (CD). CD spectra are measured as either the

Figure 3-1: (a) Light polarized in a single plane may be divided into left- and right- handed electric field vector components. (b) After passage through an optically active solution, the right-handed circularly polarized electric field vectors are absorbed and also rotated; the resulting combined vectors (center) trace out an ellipse.

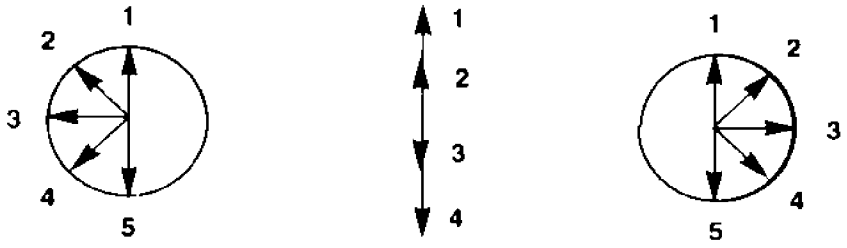

(a)

Before

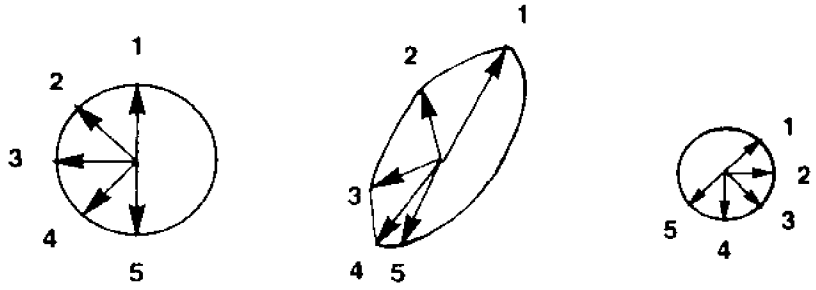

(b)

After

change in absorbance or extinction coefficient for left- and right- circularly polarized light vs. wavelength. Beer's law holds for these values and allows for interconversion between these terms:

$$\Delta A = A_L - A_R = \epsilon_L bc - \epsilon_R bc = (\Delta\epsilon)bc. \qquad (I)$$

Equation I gives the relationship between change in absorbance and change in extinction coefficient.

Although porphyrins are achiral, upon binding at a chiral site on DNA, an induced CD is observed. Pasternack and coworkers (7) demonstrated that the sign of the induced CD band in the Soret region (region of maximum optical density) can be used to determine the mode of binding. Intercalated complexes are characterized by a negative CD band, whereas external (i.e non-intercalated) complexes are marked by a positive CD band. Pasternack's CD work was done at r_0 = 0.03 (the ratio of [porphyrin]/[nucleic acid base pairs]); ionic strength = 0.2 and ph = 6.8.

Metal chelates of meso-[tetra(4-N-methylpyridyl)]porphine (TMPyP, see Fig. 1-1) without axial ligands, such as Cu(II) and Ni(II) derivatives as well as unmetallated TMPyP therefore showed negative CD bands with calf thymus DNA and poly(dG-dC)-(dG-dC) positive bands were seen with poly(dA-dT).(dA-dT) Chelates with axial ligands such as Co(III), Fe(III) and Zn(II), showed a positive band with CTDNA and poly(dA-dT).(dA-dT); no bands or small positive bands were seen with poly(dG-dC).(dG-

dC). Axial ligands therefore hinder intercalation. TMPyP also gives a positive band with CTDNA and poly(dA-dT).(dA-dT); this indicates that it is able to bind to stretches of DNA containing both kinds of basepairs.

The relationship between the sign of the CD spectrum and the binding mode has been confirmed by Pasternack in experiments such as DNA unwinding assays and by ^{1}H and ^{31}P NMR spectroscopy (7-10). This relationship has also been confirmed in work done by Fiel and coworkers (1-3,5,6).

Evidence for external or intercalative binding can be obtained from changes in the UV-visible absorption (non-CD) spectrum as well. Pasternack also found that meso-[tetra(4-N-methylpyridyl)]porphine (TMPyP) and its metallocomplexes intercalated into poly(dG-dC).(dG-dC) produced a substantial decrease in intensity or hypochromicity of the porphyrin's absorption maximum in the visible region (the Soret band) of approximately 35 % or more and a corresponding shift of the Soret band to longer wavelength: a bathochromic shift of 15 nm or more. Although other intercalating cationic porphyrins display differing hypochromicities and bathochromic shifts, the general rule obtained from these kinds of studies (7-9) is that intercalation is characterized by large hypochromicity relative to unbound porphyrin.

Externally bound complexes of TMPyP, such as axially ligated Zn(II)TMPyP, are marked by either a small hypochromicity (10 % or less) or an increase in intensity (hyperchromicity) of the Soret absorption band. The bathochromic shift

is often smaller (8 nm or less). Again, the general rule for porphyrins is that AT/porphyrin complexes are characterized by small hypochromicity or by hyperchromicity of the Soret band.

Fluorescence emission spectra have been used to indicate where porphyrin binding sites are on DNA. Whether binding is electrostatic, in the major or minor groove, or is caused by intercalation, the electronic environment of the porphyrin has changed when compared to free porphyrin in solution. Excitation is at the wavelength of maximum absorption (the Soret band) and the emission spectrum of porphyrin alone in solution is compared with that of the porphyrin when it is in the presence of DNA (at fixed r_0, pH and ionic strength).

Hypochromicity in the fluorescence emission spectrum of a porphyrin in the presence of nucleic acid, signals either the formation of an externally bound, electrostatic complex (not bound in a groove) or intercalation. Hypochromicity when an electrostatic complex is formed can be caused by radiationless deactivation of excited molecules (11). Hypochromicity upon intercalation into DNA is a common phenomenon (12,13) and is considered to be the result of the deactivation of the excited state by an interaction between the excited intercalator and the base guanine (13,14).

The extent of fluorescence emission hypochromism can be used to distinguish between intercalation or electrostatic, external binding. That produced by intercalation is extensive, e.g. for meso-[tetra(4-N-methylpyridyl)]porphine (TMPyP) and poly(dG-dC).(dG-dC) it is a 75 % reduction (16); whereas, in

the case of electrostatic interaction, it is usually much less profound, e.g. for Zn(II)TMPyP and poly(dG-dC).(dG-dC), it is a 25 % reduction of intensity (15).

By contrast, hyperchromicity is promoted by the absence of water from the solvation shell of the molecule; the inhibition of deactivation by proton transfer to water (11) may be a mechanism of action for this effect. Hyperchromicity is also favored in molecules with a rigid structure compared to those that have a more flexible structure (16); both of these conditions are encountered when a porphyrin is bound in the minor groove of DNA. Therefore, hyperchromicity is used as evidence for the insertion of a positive periphery porphyrin into the minor groove of DNA.

In order to examine the contribution of the acridine chromophore to the CD, absorbance and fluorescence spectra of the conjugate, the compound 9-(propylamino)-acridine was synthesized as an analogue of the acridine chromophore of the conjugate. 9-(propylamino)-acridine possesses the same propylamino chain as the acridine chromophore of the conjugate and this chain is in the same 9- position on the acridine function. A comparison of the absorbance spectra of 9-(propylamino)-acridine and the porphyrin-acridine conjugate reveals that they absorb in the same region of the spectrum (Figure 3-2(b)) and that the ratio between the extinction coefficient of meso-[tetra-(4-[N-(trimethylammoniumethyl)]benzamidyl)]porphine (TAP), and 9-(propylamino)-acridine is 25.7 at the Soret maximum of TAP, 414 nm, which is close to the maximum of the

acridine, which is at 409 nm. Therefore, in the absorbance and CD spectra of the conjugate, any change in the absorbance of the acridine would have a negligible effect on the absorbance of the conjugate. In essence, changes in the spectrum of the conjugate reflect changes in the spectrum of the porphyrin portion of this molecule.

The fluorescence spectrum of the conjugate also requires similar consideration. 9-(propylamino)-acridine has a maximum absorbance at 409 nm, which is close to the maximum for TAP (414 nm). When 9-(propylamino)-acridine is excited at 414 nm, its emission spectrum yields a band very close to the excitation wavelength with a maximum at 447 nm (Figure 3-2(a)). However, TAP excited at 414 nm produces an emission band at much lower frequency with a maximum at 644 nm. The fluorescence emission spectrum of the conjugate therefore contains two separate emission bands from different parts of the molecule. The application of these fluorescence phenomena will be discussed in the following sections.

The techniques discussed above were used to determine the nature of the binding sites for the porphyrin-acridine conjugate and its analogue TAP.

Figure 3-2: (A) The fluorescence emission spectrum of 9-(propylamino)-acridine (concentration = 30μM). Excitation at 414 nm. The peak due to light-scattering is indicated by an arrow. (B) The absorbance of TAP (1), conjugate (2) and 9-(propylamino)-acridine (3) at concentrations of 1, 2 and 30 μM respectively. All compounds were dissolved in buffer composed of 0.1 M NaCl, 26 mM NaH_2PO_4 and 1 mM EDTA, pH = 7.2.

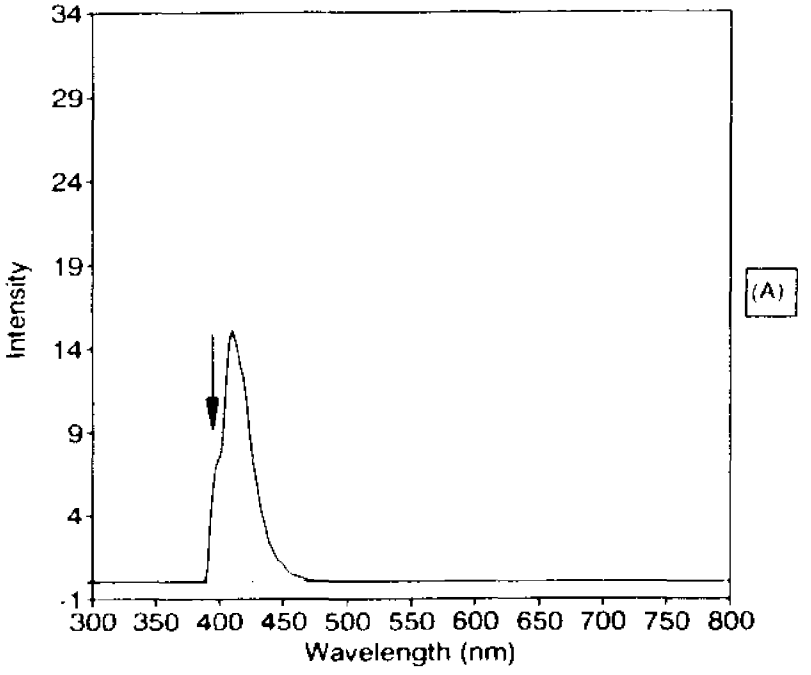
34
29
24
19
14
9
4
-1
Intensity
300 350 400 450 500 550 600 650 700 750 800
Wavelength (nm)
(A)

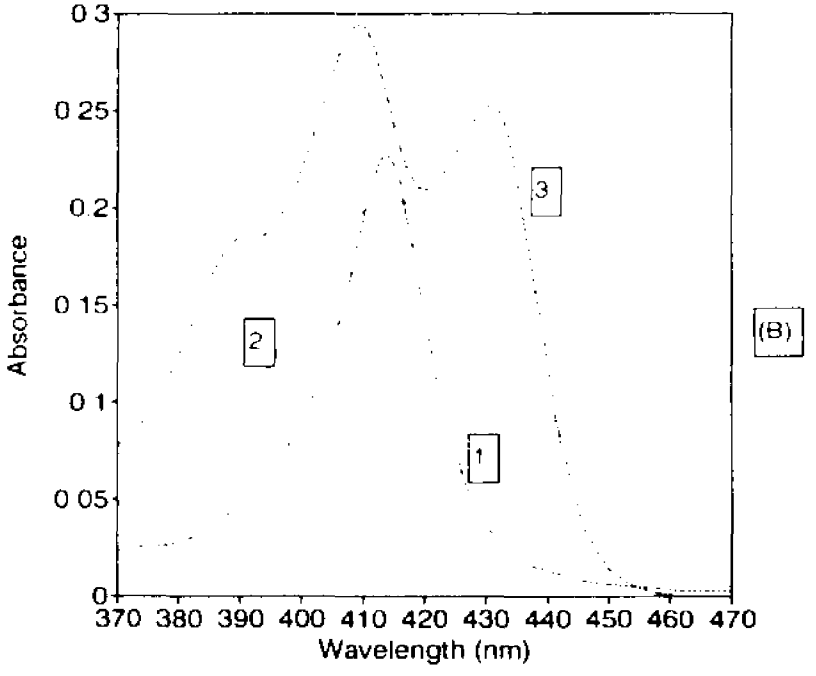
0 3
0 25
0 2
0 15
0 1
0 05
0
Absorbance
370 380 390 400 410 420 430 440 450 460 470
Wavelength (nm)
1
2
3
(B)

3.2 Materials and Methods

Calf Thymus DNA (CTDNA), poly(dA-dT).(dA-dT) and poly(dG-dC).(dG-dC) were purchased from Sigma Chemical Company. CTDNA was treated to remove protein as described by Pasternack (7) with a few changes. A sufficient volume of buffer, composed of 0.1 M NaCl, 26 mM NaH_2PO_4/Na_2HPO_4 and 1 mM EDTA, pH = 7.2, was added to CTDNA to give a final concentration of 1 mg/mL. Dissolution was achieved by stirring for 40 hrs at 4^0C. Protein was removed from the CTDNA by repeated extraction with a solution of chloroform and isoamyl alcohol (24/1, volume/volume); the organic and aqueous layers were separated by centrifugation. The protein content of the aqueous layer was monitored by the use of Bradford reagent (obtained from Biorad). After the final centrifugation, the top two-thirds of the DNA solution was carefully pipetted off and then subjected to dialysis against the pH 7.2 buffer at 4^0C. All buffers were made using distilled and deionized water.

Poly(dA-dT).(dA-dT) and poly(dG-dC).(dG-dC) were used without further purification. Stock solutions were made by adding the pH 7.2 buffer to these polynucleotides at room temperature. All DNA solutions were stored below 0^0C.

The integrity of the DNA was determined by comparing their molar extinction coefficients with published results (17-19). Concentrations were determined spectrophotometrically, as moles of base pairs/litre (M), using extinction coefficients of 1.31×10^4 M^{-1} cm^{-1} at 260 nm for Calf Thymus DNA (CTDNA) (19); 1.32×10^4 M^{-1} cm^{-1} at 262 nm for poly(dA-dT)$_2$

(17) and a value of 1.68 x 10^4 M^{-1} cm^{-1} at 254 nm for poly(dG-dC)$_2$ (18).

9-(propylamino)-acridine was synthesized by a literature procedure (20) and its identity and purity verified by NMR spectroscopy and by melting point determination. The n-propylammonium chloride necessary for the reaction was prepared by dissolving n-propylamine in methanol; this was added to dilute hydrochloric acid using a 1/1.1 molar ratio of amine to acid. The aqueous methanol solution was thoroughly mixed.

The hydrochloride was obtained by removing as much solution as possible from the reaction flask by rotary evaporation and heating the viscous residue under reduced pressure in an Erlenmeyer flask lightly covered with aluminum foil at 110°C. The salt sublimed and was obtained as a white flake on the upper walls of the flask.

All other chemicals and buffer components were molecular biology grade and were purchased from Fisher Scientific.

Circular dichroism spectra were obtained from a Jobin Yvon spectropolarimeter using a spectral band pass of 20 Å. Absorption spectra were obtained from a Cary 13 spectrophotometer. Fluorescence emission spectra were obtained using an Aminco-Bowman 125 spectrophotofluorometer. The reference, exit, entrance and signal PM tube slit widths were 0.5, 1.0, 0.5 and 2.0 mm respectively. The wavelength of excitation was 414 nm and emission spectra were obtained from 200 to 800 nm.

3.3 Results and Discussion

The interactions of the newly synthesized, water-soluble porphyrins, meso-[tetra(4-N-[trimethylammoniumethyl])benzamidyl]porphine (TAP) and 5-[4-(N-[9-acridinyl]-3-aminopropoxy)-phenyl]-10,15,20-tri[4-(N-[trimethylammoniumethyl])benzamidyl]porphine (ATB), with natural and synthetic DNA were monitored with circular dichroism, visible absorption and fluorescence emission spectroscopy. The nucleic acids used were calf thymus DNA, poly(dG-dC).(dG-dC) and poly(dA-dT).(dA-dT).

Figure 3-3 is a plot of absorbance (at the Soret maximum) vs. concentration for ATB through the range of concentrations used in the experiments. This graph is linear, indicating there is no stacking of conjugate in this range. Figure 3-4 shows the absorbance spectrum of the conjugate at pH 7.2 and 2.5. The large shift to lower frequency and hyperchromism in the Soret band at pH 2.5 is characteristic of non-N-alkylated porphyrins protonated at the pyrrolenic nitrogens (21-24). At pH 7.2, the porphyrin macrocycle of the conjugate is unprotonated. The pKa values for 9-(propylamino)-acridine are pKa_1 = 9.2 and pKa_2 = 5.5 (23) at the positions indicated in Figure 3-5(a); therefore, at pH = 7.2, the monoprotonated species (Fig. 3-5(a)) exists. Considering the structural similarity of the acridine moiety of the conjugate to 9-(propylamino)-acridine, a similar state of ionization exists in the former. This gives a structure at pH 7.2 that is shown in Figure 3-5(b).

Figure 3-3: A plot of absorbance vs. concentration for the acridine-porphyrin conjugate over the concentration range used in the experiments.

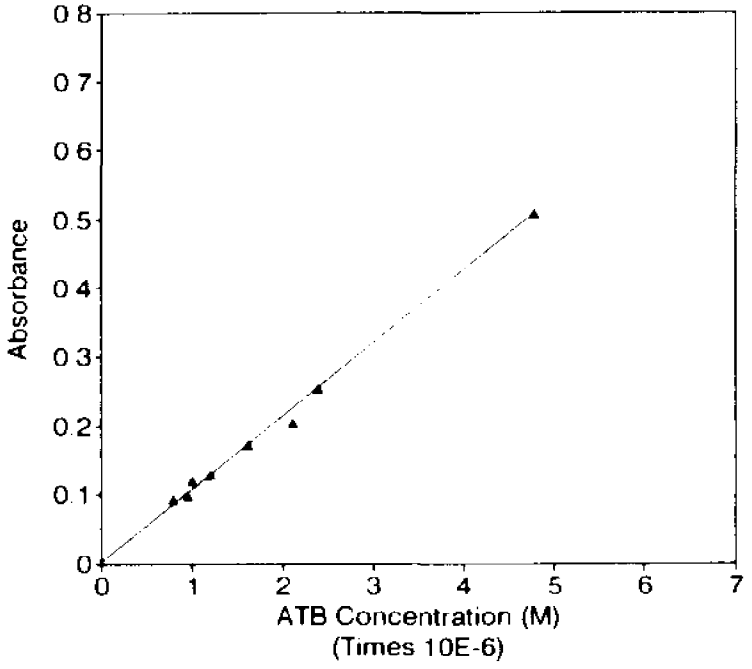
0.8
0.7
0.6
0.5
0.4
0.3
0.2
0.1
0
Absorbance
0
1
2
3
4
5
6
7
ATB Concentration (M)
(Times 10E-6)

Figure 3-4: The absorbance spectrum of the acridine-porphyrin conjugate at pH = 7.2 (solid line) and pH = 2.5 (dashed line). Buffer at pH 2.5 was composed of 0.1 M NaCl and 25 mM potassium acid phthalate.

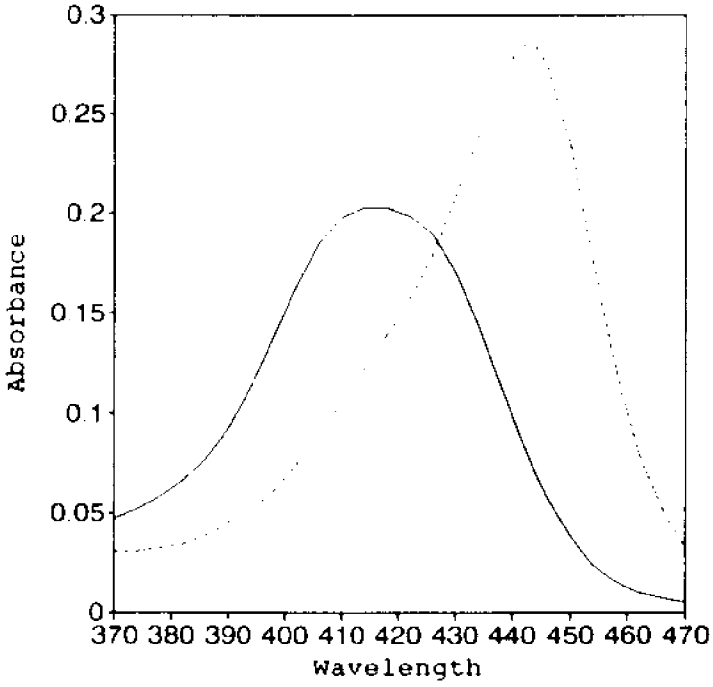
0.3
0.25
0.2
0.15
0.1
0.05
0
Absorbance
370 380 390 400 410 420 430 440 450 460 470
Wavelength

Figure 3-5. (a) The molecular structure of 9-(propylamino)-acridine at pH = 7.2. (b) The molecular structure of the conjugate at pH = 7.2.

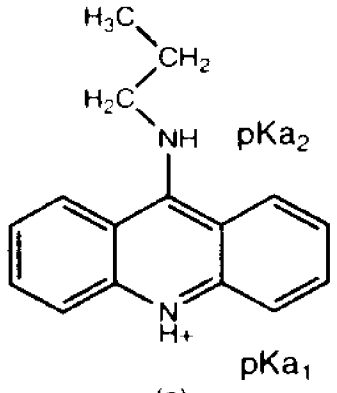
H3C
CH2
H2C
NH
pKa2
N
H+
pKa1

(a)

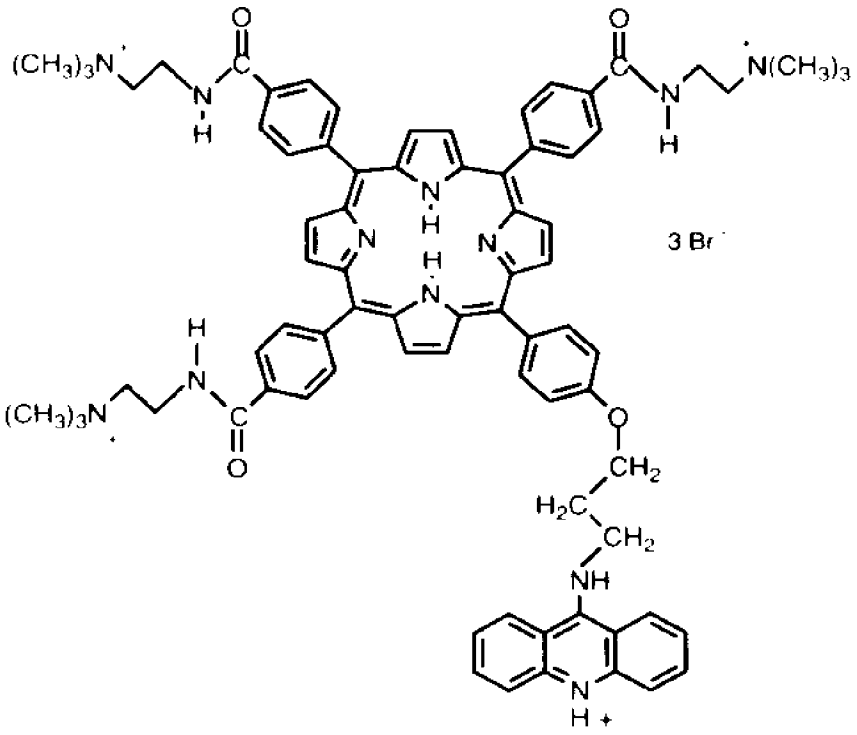
(CH3)3N
O
N
H
N(CH3)3
3 Br
(CH3)3N
O
CH2
H2C
CH2
NH
N
H +

(b)

3.3.1 Circular Dichroism Spectra of The Porphyrin-DNA Complexes.

Figures 3-6 and 3-7 show the CD spectra obtained when TAP and ATB, respectively, are in the presence of poly(dA-dT).(dA-dT), calf thymus DNA (CTDNA) and poly(dG-dC).(dG-dC). The drug /base-pair ratio (r_o) was 0.004 and the porphyrin concentration was 1 μM. Buffer composition was 0.1 M NaCl, 26 mM NaH_2PO_4 /$NaHPO_2$ and 1 mM EDTA, pH = 7.2.

The CD spectra of TAP with poly(dG-dC).(dG-dC) shows a pronounced negative band with a maximum at 425 nm while that of poly(dA-dT).(dA-dT) contains two positive bands with maxima at 418 and 449 nm; the latter is the greatest in amplitude of the two. In the case of calf thymus DNA, there is a negative and a positive band in the Soret region. These bands overlap, with maxima at 429 and 442 nm respectively; they indicate that in calf thymus DNA there is interaction with both GC and AT sites.

The conjugate, on the other hand, yields CD spectra with calf thymus DNA, poly(dG-dC).(dG-dC) and poly(dA-dT).(dA-dT) that are markedly similar. The spectrum of poly(dG-dC).(dG-dC) yields adjacent negative and positive CD bands centered at 405 and 433 nm respectively. The spectrum of poly(dA-dT).(dA-dT) also contains bands centered at the same wavelengths, although the amplitudes are greater. The spectrum of ATB with CTDNA shows a similar negative and a positive band of much smaller amplitude; one of the bands is shifted to longer wavelength-450 nm instead of 433 nm.

Figure 3-6: The circular dichroism spectrum of TAP in the presence of (A) poly(dG-dC).(dG-dC) (B) poly(dA-dT).(dA-dT) and (c) calf thymus DNA. The porphyrin concentration was 1 μM and the DNA concentration was 264 μM. The buffer consisted of 0.1 M NaCl, 26 mM NaH_2PO_4 and 1 mM EDTA, pH = 7.2.

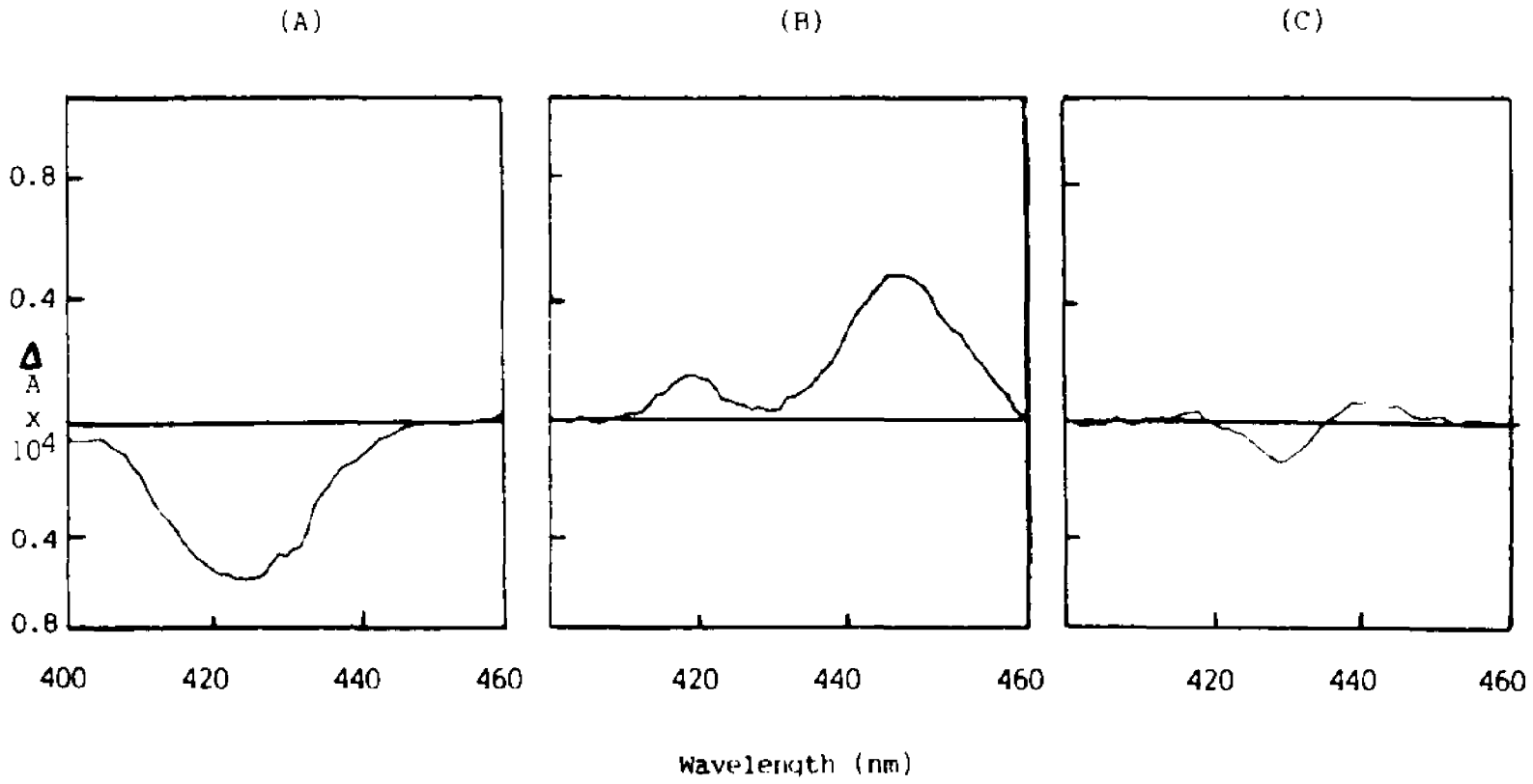
(A)
(B)
(C)
0.8
0.4
Δ
A
x
10⁴
0.4
0.8
400
420
440
460
420
440
460
420
440
460
Wavelength (nm)

Figure 3-7: The circular dichroism spectrum of ATB in the presence of (A) poly(dA-dT).(dA-dT) (B) calf thymus DNA and (C) poly(dG-dC).(dG-dC). The porphyrin concentration was 1 μM and the DNA concentration was 264 μM. The buffer was composed of 0.1 M NaCl, 26 mM NaH_2PO_4 and 1 mM EDTA, pH = 7.2.

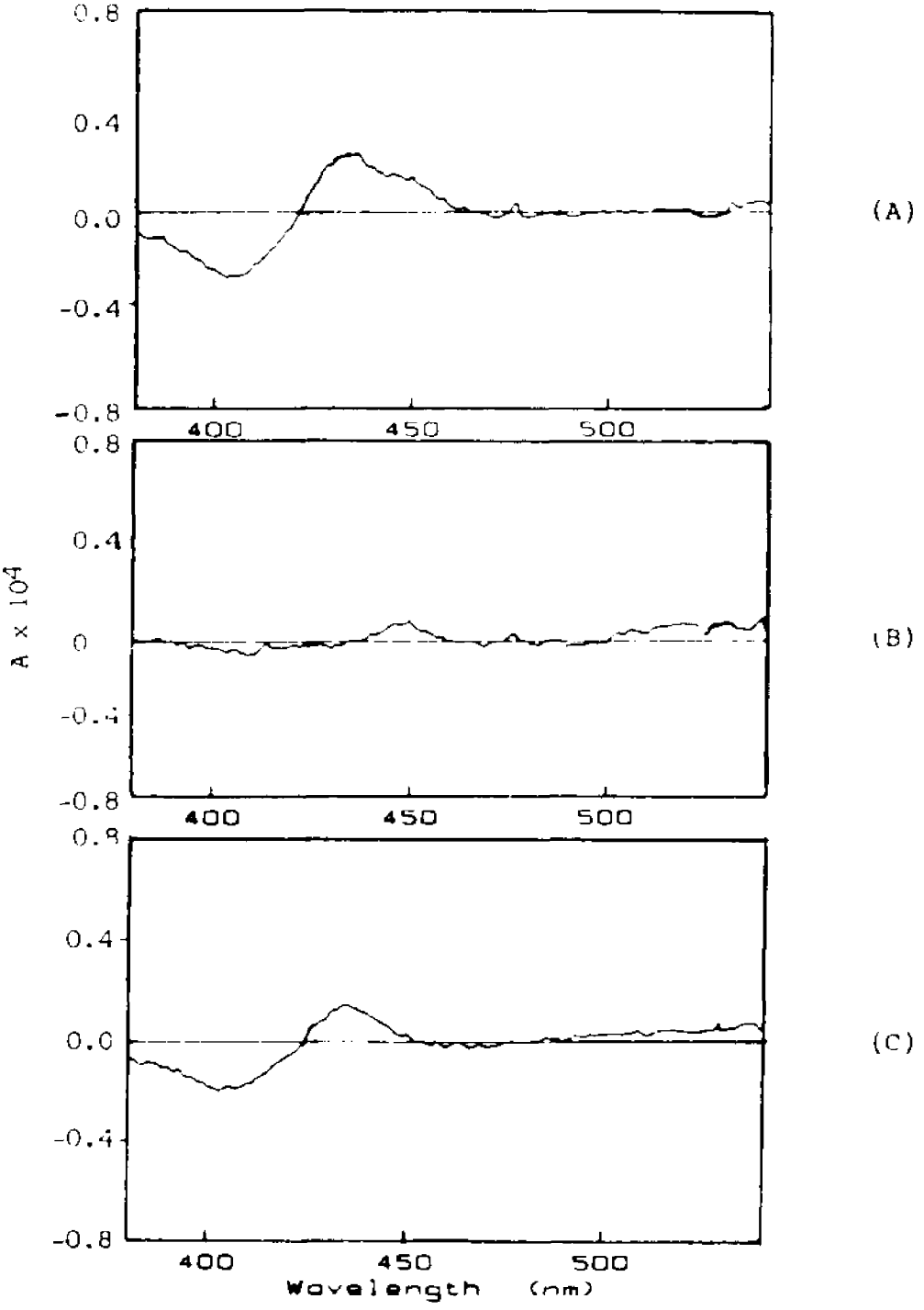
0.8
0.4
0.0
-0.4
-0.8
400
450
500
(A)
0.8
0.4
0
-0.4
-0.8
400
450
500
(B)
A x 10⁴
0.8
0.4
0.0
-0.4
-0.8
400
450
500
(C)
Wavelength (nm)

These results could be due to dipole-dipole interaction between electric dipole-allowed transitions in electronically isolated, degenerate chromophores (degenerate chromophores have absorbance maxima at the same wavelength) with a chiral orientation relative to each other (porphyrin and acridine). This would produce an "exciton couplet". The results could also be due to a different mode of interaction of the porphyrin chromophore with the nucleic acids. However, when the extinction coefficient of the porphyrin meso-[tetra(4-[N-(trimethylammoniumethyl)]benzamidyl)]porphine (TAP) and of 9-(propylamino)-acridine are compared, such dipole-dipole interaction is improbable. Using TAP as the model for the porphyrin macrocycle of the porphyrin-acridine conjugate, and 9-(propylamino) -acridine as an analogue for the acridine moiety, this becomes apparent. The extinction coefficient for TAP is 2.11 x 10^5 M^{-1} cm^{-1} at the Soret maximum, while that for 9-(propylamino)-acridine, also at 414 nm, is 8.20 x 10^3 M^{-1} cm^{-1} at, the ratio of the extinction coefficient for TAP/the extinction coefficient (E_o) for 9-(propylamino)-acridine is 25.7 (spectra shown in Figure 3-2). This number indicates that the acridine moiety is too weak an oscillator to significantly influence the absorbance properties and hence the CD spectrum of the porphyrin. Normally, such dipole-dipole interactions occur at an E_o value of 1 (e.g. between identical drug molecules bound on DNA).

The CD spectra of the conjugate therefore reveal the interactions of the porphyrin macrocycle of the conjugate. The

existence of similar negative and positive bands in the CD spectra of the conjugate indicates that the conjugate is capable of interaction with both GC and AT base pairs in a mode that is not observed with TAP. This new mode of interaction may be caused by the presence of the acridine moiety.

3.3.2 Absorption Spectra of the Porphyrin-DNA Complexes.

Figure 3-8 illustrates the red shifts and changes in the intensity of the Soret band that occur when the optical density spectrum of meso-[tetra(4-[N-(trimethylammoniumethyl)]-benzamidyl)]porphine (TAP) is scanned in the absence and then in the presence of the three types of DNA, using the same buffer and concentrations as in the CD work. Also, as in the CD experiments, due to the large difference in extinction coefficient between porphyrin and acridine chromophores (the porphyrin absorbs, at 414 nm, 25.7 times more than the acridine) the interactions of the porphyrin chromophore are, in essence, been probed.

In the presence of poly(dA-dT).(dA-dT), the Soret band normally found at 414 nm was displaced to 422 nm, a shift of 8 nm, with a hyperchromic change in absorbance. Change in absorbance (C) was defined as:

$$C = [(A_2 - A_1)/A_1] \times 100\ \% \qquad (II)$$

where A_1 = maximum absorbance of the Soret band in the absence of DNA and A_2 = maximum absorbance of the Soret band in the

Figure 3-8: The absorbance spectrum of TAP in the absence (solid line) and presence (dashed line) of (A) poly(dA-dT) .(dA-dT) (B) calf thymus DNA and (C) poly(dG-dC).(dG-dC). The porphyrin and the DNA concentrations were 1 and 264 μM, respectively. The buffer was composed of 0.1 M NaCl, 26 mM NaH_2PO_4 and 1 mM EDTA, pH = 7.2.

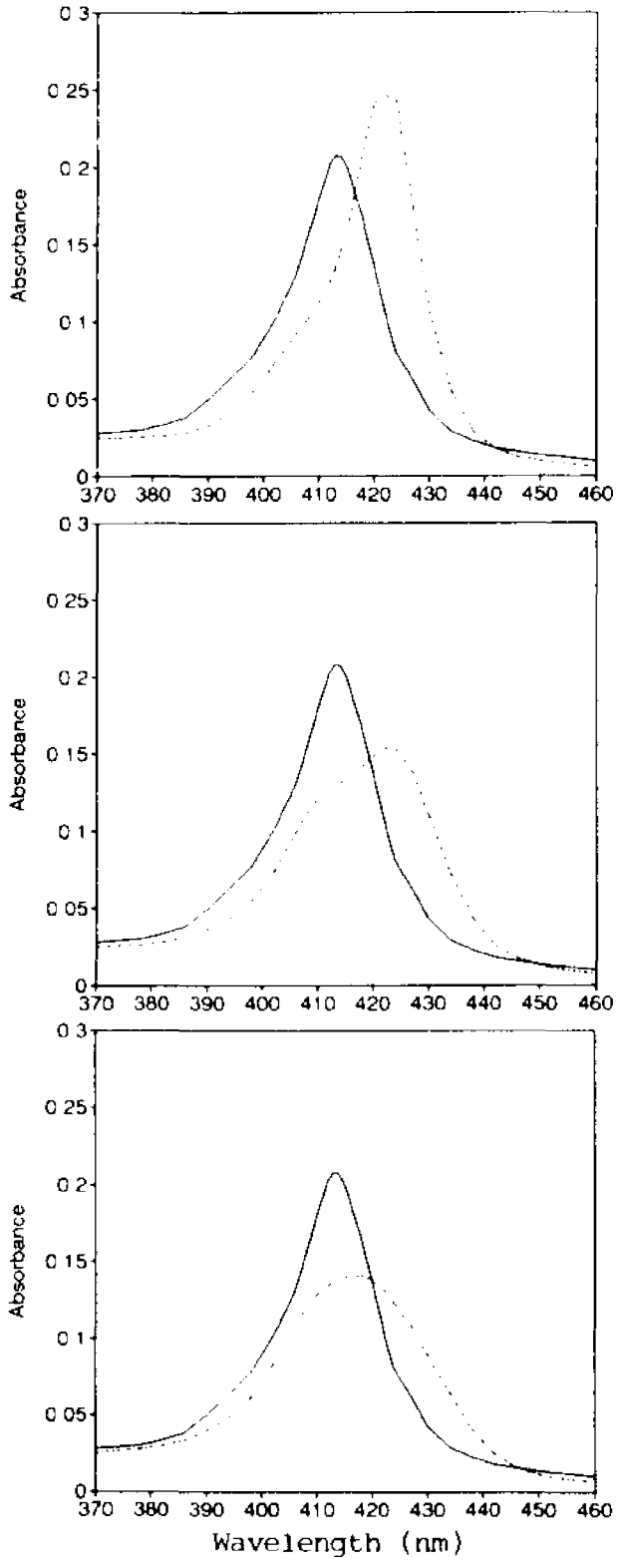
Absorbance
0.3
0.25
0.2
0.15
0.1
0.05
0
370 380 390 400 410 420 430 440 450 460
(A)
Absorbance
0.3
0.25
0.2
0.15
0.1
0.05
0
370 380 390 400 410 420 430 440 450 460
(B)
Absorbance
0.3
0.25
0.2
0.15
0.1
0.05
0
370 380 390 400 410 420 430 440 450 460
(C)
Wavelength (nm)

presence of DNA. The value for TAP and poly(dA-dT).(dA-dT) was 11.4 %.

For poly(dG-dC).(dG-dC) and TAP, there was also a red shift of the Soret band, but to 418 nm, a change of 4 nm. The noteworthy feature of this spectrum was the -37.8 % change in Soret band intensity, a marked hypochromic effect. With calf-thymus DNA the Soret produced a maximum absorbance at 423 nm, a change of 9 nm and a large, hypochromic -31.9 % change in the Soret intensity.

An examination of the spectrum of the TAP/calf thymus DNA complex shows that the band is produced by a combination of binding modes. The marked hypochromicity is significantly similar to that produced by the TAP/poly(dG-dC).(dG-dC) complex (-37.8 and -31.9 %, respectively), but the shift to longer wavelength is more like that observed with the TAP/poly(dA-dT).(dA-dT) complex (9 and 8 nm respectively). Therefore, with calf thymus DNA, binding to both GC and AT sites occurs; the hyperchromic effect with AT binding sites is consistent with groove binding and the markedly hypochromic effect with GC sites is consistent with intercalation into GC-rich sites.

The absorption spectra of the conjugate, 5-[4-(N-[9-acridinyl]-3-aminopropoxy)phenyl]-10,15,20-tri[4-(N-[trimethylammoniumethyl])benzamidyl]porphine (ATB) varied in the presence of the three types of DNA to a smaller extent (see Figure 3-9). The complex formed with poly(dG-dC).(dG-dC) possessed an absorbance maximum that was shifted to longer wavelength, from 415 nm to 420 nm, a 5 nm shift. The change in absorbance was

Figure 3-9:The absorbance spectrum of ATB in the absence (solid line) and presence (dashed line) of (A) poly(dA-dT).(dA-dT) (B) calf thymus DNA and (C) poly(dG-dC).(dG-dC). The porphyrin and the DNA concentrations were 1 and 264 μM, respectively. The buffer consisted of 0.1 M NaCl, 26 mM NaH_2PO_4 and 1 mM EDTA, pH = 7.2.

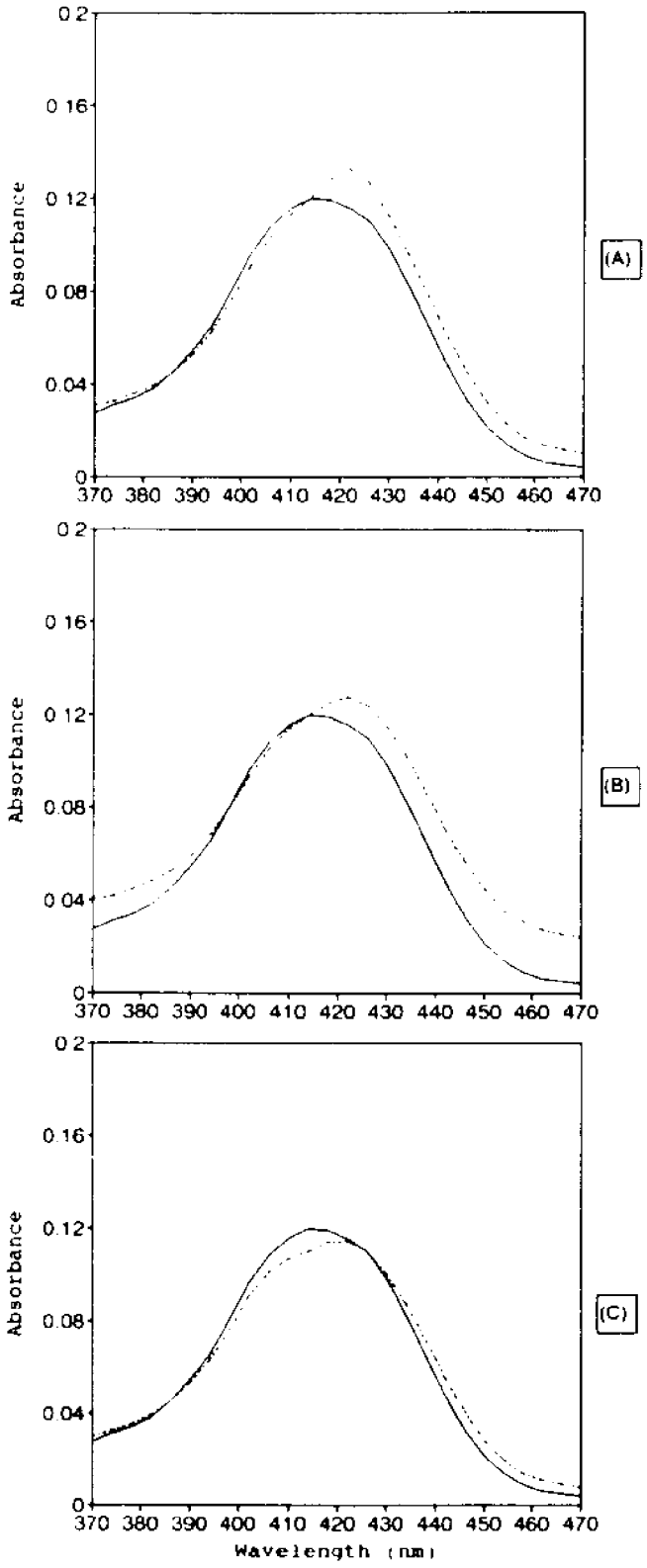
0.2
0.16
0.12
0.08
0.04
0
Absorbance
370 380 390 400 410 420 430 440 450 460 470
(A)
(B)
(C)
Wavelength (nm)

8.85 %, a small hypochromic effect. For poly(dA-dT).(dA-dT), the shift was from 415 nm to 421 nm, a 6nm difference. Of significance, the change in absorbance was 10.6 %, which is similar to that obtained with this kind of DNA and TAP (11.4 %). For calf thymus DNA, the red shift was from 422 to 415 nm, a difference of 7 nm; the change in absorbance was a hyperchromic 6.33 %.

These data, summarized in Table 3-A, indicate that the porphyrin moiety of the conjugate does not intercalate. The small hypochromicity observed when the conjugate is in the presence of GC base pairs alone (-8.85 % change in optical density) is by no means close to the -31.8 % obtained when TAP (without acridine) interacts with GC base pairs. In addition, a hyperchromic change in absorbance is observed when the porphyrin-acridine conjugate is in the presence of poly (dA-dT) .(dA-dT) (10.6 %) and calf thymus DNA (6.33 %). The similarity of the former value to that obtained with TAP and poly(dA-dT) .(dA-dT) (11.4 %) implies that the porphyrin macrocycle of the conjugate is not intercalated into the nucleic acid. This mode of binding is also obtained with calf thymus DNA and poly(dG-dC).(dG-dC).

The optical density data gives no indication that the conjugate is able to intercalate into DNA, whereas the porphyrin without the acridine (TAP) has provided evidence that it intercalates. This may be due to the larger bulk of the conjugate as compared to TAP.

Table 3-A

Absorbance Maxima For TAP/ATB - DNA Complexes

	TAP		ATB	
	Wmax	Amax (Δ A)	Wmax	Amax (Δ A)
Nucleic Acid				
None	414	.207 (0%)	415	.120 (0%)
Poly(dG-dC)$_2$	418	.141 (-32%)	420	.115 (-4.16%)
CTDNA	423	.154 (-25.5%)	420	.128 (6.33%)
Poly(dA-dT)$_2$	422	.253 (21.8%)	421	.133 (10.6%)

Wmax = Wavelength of maximum absorbance (nm)
Amax = Maximum absorbance
Δ A = Change in absorbance
CTDNA = Calf thymus DNA

3.3.3 The Fluorescence Emission Spectra of the Porphyrin-DNA Complexes.

Buffer composition and porphyrin and DNA concentrations in the fluorescence experiments were the same as in the CD and the absorbance experiments. Solutions of meso-[tetra(4-[N-(trimethylammoniumethyl)]benzamidyl)]porphine and the conjugate 5-[4-(N-[9-acridinyl]-3-aminopropoxy)phenyl]-10,15,20-tri-[4-(N-[trimethylammoniumethyl])benzamidyl]porphine (ATB) as well as their nucleic acid complexes were irradiated at 414 nm and the emission spectra scanned from 200 to 800 nm. The spectra are reproduced in Figures 3-10 (TAP) and 3-11 (ATB).

Tables 3-B and 3-C are listings of the position and intensity of fluorescence emission band maxima, as well as the changes seen in the characteristics of these maxima.

The data indicate that TAP interacts with poly(dG-dC)-(dG-dC) and poly(dA-dT).(dA-dT) in different ways. The hypochromicity of poly(dG-dC).(dG-dC) is large while that of poly-(dA-dT).(dA-dT) is small. Calf thymus DNA is intermediate in its hypochromicity when compared to these two types of DNA. However, the red shift of calf thymus DNA is more like that of poly(dG-dC).(dG-dC). These data indicate a preference for GC rich sites on the natural DNA, but also that binding is occuring at both AT and GC rich sites.

The spectra for the ATB complexes were remarkably different from those for TAP. The synthetic polynucleotide complexes had similar hypochromicities, while calf thymus DNA had slightly less. There were almost no red shifts. The spectra

Figure 3-10: The fluorescence emission spectrum of TAP in the absence (thin line) and in the presence (thicker line) of (A) poly(dA-dT).(dA-dT) (B) calf thymus DNA (C) poly(dG-dC).(dG-dC). The porphyrin concentration was 1 μM and the DNA concentration was 264 μM. Buffer composition was 0.1 M NaCl, 26 mM NaH_2PO_4 and 1 mM EDTA; pH = 7.2. Excitation was at 414 nm.

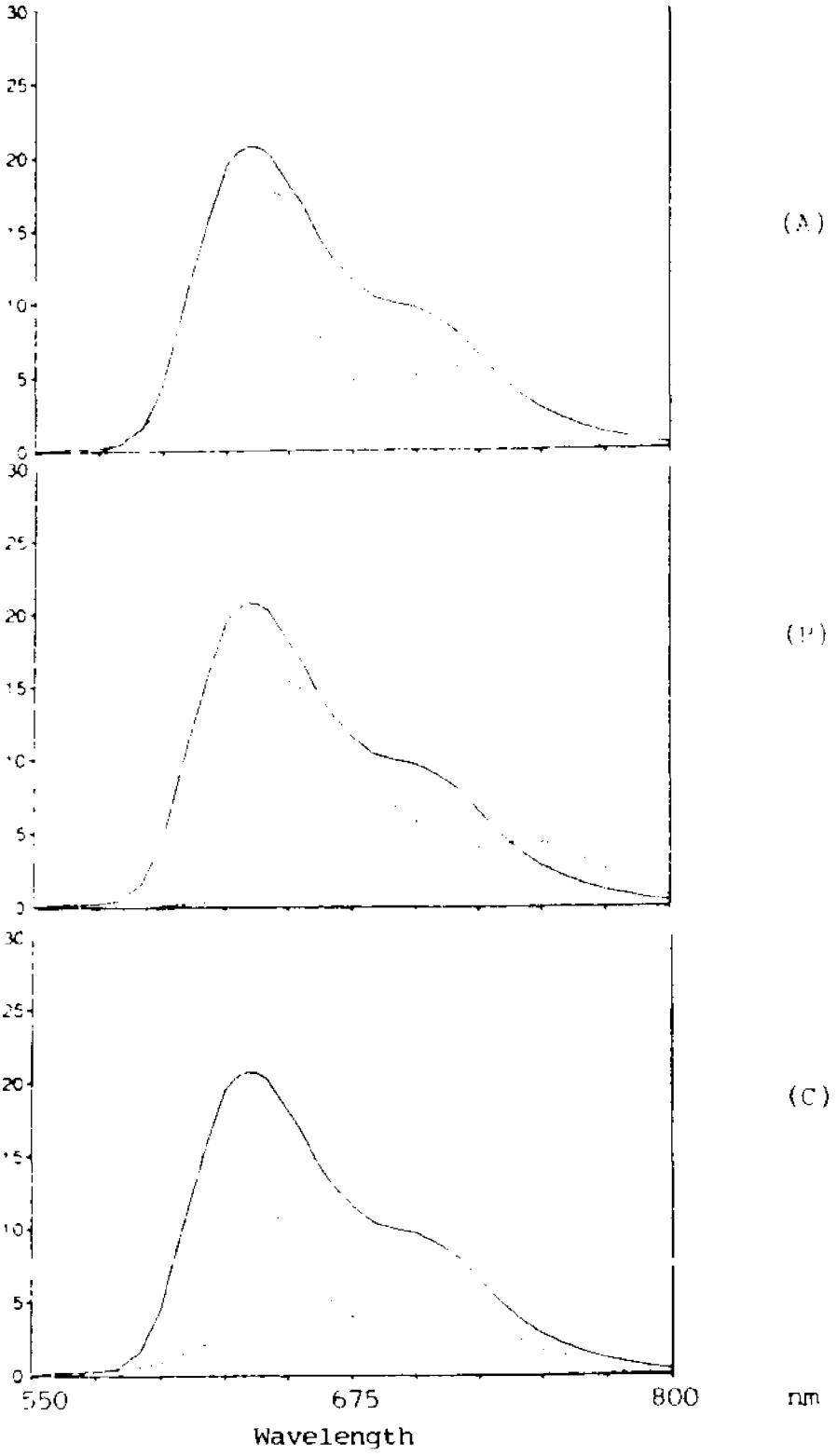
30
25
20
15
10
5
0
(A)
(B)
(C)
550
675
800
nm
Wavelength

Figure 3-11: The fluorescence emission spectrum of ATB in the absence (solid line) and in the presence (dotted line) of (A) poly(dA-dT).(dA-dT) (B) calf thymus DNA and (C) poly(dG-dC).(dG-dC). The buffer was composed of 0.1 M NaCl, 26 mM NaH_2PO_4 and 1 mM EDTA, pH = 7.2. The porphyrin and DNA concentrations were 1 and 264 μM, respectively. Excitation was at 414 nm.

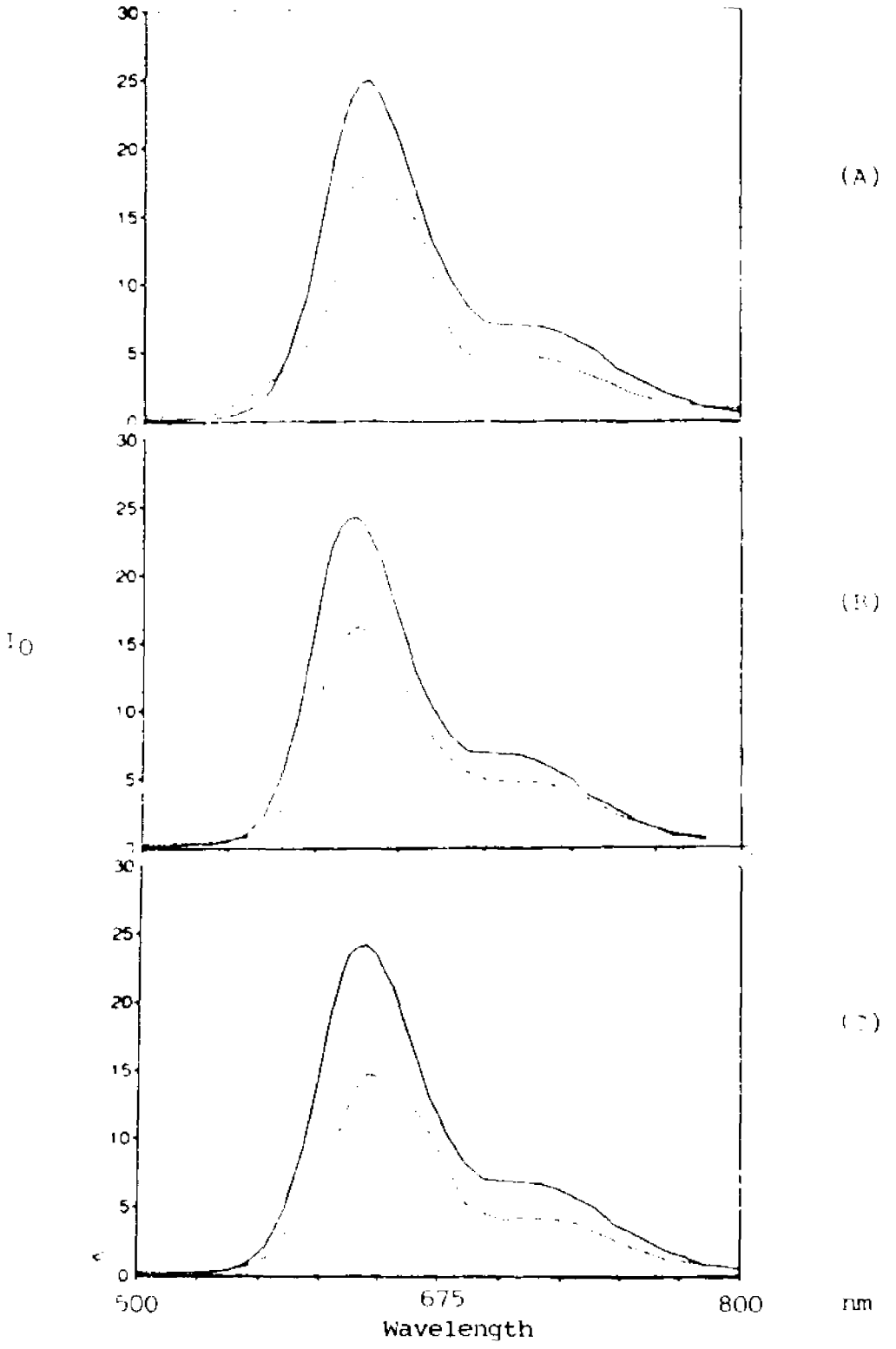
30
25
20
15
10
5
0
(A)
(B)
(C)
I0
500
675
800
nm
Wavelength

Table 3-B

Fluorescence Maxima For TAP-DNA Complexes

	W_1	I_1	ΔI_1	W_2
Nucleic Acid				
None	644	21.0	-	681
Poly(dG-dC)$_2$	656	11.5	-45.2%	713
CTDNA	658	15.4	-26.7%	749
Poly(dA-dT)$_2$	649	17.8	-15.2%	713

W_1 = Wavelength of maximum intensity
I_1 = Maximum intensity
ΔI_1 = Change in intensity
W_2 = Wavelength of secondary maximum
CTDNA = calf thymus DNA

Table 3-C

Fluorescence Maxima For ATB-DNA Complexes

Nucleic Acid	W_1	I_1	ΔI_1	W_2
None	657	24.8	-	687
Poly(dG-dC)$_2$	659	15.2	-38.7%	690
CTDNA	659	17.8	-28.2%	690
Poly(dA-dT)$_2$	656	16.2	-34.7%	711

W_1 = Wavelength of maximum intensity
I_1 = Maximum intensity
ΔI_1 = Change in intensity
W_2 = Wavelength of secondary maximum
CTDNA = calf thymus DNA

indicate that the mode of interaction in all three cases are very similar, with no distinct preference for GC or AT rich areas on calf thymus DNA. The data are consistent with the CD, and to a lesser extent, with the absorbance results. The porphyrin no longer distinguishes between different kinds of DNA as before (as in the case of TAP); this is the effect of the acridine and may be an effect caused by the size of the conjugate or by the binding mode of the conjugate (possibly by intercalation at the acridine).

The fluorescence emission spectra of the acridine are seen as a small shoulder located at a slightly longer wavelength relative to the band produced by light-scattering at the wavelength of excitation (Figure 3-12). It is noteworthy that a similar situation occurs with 9-(propylamino)-acridine. The band produced by light-scattering makes the solicitation of data on the acridine from these spectra impossible. Instead, information on acridine intercalation as the mode of interaction of the conjugate may be obtained from the equilibrium binding data discussed in chapter four.

Figure 3-12: The shoulder observed (indicated by arrow) in the fluorescence emission spectrum of the acridine-porphyrin conjugate in the presence of calf thymus DNA. Excitation was at 414 nm. The porphyrin concentration was 1 μM and the DNA concentration was 264 μM. The buffer consisted of 0.1 M NaCl, 26 mM NaH_2PO_4 and 1 mM EDTA, pH = 7.2.

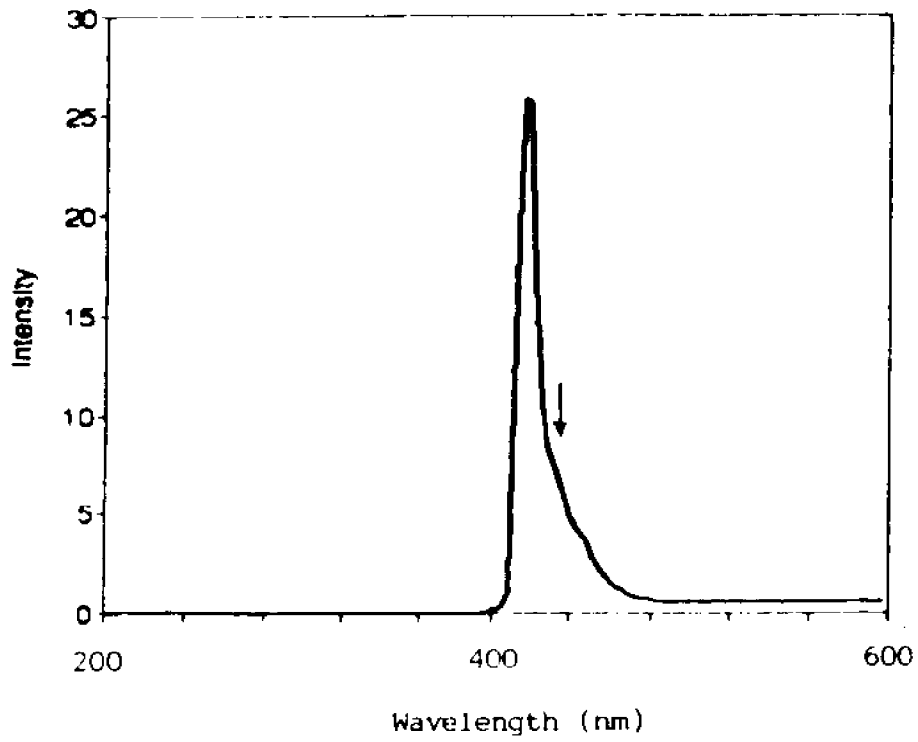
30
25
20
15
10
5
0
Intensity
200
400
600
Wavelength (nm)

Chapter Four

Affinity Constants for Porphyrin-DNA Binding

4.1 Introduction

The determination of affinity constants for porphyrin-nucleic acid binding is of great importance in the application of these ligands as probes of nucleic acid structure and dynamics and also in the possible use of these molecules as potent DNA alkylators. It is necessary to know what base sequences or types of DNA the porphyrin has a preference for binding to, the strength of the binding and also what structural factors enhance or diminish binding.

A variety of factors should be considered in order to select a method that will accurately provide affinity constants for the binding of this class of heterocyclic drug to DNA. The use of UV-visible titration is severely limited, it is difficult to accurately determine the extinction coefficient of porphyrin bound to nucleic acid (1,2); in addition, the Soret band of a porphyrin is greatly modified usually when only intercalation occurs (3,4,5).

Equilibrium dialysis has also been used to measure equilibrium constants for porphyrin binding (6,7); in order to do so, it is necessary to incubate the porphyrin solution in the dialysis chamber for a few days. During this period, precipitation of the porphyrin may be observed or there may be adsorption to the walls of the dialysis chamber; the DNA may also be degraded because the DNA solution is incubated at 25^0C

during this time. The occurrence of the first two events is primarily controlled by the solubility properties of the porphyrin.

Binding analyses carried out by the direct fluorescence quenching method or the UV-visible titration method, would be complicated by the possible binding of the conjugate to DNA only at the acridine moiety, for which it would be difficult to measure changes in fluorescence intensity (Chapter Three).

By contrast, measurement of apparent affinity constants by the ethidium bromide competitive binding method does not depend on the mode of binding of the porphyrin or the conjugate and does not require the time necessary for the equilibrium dialysis method. The proportional decrease of the magnitude of the affinity constant for ethidium bromide intercalation into DNA as the concentration of an inhibitor of that binding increases, is used to obtain the affinity constant for the inhibitor according to the classical method of LePecq and Paoletti (8). A plot of the reciprocal of the ethidium bromide affinity constant versus the concentration of inhibitor (here, a porphyrin or the acridine-porphyrin conjugate) produces a straight line from whose slope the equilibrium constant of the inhibitor can be obtained as indicated by equation (I).

$$\frac{1}{K_{EB'}} = \frac{K_{por}\ (Por)}{K_{EB}} \qquad (I)$$

In equation (I), $K_{EB'}$ = the affinity constant of ethidium bromide in the presence of porphyrin, K_{EB} = the affinity constant of ethidium bromide in the absence of porphyrin, K_{por} = the affinity constant of porphyrin and (Por) = the concentration of porphyrin. The ethidium bromide affinity constant is obtained by the construction of a Scatchard plot (9); the concentration of bound ethidium bromide is determined by the use of spectrofluorometry according to Lepecq and Paoletti (8) (see reference (8) for the derivation of an equation yielding this quantity).

One of the first uses of the ethidium bromide competitive binding technique was to determine affinity constants for the binding of quinacrine, a trypanocidal acridine, to calf thymus DNA (8) and since then, it has become a standard method in nucleic acid chemistry (e.g. to determine the affinity constants for the binding of a series of acridine-purine and acridine-pyrimidine conjugates to DNA (10)). This method has also been used to examine the binding of the porphyrins meso-[tetra-(aminomethylphenyl)]porphyrin (TAMPP) (11) and meso-[tetra(4-N-methylpyridyl)]porphine (TMPyP) (12), and some of their metal ion complexes. The independence of this method from the mode of binding of the porphyrin has enabled Sari and collaborators to examine the magnitude of binding to calf thymus DNA as a function of charge and structure for several porphyrins and metalloporphyrins (13). Sari demonstrated that for a given symmetrical tetracationic porphyrin such as TMPyP (Figure 4-1), the ability to bind to calf thymus DNA decreased as the

total number of charges were decreased. In addition, shifting the positive charges from the para to the meta and then to the ortho positions, resulted in a decrease in the affinity constant (holding the total number of charges constant for the three isomers). It would therefore be expected that the conjugate which has four positive charges should experience no decrease in affinity constant, when compared to its tetracationic analogue that has no acridine, if the charge and its position alone determines magnitude of binding. Any decrease or increase in affinity constant would thus be due to steric factors or a new mode of binding.

The results obtained by Sari for meso-[tetra(4-N-methylpyridyl)]porphine (TMPyP) and its meta isomer (Figure 4-1) are similar to those determined by Fiel (14) and Dougherty (15) using UV-visible spectrophotometry. This chapter describes the methods used to obtain affinity constants for meso-[tetra(4-[N-(trimethylammoniumethyl)]benzamidyl)]porphine (TAP) and the acridine-porphyrin conjugate, 5-[4-(N-[9-acridinyl]-3-aminopropoxy)phenyl]-10,15,20-tri[4-(N-[trimethylammoniumethyl])-benzamidyl]porphine (ATB), as they interact with poly(dG-dC).(dG-dC), poly(dA-dT).(dA-dT) and calf thymus DNA in buffer at pH 7.2 and composed of 0.1 M NaCl, 26 mM sodium phosphate and 1 mM EDTA.

The results will be discussed with regard to the findings of the spectroscopic studies and with regard to possible modes of binding of ATB to the polynucleotides.

Figure 4-1: Isomers of meso-[tetra(4-N-methylpyridyl)porphine (TMPyP).

Para Isomer

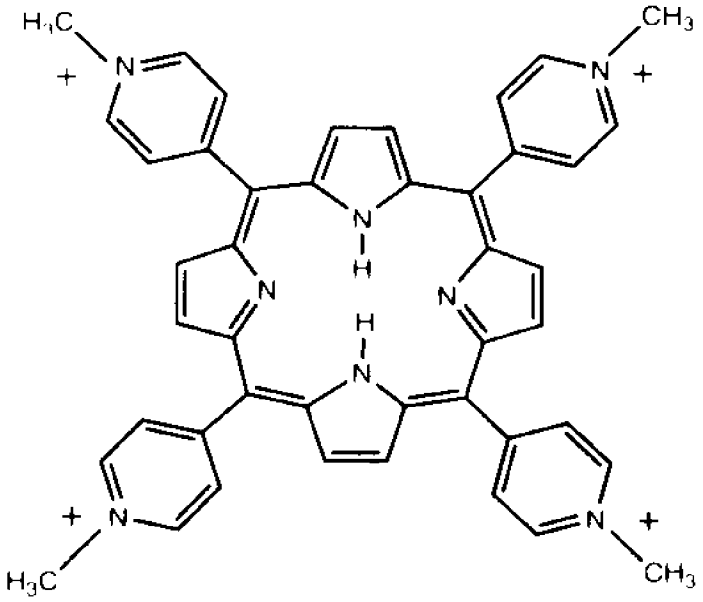

Meso Substituent

Meta Isomer

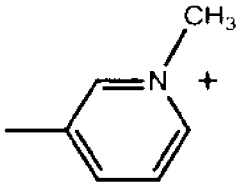

Ortho Isomer

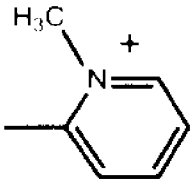

4.2 Materials and Methods

Reagents and instruments for the fluorometric determination of affinity constants were the same as those used in the CD, UV-Visible and fluorescence spectroscopic work (section 3-2), but with the following additions: ethidium bromide was purchased from Aldrich Chemical Company; silica fluorescence cells with a range of 300 - 700 nm were used for intensity measurements; the wavelength of excitation was 520 nm and that of emission was set at 600 nm. The temperature was held constant at 25^{0}C.

Determination of the affinity binding constant for ethidium bromide (EB) binding to a polynucleotide (either calf thymus DNA, poly(dG-dC).(dG-dC) or poly(dA-dT).(dA-dT)) was performed as follows: 30 μL of EB stock solution was added to 2 mL of plain buffer in a cuvette. The fluorescence intensity was read using the previously listed excitation and emission wavelengths. 10 μL aliquots were then added until the total volume of added EB was 120 μL.

The titration was repeated with the buffer containing DNA and porphyrin (or no porphyrin), but with the total volume kept at 2 mL and all other conditions the same as before. The procedure was repeated with a total of eight different values of TAP concentration and seven values of conjugate (ATB) concentration for each of the three types of DNA.

In order to calculate the concentration of EB bound to DNA, it was necessary to determine K_t, the slope of a straight

line obtained when a plot of EB concentration versus fluorescence intensity is made for the titration of EB into plain buffer. It was also necessary to obtain K_b, the slope of the straight-line obtained when a similar titration of EB into buffer is carried out, but with DNA present at a concentration greater than or equal to 100 times the maximum EB concentration in the cuvette. The ratio K_b/K_f defines the value v which is necessary to calculate the concentration of ethidium bromide bound to DNA, given by equation (II):

$$EBb = \frac{I_t - I_o}{(v - 1)K_f} \qquad \text{(II)}$$

Where I_t = the EB fluorescence intensity in the presence of DNA and porphyrin and I_o = the EB fluorescence intensity of EB in plain buffer. A Scatchard plot is then constructed by plotting r/c vs. r, where r = EBb/total DNA concentration and c = the concentration of free (unbound) EB. The slope of such a plot is the negative value of the affinity constant.

Competition occurs when there is a proportional decrease of the magnitude of the slope of the Scatchard plot (EB affinity constant decreasing) as the concentration of competitor (here TAP or the conjugate) is increased (in separate titrations).

DNA and porphyrin concentrations were determined by the use of spectrophotometry as previously described (section 3-2). Computations associated with these plots are reported in the Appendix (A-1). A typical Scatchard plot is illustrated in

Figure 4-2, the computations necessary to obtain it are shown in Table 4-2(a).

A modification was made in the computation of the Scatchard plots in order to account for the negative cooperativity encountered when EB binds to DNA; the concentration of free EB (c) which is used to calculate r/c, was replaced with the total concentration of ethidium bromide (bound and free). This modification yields the minimum binding constant for ethidium bromide; use of the free EB concentration as c in r/c yields a curved plot that is caused by negative cooperative binding (Figure 4-3), replacement of the free EB concentration with the total concentration of EB gives a straight line that is a tangent to the curve. This straight line represents the lowest slope of the curve and hence the smallest equilibrium constant (Figure 4-3).

The addition of aliquots of ethidium bromide stock solution to the cuvettes containing DNA and porphyrin resulted in a small, gradual decline in the concentration of the porphyrin (see computations accompanying Figure 4-3). In the plots of the reciprocal of the EB binding constant vs. porphyrin concentration, the latter value was taken from the porphyrin concentration at the midpoint of the titration.

Figure 4-2: Scatchard plot for ethidium bromide binding to calf thymus DNA in the presence of TAP.

Scatchard Plot for EB Binding to DNA with TAP as Inhibitor.

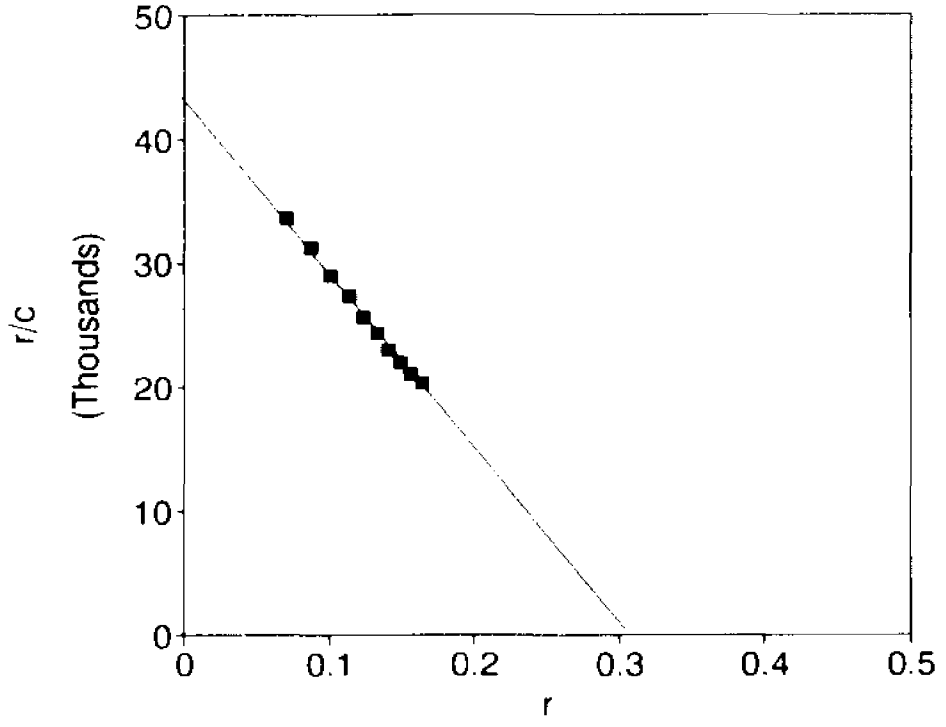

Table 4-2(a): Computations necessary to obtain Scatchard plot shown in Figure 4-2.

Veb = Volume of ethidium bromide (EB).
Io = Fluorescence intensity of EB in plain buffer.
It = Fluorescence Intensity of EB in the presence of DNA and porphyrin.
EBt = Total concentration (bound and unbound) of ethidium bromide.
DNAt = Total DNA concentration.
EBb = Concentration of EB bound to DNA.
PORt = Total (bound and unbound) concentration of porphyrin.

Veb	Io	It	EBt	DNAt	EBb	PORt	r	r/c
30	0.154	0.59	2.11E-06	4.45E-06	3.15E-07	4.67E-07	0.070915	33556.55
40	0.205	0.74	2.8E-06	4.43E-06	3.87E-07	4.65E-07	0.087446	31187.03
50	0.255	0.87	3.49E-06	4.4E-06	4.45E-07	4.63E-07	0.101015	28962.28
60	0.301	0.99	4.17E-06	4.38E-06	4.98E-07	4.6E-07	0.113721	27303.75
70	0.355	1.1	4.84E-06	4.36E-06	5.39E-07	4.58E-07	0.123561	25551.64
80	0.409	1.21	5.5E-06	4.34E-06	5.8E-07	4.56E-07	0.133491	24271.08
90	0.458	1.3	6.16E-06	4.32E-06	6.09E-07	4.54E-07	0.140998	22897.18
100	0.503	1.39	6.81E-06	4.3E-06	6.42E-07	4.52E-07	0.149245	21917.05
110	0.556	1.48	7.45E-06	4.28E-06	6.69E-07	4.5E-07	0.156211	20953.86
120	0.595	1.56	8.09E-06	4.26E-06	6.98E-07	4.47E-07	0.163915	20250.59

Regression Output:

Constant		44141.86
Std Err of Y Est		131.8822
R Squared		0.999181
No. of Observations		9
Degrees of Freedom		7
X Coefficient(s)	-149244	
Std Err of Coef.	1614.847	

Table 4-2(a)

Figure 4-3: Scatchard plots for ethidium bromide binding to calf thymus DNA; the curved line (triangles) is produced by negative cooperative binding; the straight line (squares) is obtained when the unbound ethidium bromide concentration is replaced by the total concentration (bound and unbound) of ethidium bromide in the scatchard equation and represents the minimum affinity constant obtainable from the curved plot.

Scatchard Plot for EB Binding to DNA with TAP as Inhibitor.

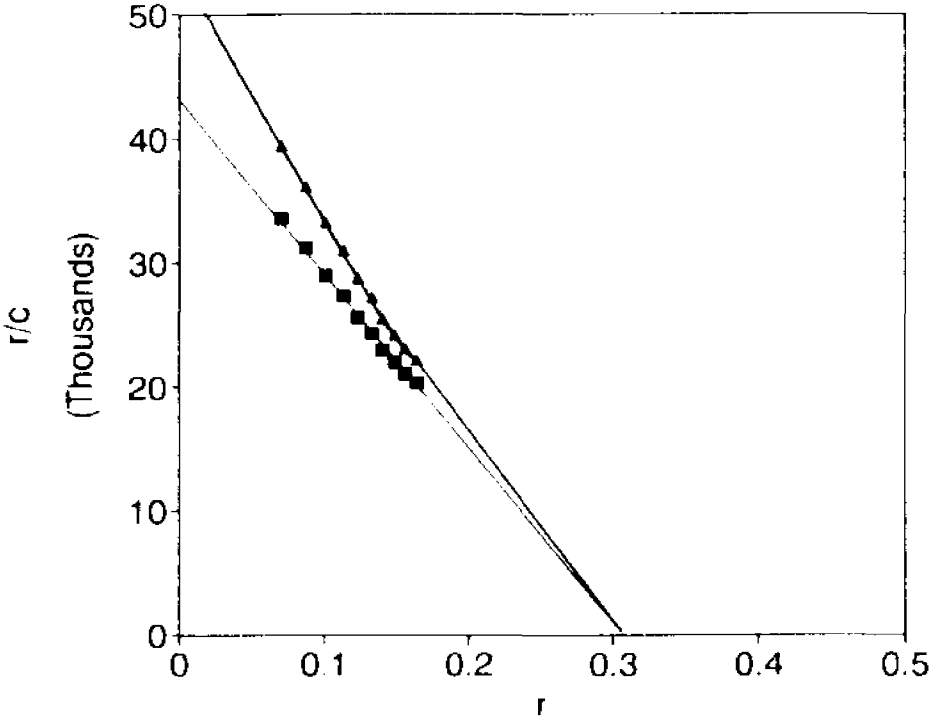

Results and discussion

Tables 4-A and 4-B list the affinity constants derived for meso-[tetra(4-[N-(trimethylammoniumethyl)benzamidyl])]-porphine (TAP) and the porphyrin-acridine conjugate, respectively, in 0.1 M NaCl, 26 mM sodium phosphate and 1 mM EDTA, pH = 7.2 as measured by the method of Lepecq and Paoletti (8).

An examination of Figure 4-4 shows that TAP binds to all three types of DNA with two types of binding: low (small slope) and high (large slope) affinity binding over the concentration of porphyrin indicated. It is possible that the high affinity binding represents a kind of saturative binding in which the ethidium bromide cannot displace any more porphyrin from the polynucleotide. This phenomenon clearly occurs above a (DNA)/(Porphyrin) ratio ($1/r_0$) of 8.72, 6.71 and 3.82 for poly(dA-dT).(dA-dT), calf thymus DNA and poly(dG-dC).(dG-dC) respectively. These values represent a much higher proportion of porphyrin/DNA than those used in the CD, UV-visible and fluorescence spectroscopic studies [(DNA)/(Porphyrin) ratio, $1/r_0$, = 264], the affinity constants for binding in the spectroscopic work may be therefore be extrapolated from the low affinity binding conditions (the Porphyrin concentration would be close to zero to obtain $1/r_0$ = 264 in the Scatchard analysis).

The low affinity binding is therefore of preferential interest and it is this that will be primarily referred to hereafter; the data clearly shows that TAP binds preferentially to AT base pair rich regions in DNA and rather weakly

Table 4-A

Affinity Constants *
For TAP Binding to DNA

DNA	K
pAT	1.00E+07
	3.40E+07
CT	2.40E+06
	8.20E+06
pGC	4.30E+05
	1.50E+06

*Affinity constants are for two types of binding: low affinity (1st number) and high affinity binding (2nd number).

pAT: Poly(dA-dT).(dA-dT)
pGC: Poly(dG-dC).(dG-dC)
CT: Calf Thymus DNA
K: Affinity Constant (M^{-1})

Table 4-B

Affinity Constants
for ATB Binding to DNA

DNA	K
pAT	3.20E+05
CT	1.40E+05
pGC	2.70E+05

pAT: Poly(dA-dT).(dA-dT)
pGC: Poly(dG-dC).(dG-dC)
CT: Calf Thymus DNA
K: Affinity Constant (M^{-1})

Figure 4-4: Plots of 1/slope (i.e. 1/affinity constant) vs. TAP concentration for ethidium bromide binding to DNA with TAP as inhibitor. All compounds and nucleic acids were dissolved in 0.1 M NaCl, 26 mM NaH_2PO_4 and 1 mM EDTA, pH = 7.2. The temperature of the cuvette was maintained at 25^0C. Concentrations of reagents and nucleic acids are reported in appendix A-1.

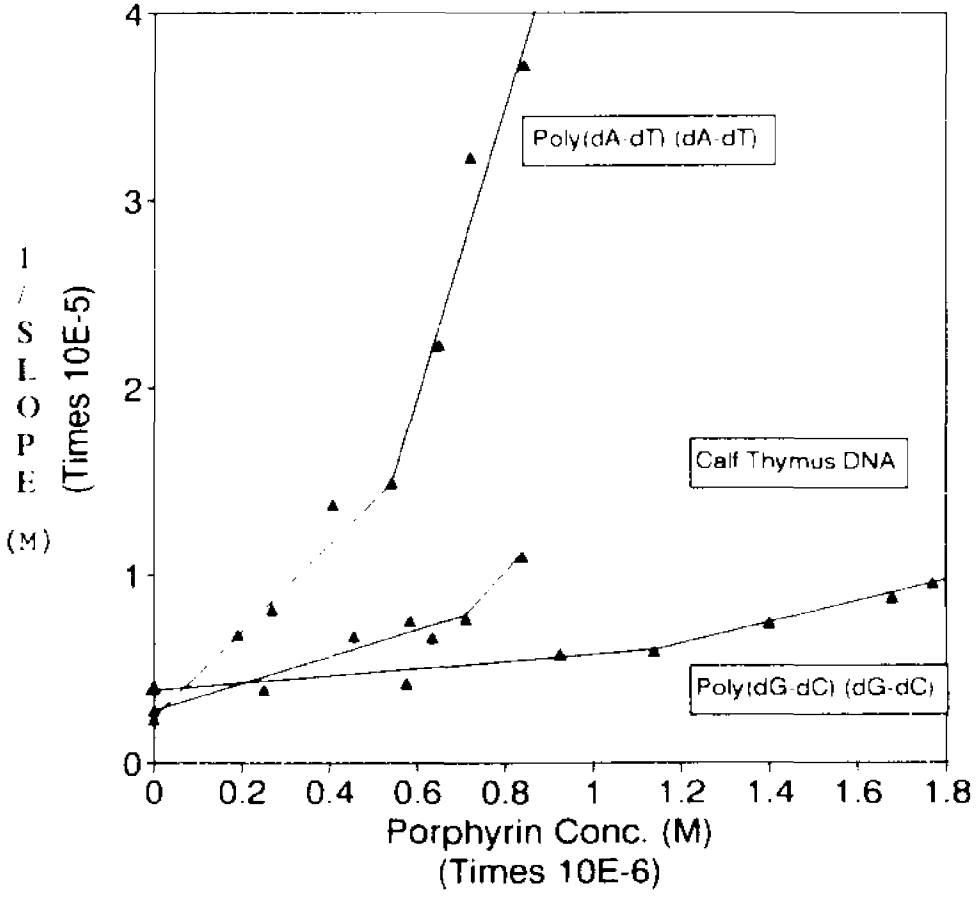
1 / SLOPE (M)
(Times 10E-5)
4
3
2
1
0
Poly(dA-dT) (dA-dT)
Calf Thymus DNA
Poly(dG-dC) (dG-dC)
0
0.2
0.4
0.6
0.8
1
1.2
1.4
1.6
1.8
Porphyrin Conc. (M)
(Times 10E-6)

Figures 4-5 and 4-6: Plots of 1/slope (i.e. 1/affinity constant) vs. ATB concentration for ethidium bromide binding to DNA with ATB as inhibitor. All compounds and nucleic acids were dissolved in 0.1 M NaCl, 26 mM NaH_2PO_4 and 1 mM EDTA, pH = 7.2. The temperature of the cuvette was maintained at 25^0C. Concentrations of reagents and nucleic acids are reported in appendix A-1.

Figure 4-5

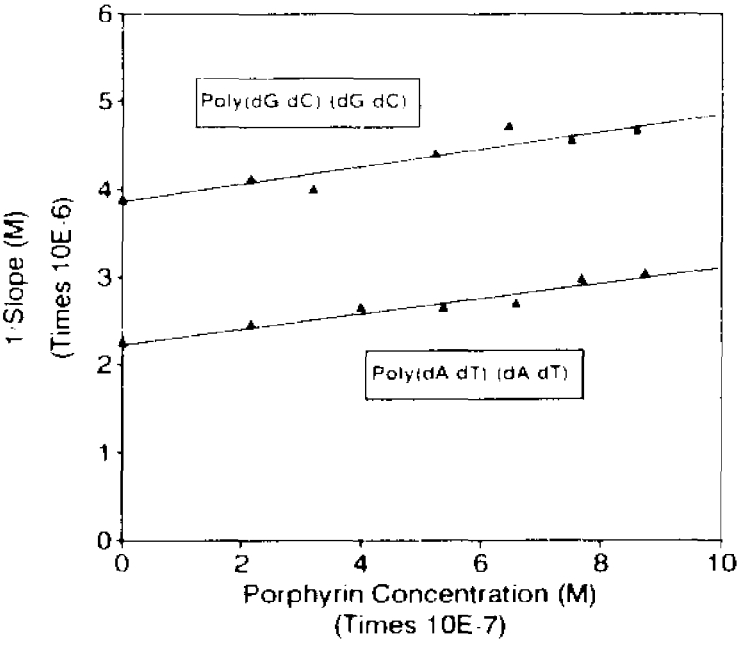

Figure 4-6

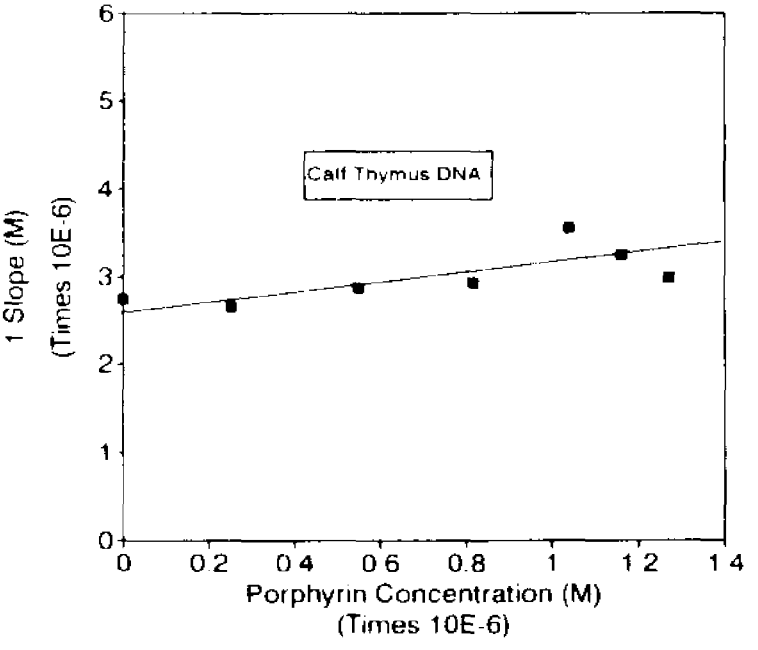

to GC rich areas (1×10^7 and 4.3×10^5 M^{-1}) respectively. Binding to calf thymus DNA is intermediate between these two values (2.4×10^6 M^{-1}).

The affinity constants for the binding of the conjugate to the three kinds of nucleic acid show no such variation at the porphyrin concentrations tested (up to 1 μM, $1/r_0$ as low as 4.36) (Figures 4-5 and 4-6). In addition, the magnitude of the constants have undergone a marked decrease (especially in the case of binding to poly(dA-dT).(dA-dT)) and are now 3.2×10^5, 1.4×10^5 and 2.7×10^5 M^{-1} for poly(dA-dT).(dA-dT), calf thymus DNA and poly(dG-dC) .(dG-dC). These figures indicate no preference for binding to one of the two base pairs, another significant difference between the conjugate and TAP. Appendix A-1 contains the data points for construction of the graphs in Figures 4-4, 4-5 and 4-6.

These results are, however, remarkably consistent with the UV-visible, CD and fluorescence results for the binding of the conjugate to the three kinds of nucleic acid, which gave nearly equivalent spectroscopic signatures for binding of the conjugate to the three kinds of DNA. It is noteworthy that the amplitudes of the CD bands for binding of the conjugate to poly(dA-dT).(dA-dT) and poly(dG-dC).(dG-dC) are nearly equal, while those for conjugate binding to calf thymus DNA are much weaker. These amplitudes represent the strength of the interaction and are consistent with the results obtained here.

The equilibrium constant data are therefore indicators that the binding of the conjugate is not directed by the por-

phyrin macrocycle, but is influenced by the acridine moiety toward modes that are similar or identical for all three types of nucleic acid studied.

Conclusion

The binding of 9-aminoacridines to DNA has been well defined (16,17); intercalation is the major mode of interaction of these flat, heterocyclic molecules. Intercalation of the acridine moiety of molecules analogous to the porphyrin-acridine conjugate, such as hemin-acridine and acodazole-hemin metallocomplexes has also being observed (18). The altered binding constants and spectroscopic data of the conjugate, as compared to the untethered porphyrin (TAP), matches the binding characteristics and expected spectroscopic properties of the conjugate if the acridine had intercalated between the base pairs of all three types of DNA and the porphyrin was projected outward from the intercalation site. 9-aminoacridine exhibits almost equal equilibrium constants for intercalation into poly(dA-dT).(dA-dT) and poly(dG-dC).(dG-dC) (19); in addition, there has been no evidence of identical spectroscopic properties and equilibrium constants for cationic porphyrins interacting with poly(dA-dT) .(dA-dT) and poly(dG-dC).(dG-dC) and calf thymus DNA.

The data gathered here therefore shows that the prime factor in the binding of the conjugate to DNA is the acridine portion of the molecule and not the porphyrin and that the mode of binding indicated is intercalation.

These studies form the foundation for more advanced studies into possible DNA footprinting and alkylating applications for cationic acridine-porphyrin heterodimers. The synthetic

route used provides relatively large amounts of precursors and conjugate to aid the synthesis of various conformational isomers, structural derivatives and their metalloderivatives. It is hoped that these compounds will provide insight into the molecular geometry of nucleic acids and that they will be of use in the modification of nucleic acid structure.

Appendix A-1: Determination of Porphyrin / Nucleic Acid Affinity Constants.

Determination of Affinity Constants for
TAP Binding to DNA

DNA	Slope	1/M	PORm	Page	Table
	443000	2.3E-06	0	139	AT1
	147000	6.8E-06	1.9E-07	140	AT2
	123000	8.1E-06	2.9E-07	141	AT3
pAT	72800	1.4E-05	4.1E-07	142	AT4
	67200	1.5E-05	5.4E-07	143	AT5
	45000	2.2E-05	6.5E-07	144	AT6
	31000	3.2E-05	7.2E-07	145	AT7
	26900	3.7E-05	8.4E-07	146	AT8
	258000	3.9E-06	0	147	GC1
	252000	4E-06	2.2E-07	148	GC2
	238000	4.2E-06	5.8E-07	149	GC3
pGC	173000	5.8E-06	9.3E-07	150	GC4
	169000	5.9E-06	1.1E-06	151	GC5
	135000	7.4E-06	1.4E-06	152	GC6
	114000	8.8E-06	1.7E-06	153	GC7
	105000	9.5E-06	1.8E-06	154	GC8
	364000	2.7E-06	0	155	CT1
	149000	6.7E-06	4.6E-07	156	CT2
	133000	7.5E-06	5.9E-07	157	CT3
CTDNA	151000	6.6E-06	6.4E-07	158	CT4
	130000	7.7E-06	7.1E-07	159	CT5
	91200	1.1E-05	8.4E-07	160	CT6

pAT = Poly(dA-dT).(dA-dT)
pGC = Poly(dG-dC).(dG-dC)
CTDNA = Calf Thymus DNA
Slope = Slope of the Scatchard Plot (EB/DNA Binding)
PORm = Porphyrin concentration at the midpoint of the titration

Determination of Affinity Constants
for ATB Binding to DNA

DNA	Slop	1/m	PORm	Page	Table
	443000	2.3E-06	0	139	AT1
	405000	2.5E-06	2.2E-07	161	AT9
	375000	2.7E-06	4E-07	162	AT10
pAT	377000	2.7E-06	5.4E-07	163	AT11
	371000	2.7E-06	6.6E-07	164	AT12
	336000	3E-06	7.7E-07	165	AT13
	329000	3E-06	8.7E-07	166	AT14
	258000	3.9E-06	0	147	GC1
	253000	4E-06	2.2E-07	167	GC9
pGC	250000	4E-06	3.2E-07	168	GC10
	227000	4.4E-06	5.2E-07	169	GC11
	212000	4.7E-06	6.5E-07	170	GC12
	236000	4.2E-06	7.5E-07	171	GC13
	214000	4.7E-06	8.6E-07	172	GC14
	364000	2.7E-06	0	155	CT1
	376000	2.7E-06	2.5E-07	173	CT7
	347000	2.9E-06	5.5E-07	174	CT8
CTDNA	282000	3.5E-06	1E-06	175	CT9
	308000	3.2E-06	1.2E-06	176	CT10
	333000	3E-06	1.3E-06	177	CT11
	341000	2.9E-06	8.2E-07	178	CT12

pAT = Poly(dA-dT).(dA-dT)
pGC = Poly(dG-dC).(dG-dC)
CTDNA = Calf Thymus DNA
Slope = Slope of the Scatchard Pl (EB/DNA Binding)
PORm = Porphyrin concen- at the midpoint of the titration

V	Io	It	EBt	DNAt	EBb	r	r/c
30	0.137	1.44	2.1E-06	4.45E-06	8.6E-07	0.193404	92162.07
40	0.183	1.71	2.78E-06	4.43E-06	1.01E-06	0.227769	81804.34
50	0.225	1.88	3.46E-06	4.4E-06	1.09E-06	0.248072	71626.33
60	0.271	2.05	4.14E-06	4.38E-06	1.17E-06	0.267959	64788.23
70	0.313	2.18	4.8E-06	4.36E-06	1.23E-06	0.282579	58846.95
80	0.36	2.28	5.46E-06	4.34E-06	1.27E-06	0.292005	53465.65
90	0.41	2.37	6.11E-06	4.32E-06	1.29E-06	0.299521	48982.74
100	0.451	2.435	6.76E-06	4.3E-06	1.31E-06	0.30464	45052.33
110	0.49	2.5	7.4E-06	4.28E-06	1.33E-06	0.310101	41889.51
120	0.53	2.55	8.04E-06	4.26E-06	1.33E-06	0.313121	38956.4

Regression Output:

Constant		181105.4
Std Err of Y Est		2432.286
R Squared		0.983259
No. of Observations		10
Degrees of Freedom		8
X Coefficient(s)	-443010	
Std Err of Coef.	20437.66	

AT1

V	Io	It	EBt	DNAt	EBb	PORt	r	r/c
30	0.028	0.226	2.13E-06	4.45E-06	6.58E-07	1.96E-07	0.147852	69476.91
40	0.0365	0.28	2.82E-06	4.43E-06	8.09E-07	1.95E-07	0.182724	64714.83
50	0.046	0.331	3.51E-06	4.4E-06	9.47E-07	1.94E-07	0.214914	61190.93
60	0.057	0.375	4.19E-06	4.38E-06	1.06E-06	1.93E-07	0.240969	57453.28
70	0.0645	0.409	4.87E-06	4.36E-06	1.14E-06	1.92E-07	0.262317	53868.68
80	0.073	0.441	5.54E-06	4.34E-06	1.22E-06	1.92E-07	0.281565	50838.06
90	0.0835	0.473	6.2E-06	4.32E-06	1.29E-06	1.91E-07	0.299448	48290.53
100	0.091	0.495	6.86E-06	4.3E-06	1.34E-06	1.9E-07	0.312081	45511.85
110	0.099	0.523	7.51E-06	4.28E-06	1.41E-06	1.89E-07	0.32909	43837.18
120	0.108	0.54	8.15E-06	4.26E-06	1.43E-06	1.88E-07	0.336889	41331.27

Regression Output:

Constant		92113.98
Std Err of Y Est		727.8897
R Squared		0.99467
No. of Observations		10
Degrees of Freedom		8
X Coefficient(s)	-147488	
Std Err of Coef.	3817.187	

AT2

V	Io	It	EBt	DNAt	EBb	PORt	r	r/c
30	0.036	0.226	2.1E-06	4.45E-06	4.95E-07	2.95E-07	0.111371	53071.09
40	0.048	0.285	2.78E-06	4.43E-06	6.18E-07	2.93E-07	0.139605	50139.77
50	0.059	0.34	3.46E-06	4.4E-06	7.33E-07	2.92E-07	0.166334	48026.14
60	0.071	0.389	4.14E-06	4.38E-06	8.29E-07	2.9E-07	0.189154	45734.5
70	0.083	0.428	4.8E-06	4.36E-06	9E-07	2.89E-07	0.206211	42943.3
80	0.094	0.465	5.46E-06	4.34E-06	9.67E-07	2.88E-07	0.222823	40798.5
90	0.105	0.501	6.11E-06	4.32E-06	1.03E-06	2.86E-07	0.238981	39082.19
100	0.1145	0.53	6.76E-06	4.3E-06	1.08E-06	2.85E-07	0.251949	37260.03
110	0.125	0.55	7.4E-06	4.28E-06	1.11E-06	2.83E-07	0.258937	34977.98
120	0.138	0.578	8.04E-06	4.26E-06	1.15E-06	2.82E-07	0.269346	33510.18

Regression Output:

Constant	67765.98
Std Err of Y Est	906.6645
R Squared	0.983168
No. of Observations	10
Degrees of Freedom	8
X Coefficient(s)	-122702
Std Err of Coef.	5676.151

V	Io	It	EBt	DNAt	EBb	PORt	r	r/c
30	0.036	0.197	2.1E-06	4.45E-06	4.16E-07	4.15E-07	0.093545	44576.75
40	0.047	0.253	2.78E-06	4.43E-06	5.32E-07	4.13E-07	0.120281	43199.55
50	0.058	0.3	3.46E-06	4.4E-06	6.25E-07	4.11E-07	0.141994	40998.2
60	0.071	0.355	4.14E-06	4.38E-06	7.34E-07	4.09E-07	0.16745	40486.78
70	0.082	0.402	4.8E-06	4.36E-06	8.27E-07	4.07E-07	0.189592	39482.47
80	0.093	0.431	5.46E-06	4.34E-06	8.74E-07	4.05E-07	0.201224	36843.86
90	0.104	0.466	6.11E-06	4.32E-06	9.36E-07	4.03E-07	0.216548	35413.62
100	0.116	0.51	6.76E-06	4.3E-06	1.02E-06	4.01E-07	0.236818	35022.45
110	0.127	0.541	7.4E-06	4.28E-06	1.07E-06	4E-07	0.250025	33774.14
120	0.1374	0.565	8.04E-06	4.26E-06	1.11E-06	3.98E-07	0.259462	32280.47

Regression Output:

Constant		51865.19
Std Err of Y Est		746.3894
R Squared		0.971189
No. of Observations		10
Degrees of Freedom		8
X Coefficient(s)	-72763.9	
Std Err of Coef.	4430.957	

V	Io	It	EBt	DNAt	EBb	PORt	r	r/c
30	0.152	0.79	2.1E-06	4.45E-06	3.93E-07	5.54E-07	0.088318	42086.02
40	0.22	1.015	2.78E-06	4.43E-06	4.9E-07	5.51E-07	0.110594	39720.42
50	0.249	1.235	3.46E-06	4.4E-06	6.07E-07	5.48E-07	0.137837	39797.98
60	0.298	1.45	4.14E-06	4.38E-06	7.09E-07	5.46E-07	0.161828	39127.5
70	0.345	1.625	4.8E-06	4.36E-06	7.88E-07	5.43E-07	0.180682	37626.95
80	0.397	1.775	5.46E-06	4.34E-06	8.49E-07	5.4E-07	0.195455	35787.58
90	0.447	1.92	6.11E-06	4.32E-06	9.07E-07	5.38E-07	0.209934	34332.01
100	0.493	2.05	6.76E-06	4.3E-06	9.59E-07	5.35E-07	0.222968	32974.15
110	0.538	2.19	7.4E-06	4.28E-06	1.02E-06	5.33E-07	0.237699	32109.14
120	0.583	2.31	8.04E-06	4.26E-06	1.06E-06	5.3E-07	0.249668	31061.98

Regression Output:

Constant	48532.67
Std Err of Y Est	955.7084
R Squared	0.942511
No. of Observations	10
Degrees of Freedom	8
X Coefficient(s)	-67244.6
Std Err of Coef.	5871.694

AT5

V	Io	It	EBt	DNAt	EBb	PORt	r	r/c
30	0.029	0.148	2.13E-06	4.45E-06	3.78E-07	6.62E-07	0.084945	39916.47
40	0.038	0.191	2.82E-06	4.43E-06	4.86E-07	6.59E-07	0.109754	38871.04
50	0.047	0.23	3.51E-06	4.4E-06	5.81E-07	6.56E-07	0.131917	37559.79
60	0.057	0.267	4.19E-06	4.38E-06	6.67E-07	6.53E-07	0.152119	36269.1
70	0.065	0.308	4.87E-06	4.36E-06	7.72E-07	6.5E-07	0.176878	36323.13
80	0.076	0.338	5.54E-06	4.34E-06	8.32E-07	6.46E-07	0.191629	34599.7
90	0.084	0.371	6.2E-06	4.32E-06	9.11E-07	6.43E-07	0.210924	34014.67
100	0.093	0.403	6.86E-06	4.3E-06	9.84E-07	6.4E-07	0.228917	33383.71
110	0.102	0.433	7.51E-06	4.28E-06	1.05E-06	6.37E-07	0.245588	32714.07
120	0.111	0.46	8.15E-06	4.26E-06	1.11E-06	6.34E-07	0.260171	31919.07

Regression Output:

Constant	43633.49
Std Err of Y Est	345.6772
R Squared	0.985163
No. of Observations	10
Degrees of Freedom	8
X Coefficient(s)	-45048.2
Std Err of Coef.	1954.591

AT6

V	Io	It	EBt	DNAt	EBb	PORt	r	r/c
30	0.029	0.1235	2.13E-06	4.45E-06	3E-07	7.36E-07	0.067457	31698.37
40	0.038	0.164	2.82E-06	4.43E-06	4E-07	7.32E-07	0.090385	32011.44
50	0.047	0.2	3.51E-06	4.4E-06	4.86E-07	7.29E-07	0.110292	31402.45
60	0.057	0.2355	4.19E-06	4.38E-06	5.67E-07	7.25E-07	0.129301	30828.74
70	0.065	0.265	4.87E-06	4.36E-06	6.35E-07	7.22E-07	0.145578	29895.58
80	0.076	0.301	5.54E-06	4.34E-06	7.14E-07	7.18E-07	0.164567	29713.48
90	0.084	0.333	6.2E-06	4.32E-06	7.91E-07	7.15E-07	0.182996	29510.99
100	0.093	0.355	6.86E-06	4.3E-06	8.32E-07	7.11E-07	0.193472	28214.62
110	0.102	0.385	7.51E-06	4.28E-06	8.99E-07	7.08E-07	0.209974	27970.03
120	0.111	0.403	8.15E-06	4.26E-06	9.43E-07	7.05E-07	0.221406	27163.22

Regression Output:

Constant	34540.98
Std Err of Y Est	459.2684
R Squared	0.932554
No. of Observations	10
Degrees of Freedom	8
X Coefficient(s)	-31014.9
Std Err of Coef.	2948.957

AT7

V	Io	It	EBt	DNAt	EBb	PORt	r	r/c
30	0.028	0.104	2.13E-06	4.45E-06	2.52E-07	8.59E-07	0.056751	26667.91
40	0.0365	0.136	2.82E-06	4.43E-06	3.31E-07	8.54E-07	0.074666	26444.05
50	0.046	0.171	3.51E-06	4.4E-06	4.15E-07	8.5E-07	0.094261	26838.13
60	0.057	0.2085	4.19E-06	4.38E-06	5.03E-07	8.46E-07	0.114801	27371.61
70	0.0645	0.2445	4.87E-06	4.36E-06	5.98E-07	8.42E-07	0.13706	28146.19
80	0.073	0.282	5.54E-06	4.34E-06	6.94E-07	8.38E-07	0.15991	28872.7
90	0.0835	0.31	6.2E-06	4.32E-06	7.52E-07	8.34E-07	0.174133	28081.66
100	0.091	0.332	6.86E-06	4.3E-06	8.01E-07	8.3E-07	0.186167	27149.39
110	0.099	0.359	7.51E-06	4.28E-06	8.64E-07	8.26E-07	0.201801	26881.29
120	0.108	0.385	8.15E-06	4.26E-06	9.2E-07	8.22E-07	0.216014	26501.76

Regression Output:

Constant		32418.8
Std Err of Y Est		530.4605
R Squared		0.723834
No. of Observations		6
Degrees of Freedom		4
X Coefficient(s)	-26862.8	
Std Err of Coef.	8296.35	

AT8

V	Io	It	EBt	DNAt	EBb	r	r/c
30	0.037	0.301	2.1E-06	4.45E-06	9.78E-07	0.219765	104723.6
40	0.049	0.364	2.78E-06	4.43E-06	1.17E-06	0.263511	94641.29
50	0.063	0.419	3.46E-06	4.4E-06	1.32E-06	0.299269	86408.7
60	0.075	0.464	4.14E-06	4.38E-06	1.44E-06	0.328606	79451.58
70	0.086	0.509	4.8E-06	4.36E-06	1.57E-06	0.359061	74774.37
80	0.098	0.539	5.46E-06	4.34E-06	1.63E-06	0.376149	68872.37
90	0.111	0.563	6.11E-06	4.32E-06	1.67E-06	0.387385	63351.7
100	0.123	0.587	6.76E-06	4.3E-06	1.72E-06	0.399572	59091.68
110	0.134	0.609	7.4E-06	4.28E-06	1.76E-06	0.410993	55518.23
120	0.148	0.631	8.04E-06	4.26E-06	1.79E-06	0.419895	52240.5

Regression Output:

Constant		163121.3
Std Err of Y Est		2248.242
R Squared		0.985195
No. of Observations		10
Degrees of Freedom		8
X Coefficient(s)	-257531	
Std Err of Coef.	11161.8	

GC1

V	Io	It	EBt	DNAt	EBb	PORt	r	r/c
30	0.017	0.14	2.13E-06	4.44E-06	1.03E-06	2.19E-07	0.232385	109199.4
40	0.023	0.166	2.82E-06	4.42E-06	1.2E-06	2.18E-07	0.271502	96156.91
50	0.029	0.189	3.51E-06	4.4E-06	1.34E-06	2.17E-07	0.305267	86916.42
60	0.035	0.21	4.19E-06	4.37E-06	1.47E-06	2.16E-07	0.335515	79995.47
70	0.0405	0.228	4.87E-06	4.35E-06	1.57E-06	2.15E-07	0.361225	74180.21
80	0.046	0.245	5.54E-06	4.33E-06	1.67E-06	2.14E-07	0.385233	69555.89
90	0.051	0.257	6.2E-06	4.31E-06	1.73E-06	2.13E-07	0.400701	64619.18
100	0.0565	0.27	6.86E-06	4.29E-06	1.79E-06	2.12E-07	0.417276	60852.8
110	0.0615	0.28	7.51E-06	4.27E-06	1.83E-06	2.11E-07	0.429082	57156.79
120	0.066	0.29	8.15E-06	4.25E-06	1.88E-06	2.1E-07	0.441968	54222.89

Regression Output:

Constant	165809.9
Std Err of Y Est	1187.386
R Squared	0.996072
No. of Observations	10
Degrees of Freedom	8
X Coefficient(s)	-252850
Std Err of Coef.	5613.651

GC2

V	Io	It	EBt	DNAt	EBb	PORt	r	r/c
30	0.017	0.128	2.13E-06	4.45E-06	9.66E-07	5.89E-07	0.217144	102037.7
40	0.023	0.155	2.82E-06	4.43E-06	1.15E-06	5.86E-07	0.259498	91905.45
50	0.028	0.177	3.51E-06	4.4E-06	1.3E-06	5.83E-07	0.294354	83809.06
60	0.034	0.196	4.19E-06	4.38E-06	1.41E-06	5.8E-07	0.321597	76677.01
70	0.039	0.211	4.87E-06	4.36E-06	1.5E-06	5.77E-07	0.343106	70459.26
80	0.044	0.226	5.54E-06	4.34E-06	1.58E-06	5.75E-07	0.364808	65868.09
90	0.049	0.24	6.2E-06	4.32E-06	1.66E-06	5.72E-07	0.384688	62036.95
100	0.055	0.254	6.86E-06	4.3E-06	1.73E-06	5.69E-07	0.402719	58729.82
110	0.059	0.262	7.51E-06	4.28E-06	1.77E-06	5.66E-07	0.41277	54983.86
120	0.065	0.27	8.15E-06	4.26E-06	1.78E-06	5.64E-07	0.418812	51382.04

Regression Output:

Constant	153583.5
Std Err of Y Est	813.7513
R Squared	0.997544
No. of Observations	8
Degrees of Freedom	6
X Coefficient(s)	-238472
Std Err of Coef.	4831.166

GC3

V	Io	It	EBt	DNAt	EBb	PORt	r	r/c
30	0.146	1.22	2.19E-06	7.59E-06	1.02E-06	9.44E-07	0.134455	61473.81
40	0.192	1.57	2.9E-06	7.55E-06	1.31E-06	9.4E-07	0.173363	59739.91
50	0.242	1.81	3.61E-06	7.51E-06	1.49E-06	9.35E-07	0.198233	54915.99
60	0.289	2.03	4.31E-06	7.48E-06	1.65E-06	9.31E-07	0.221178	51309.4
70	0.339	2.24	5E-06	7.44E-06	1.81E-06	9.26E-07	0.242677	48488.62
80	0.387	2.4	5.69E-06	7.4E-06	1.91E-06	9.22E-07	0.258216	45362.34
90	0.434	2.5	6.37E-06	7.37E-06	1.96E-06	9.17E-07	0.266289	41782.59
100	0.48	2.675	7.05E-06	7.33E-06	2.08E-06	9.13E-07	0.28427	40335.56
110	0.52	2.81	7.72E-06	7.3E-06	2.17E-06	9.09E-07	0.297985	38620.93
120	0.571	2.91	8.38E-06	7.26E-06	2.22E-06	9.04E-07	0.305804	36503.6

Regression Output:

Constant	89655.12
Std Err of Y Est	804.1558
R Squared	0.990883
No. of Observations	9
Degrees of Freedom	7
X Coefficient(s)	-173414
Std Err of Coef.	6286.921

GC4

Ve	Io	It	EBt	DNAt	EBb	PORt	r	r/c
5	0.047	0.32	7.16E-07	4.5E-06	1.42E-07	1.16E-06	0.031543	44072.61
10	0.094	0.58	1.43E-06	4.49E-06	2.53E-07	1.15E-06	0.056294	39425.37
15	0.14	0.82	2.14E-06	4.48E-06	3.54E-07	1.15E-06	0.078961	36958.57
20	0.185	1.02	2.84E-06	4.47E-06	4.35E-07	1.15E-06	0.0972	34206.34
25	0.23	1.18	3.54E-06	4.46E-06	4.94E-07	1.14E-06	0.110861	31288.23
30	0.274	1.34	4.24E-06	4.45E-06	5.55E-07	1.14E-06	0.124705	29401.9
35	0.317	1.48	4.94E-06	4.44E-06	6.05E-07	1.14E-06	0.136387	27630.44
40	0.365	1.59	5.63E-06	4.43E-06	6.37E-07	1.14E-06	0.144011	25590.8
45	0.41	1.69	6.32E-06	4.42E-06	6.66E-07	1.13E-06	0.150846	23885.34
50	0.457	1.78	7E-06	4.4E-06	6.88E-07	1.13E-06	0.156294	22327.75

Regression Output:

Constant	49924.37
Std Err of Y Est	682.5237
R Squared	0.991917
No. of Observations	10
Degrees of Freedom	8
X Coefficient(s)	-169214
Std Err of Coef.	5400.634

GC5

V	Io	It	EBt	DNAt	EBb	PORt	r	r/c
5	0.047	0.27	7.16E-07	4.5E-06	1.16E-07	1.42E-06	0.025766	36000.7
10	0.094	0.5	1.43E-06	4.49E-06	2.11E-07	1.41E-06	0.047027	32935.59
15	0.14	0.71	2.14E-06	4.48E-06	2.97E-07	1.41E-06	0.066188	30979.97
20	0.185	0.84	2.84E-06	4.47E-06	3.41E-07	1.4E-06	0.076247	26832.52
25	0.23	1.02	3.54E-06	4.46E-06	4.11E-07	1.4E-06	0.092189	26018.63
30	0.274	1.18	4.24E-06	4.45E-06	4.71E-07	1.4E-06	0.105987	24988.86
35	0.317	1.32	4.94E-06	4.44E-06	5.22E-07	1.39E-06	0.117624	23829.18
40	0.365	1.44	5.63E-06	4.43E-06	5.59E-07	1.39E-06	0.126377	22457.23
45	0.41	1.54	6.32E-06	4.42E-06	5.88E-07	1.39E-06	0.133168	21086.28
50	0.457	1.64	7E-06	4.4E-06	6.16E-07	1.38E-06	0.139755	19965.02

Regression Output:

Constant	39101.71
Std Err of Y Est	850.7047
R Squared	0.976829
No. of Observations	10
Degrees of Freedom	8
X Coefficient(s)	-135353
Std Err of Coef.	7370.278

GC6

V	Io	It	EBt	DNAt	EBb	PORt	r	r/c
30	0.017	0.084	2.13E-06	4.45E-06	5.83E-07	1.72E-06	0.131069	61590.34
40	0.023	0.106	2.82E-06	4.43E-06	7.22E-07	1.71E-06	0.163169	57789.03
50	0.028	0.127	3.51E-06	4.4E-06	8.61E-07	1.7E-06	0.195577	55685.22
60	0.034	0.146	4.19E-06	4.38E-06	9.75E-07	1.69E-06	0.222339	53011.27
70	0.039	0.161	4.87E-06	4.36E-06	1.06E-06	1.68E-06	0.243366	49976.92
80	0.044	0.175	5.54E-06	4.34E-06	1.14E-06	1.68E-06	0.262581	47410.55
90	0.049	0.185	6.2E-06	4.32E-06	1.18E-06	1.67E-06	0.273914	44172.9
100	0.055	0.195	6.86E-06	4.3E-06	1.22E-06	1.66E-06	0.28332	41317.46
110	0.059	0.201	7.51E-06	4.28E-06	1.24E-06	1.65E-06	0.288736	38461.62
120	0.065	0.209	8.15E-06	4.26E-06	1.25E-06	1.64E-06	0.29419	36092.75

Regression Output:

Constant		77031.45
Std Err of Y Est		1141.975
R Squared		0.970625
No. of Observations		7
Degrees of Freedom		5
X Coefficient(s)	-113661	
Std Err of Coef.	8842.862	

GC7

V	Io	It	EBt	DNAt	EBb	PORt	r	r/c
60	0.31	1.07	4.31E-06	4.39E-06	7.61E-07	1.81E-06	0.173263	40193.89
70	0.36	1.25	5E-06	4.37E-06	8.91E-07	1.8E-06	0.203885	40737.65
80	0.41	1.36	5.69E-06	4.35E-06	9.51E-07	1.79E-06	0.218681	38417.01
90	0.455	1.5	6.37E-06	4.33E-06	1.05E-06	1.78E-06	0.241706	37925.35
100	0.5	1.6	7.05E-06	4.31E-06	1.1E-06	1.77E-06	0.255645	36273.93
110	0.55	1.7	7.72E-06	4.29E-06	1.15E-06	1.76E-06	0.268538	34804.34
120	0.585	1.77	8.38E-06	4.27E-06	1.19E-06	1.75E-06	0.278022	33187.32
130	0.635	1.86	9.03E-06	4.25E-06	1.23E-06	1.75E-06	0.288762	31967.98
140	0.68	1.94	9.68E-06	4.23E-06	1.26E-06	1.74E-06	0.298407	30820.05
150	0.725	2.01	1.03E-05	4.21E-06	1.29E-06	1.73E-06	0.30575	29610.93

Regression Output:

Constant	62445.64
Std Err of Y Est	690.9952
R Squared	0.970587
No. of Observations	9
Degrees of Freedom	7
X Coefficient(s)	-105224
Std Err of Coef.	6923.434

GC8

V	Io	It	EBt	DNAt	EBb	r	r/c
5	0.13	1.08	7.08E-07	4.44E-06	3.06E-07	0.068974	97389.52
10	0.235	1.87	1.41E-06	4.43E-06	5.27E-07	0.119004	84224.76
15	0.36	2.25	2.11E-06	4.42E-06	6.09E-07	0.137907	65230.47
20	0.48	2.66	2.81E-06	4.41E-06	7.03E-07	0.159462	56709.93
25	0.595	3.12	3.51E-06	4.4E-06	8.14E-07	0.185155	52808.19
30	0.71	3.45	4.2E-06	4.38E-06	8.83E-07	0.201416	47990.06
35	0.84	3.7	4.88E-06	4.37E-06	9.22E-07	0.210755	43147.61
40	0.96	3.93	5.57E-06	4.36E-06	9.57E-07	0.219399	39399.13
45	1.03	4.15	6.25E-06	4.35E-06	1.01E-06	0.231045	36970.78
50	1.17	4.5	6.93E-06	4.34E-06	1.07E-06	0.247199	35687.15

Regression Output:

Constant		120701.9
Std Err of Y Est		4203.402
R Squared		0.963619
No. of Observations		10
Degrees of Freedom		8
X Coefficient(s)	-363678	
Std Err of Coef.	24983.62	

CTL

V	Io	It	EBt	DNAt	EBb	PORt	r	r/c
30	0.154	0.59	2.11E-06	4.45E-06	3.15E-07	4.67E-07	0.070915	33556.55
40	0.205	0.74	2.8E-06	4.43E-06	3.87E-07	4.65E-07	0.087446	31187.03
50	0.255	0.87	3.49E-06	4.4E-06	4.45E-07	4.63E-07	0.101015	28962.28
60	0.301	0.99	4.17E-06	4.38E-06	4.98E-07	4.6E-07	0.113721	27303.75
70	0.355	1.1	4.84E-06	4.36E-06	5.39E-07	4.58E-07	0.123561	25551.64
80	0.409	1.21	5.5E-06	4.34E-06	5.8E-07	4.56E-07	0.133491	24271.08
90	0.458	1.3	6.16E-06	4.32E-06	6.09E-07	4.54E-07	0.140998	22897.18
100	0.503	1.39	6.81E-06	4.3E-06	6.42E-07	4.52E-07	0.149245	21917.05
110	0.556	1.48	7.45E-06	4.28E-06	6.69E-07	4.5E-07	0.156211	20953.86
120	0.595	1.56	8.09E-06	4.26E-06	6.98E-07	4.47E-07	0.163915	20250.59

Regression Output:

Constant		44141.86
Std Err of Y Est		131.8822
R Squared		0.999181
No. of Observations		9
Degrees of Freedom		7
X Coefficient(s)	-149244	
Std Err of Coef.	1614.847	

CL2

V	Io	It	EBt	DNAt	EBb	PORt	r	r/c
30	0.159	0.54	2.11E-06	4.45E-06	2.52E-07	5.97E-07	0.056683	26821.92
40	0.227	0.675	2.8E-06	4.43E-06	2.96E-07	5.94E-07	0.066979	23887.6
50	0.28	0.79	3.49E-06	4.4E-06	3.38E-07	5.91E-07	0.076622	21968.58
60	0.339	0.92	4.17E-06	4.38E-06	3.84E-07	5.88E-07	0.087715	21059.76
70	0.395	1.02	4.84E-06	4.36E-06	4.14E-07	5.86E-07	0.094816	19607.25
80	0.45	1.125	5.5E-06	4.34E-06	4.47E-07	5.83E-07	0.102896	18708.31
90	0.503	1.24	6.16E-06	4.32E-06	4.88E-07	5.8E-07	0.112887	18332.07
100	0.555	1.32	6.81E-06	4.3E-06	5.06E-07	5.77E-07	0.117736	17289.96
110	0.6	1.41	7.45E-06	4.28E-06	5.36E-07	5.74E-07	0.125256	16801.63
120	0.65	1.49	8.09E-06	4.26E-06	5.56E-07	5.72E-07	0.13051	16123.67

Regression Output:

Constant		32942.84
Std Err of Y Est		726.2042
R Squared		0.959362
No. of Observations		10
Degrees of Freedom		8
X Coefficient(s)	-132525	
Std Err of Coef.	9643.344	

CT3

V	Io	It	EBt	DNAt	EBb	PORt	r	r/c
30	0.152	0.58	2.11E-06	4.45E-06	3.1E-07	6.49E-07	0.069799	33028.36
40	0.202	0.73	2.8E-06	4.43E-06	3.83E-07	6.46E-07	0.086531	30860.77
50	0.252	0.845	3.49E-06	4.4E-06	4.3E-07	6.43E-07	0.09766	28000.44
60	0.305	0.97	4.17E-06	4.38E-06	4.82E-07	6.4E-07	0.110052	26422.7
70	0.356	1.08	4.84E-06	4.36E-06	5.25E-07	6.36E-07	0.120397	24897.38
80	0.405	1.175	5.5E-06	4.34E-06	5.59E-07	6.33E-07	0.128666	23393.75
90	0.455	1.275	6.16E-06	4.32E-06	5.95E-07	6.3E-07	0.137679	22358.17
100	0.5	1.37	6.81E-06	4.3E-06	6.31E-07	6.27E-07	0.146773	21554.12
110	0.551	1.445	7.45E-06	4.28E-06	6.49E-07	6.24E-07	0.15154	20327.42
120	0.595	1.53	8.09E-06	4.26E-06	6.78E-07	6.21E-07	0.159241	19673.18

Regression Output:

Constant	43322.94
Std Err of Y Est	432.3803
R Squared	0.991758
No. of Observations	10
Degrees of Freedom	8
X Coefficient(s)	-151210
Std Err of Coef.	4873.704

CT4

V	Io	It	EBt	DNAt	EBb	PORt	r	r/c
30	0.159	0.6125	2.11E-06	4.45E-06	3E-07	7.27E-07	0.067469	31925.83
40	0.227	0.77	2.8E-06	4.43E-06	3.59E-07	7.23E-07	0.081182	28953.04
50	0.28	0.91	3.49E-06	4.4E-06	4.17E-07	7.2E-07	0.094651	27137.66
60	0.339	1.05	4.17E-06	4.38E-06	4.71E-07	7.16E-07	0.107341	25771.93
70	0.395	1.18	4.84E-06	4.36E-06	5.2E-07	7.13E-07	0.119089	24626.71
80	0.45	1.29	5.5E-06	4.34E-06	5.56E-07	7.09E-07	0.128048	23281.45
90	0.503	1.39	6.16E-06	4.32E-06	5.87E-07	7.06E-07	0.135863	22063.16
100	0.555	1.48	6.81E-06	4.3E-06	6.12E-07	7.03E-07	0.142361	20906.17
110	0.6	1.59	7.45E-06	4.28E-06	6.55E-07	6.99E-07	0.15309	20535.32
120	0.65	1.67	8.09E-06	4.26E-06	6.75E-07	6.96E-07	0.158477	19578.74

Regression Output:

Constant		39883.17
Std Err of Y Est		461.6329
R Squared		0.988147
No. of Observations		10
Degrees of Freedom		8
X Coefficient(s)	-129720	
Std Err of Coef.	5022.971	

CT5

V	Io	It	EBt	DNAt	EBb	PORt	r	r/c
30	0.154	0.39	2.11E-06	4.45E-06	1.71E-07	8.57E-07	0.038385	18163.63
40	0.205	0.529	2.8E-06	4.43E-06	2.34E-07	8.53E-07	0.052958	18887.1
50	0.255	0.64	3.49E-06	4.4E-06	2.79E-07	8.48E-07	0.063237	18130.86
60	0.301	0.738	4.17E-06	4.38E-06	3.16E-07	8.44E-07	0.072128	17317.47
70	0.355	0.838	4.84E-06	4.36E-06	3.49E-07	8.4E-07	0.080108	16565.7
80	0.409	0.931	5.5E-06	4.34E-06	3.78E-07	8.36E-07	0.086994	15817.11
90	0.458	0.99	6.16E-06	4.32E-06	3.85E-07	8.32E-07	0.089087	14467.1
100	0.503	1.11	6.81E-06	4.3E-06	4.39E-07	8.28E-07	0.102132	14998.48
110	0.556	1.18	7.45E-06	4.28E-06	4.51E-07	8.24E-07	0.105493	14150.66
120	0.595	1.28	8.09E-06	4.26E-06	4.96E-07	8.2E-07	0.116354	14374.77

Regression Output:

Constant		23723.94
Std Err of Y Est		534.3498
R Squared		0.91864
No. of Observations		8
Degrees of Freedom		6
X Coefficient(s)	-91172.6	
Std Err of Coef.	11076.99	

CL6

V	Io	It	EBt	DNAt	EBb	PORt	r	r/c
30	0.017	0.158	2.13E-06	4.45E-06	7.64E-07	2.19E-07	0.171713	80689.22
40	0.023	0.185	2.82E-06	4.43E-06	8.78E-07	2.18E-07	0.198259	70216.79
50	0.029	0.208	3.51E-06	4.4E-06	9.7E-07	2.17E-07	0.220138	62678.17
60	0.035	0.225	4.19E-06	4.38E-06	1.03E-06	2.16E-07	0.234806	55983.8
70	0.0405	0.24	4.87E-06	4.36E-06	1.08E-06	2.15E-07	0.247743	50875.79
80	0.046	0.253	5.54E-06	4.34E-06	1.12E-06	2.14E-07	0.258298	46637.22
90	0.051	0.265	6.2E-06	4.32E-06	1.16E-06	2.13E-07	0.268317	43270.25
100	0.0565	0.274	6.86E-06	4.3E-06	1.18E-06	2.12E-07	0.27401	39959.81
110	0.0615	0.282	7.51E-06	4.28E-06	1.19E-06	2.11E-07	0.279112	37179.75
120	0.066	0.289	8.15E-06	4.26E-06	1.21E-06	2.1E-07	0.283615	34795.33

Regression Output:

Constant	150860.2
Std Err of Y Est	774.4605
R Squared	0.997661
No. of Observations	10
Degrees of Freedom	8
X Coefficient(s)	-404890
Std Err of Coef.	6931.823

AT9

V	Io	It	EBt	DNAt	EBb	PORt	r	r/c
30	0.0185	0.177	2.13E-06	4.45E-06	8.02E-07	4.17E-07	0.18033	84738.53
40	0.024	0.207	2.82E-06	4.43E-06	9.26E-07	4.14E-07	0.20923	74102.4
50	0.03	0.233	3.51E-06	4.4E-06	1.03E-06	4.12E-07	0.233235	66407.11
60	0.036	0.253	4.19E-06	4.38E-06	1.1E-06	4.1E-07	0.250536	59734.3
70	0.043	0.272	4.87E-06	4.36E-06	1.16E-06	4.08E-07	0.265674	54558.07
80	0.0385	0.284	5.54E-06	4.34E-06	1.24E-06	4.06E-07	0.286192	51673.64
90	0.054	0.296	6.2E-06	4.32E-06	1.22E-06	4.05E-07	0.283469	45713.69
100	0.06	0.311	6.86E-06	4.3E-06	1.27E-06	4.03E-07	0.295418	43081.73
110	0.066	0.315	7.51E-06	4.28E-06	1.26E-06	4.01E-07	0.294459	39224.05
120	0.071	0.326	8.15E-06	4.26E-06	1.29E-06	3.99E-07	0.302984	37171.62

Regression Output:

Constant	153137.4
Std Err of Y Est	2660.677
R Squared	0.974304
No. of Observations	10
Degrees of Freedom	8
X Coefficient(s)	-374768
Std Err of Coef.	21518.03

AT10

V	Io	It	EBt	DNAt	EBb	PORt	r	r/c
30	0.0185	0.171	2.13E-06	4.45E-06	7.72E-07	5.48E-07	0.173504	81530.76
40	0.024	0.199	2.82E-06	4.43E-06	8.86E-07	5.45E-07	0.200084	70862.95
50	0.03	0.225	3.51E-06	4.4E-06	9.87E-07	5.43E-07	0.224043	63790.08
60	0.036	0.246	4.19E-06	4.38E-06	1.06E-06	5.4E-07	0.242454	57807.39
70	0.043	0.261	4.87E-06	4.36E-06	1.1E-06	5.37E-07	0.252912	51937.37
80	0.0385	0.2775	5.54E-06	4.34E-06	1.21E-06	5.35E-07	0.278615	50305.49
90	0.054	0.288	6.2E-06	4.32E-06	1.18E-06	5.32E-07	0.274098	44202.49
100	0.06	0.298	6.86E-06	4.3E-06	1.2E-06	5.3E-07	0.280117	40850.41
110	0.066	0.306	7.51E-06	4.28E-06	1.21E-06	5.27E-07	0.283816	37806.31
120	0.071	0.311	8.15E-06	4.26E-06	1.21E-06	5.25E-07	0.285161	34985.05

Regression Output:

Constant	147531.9
Std Err of Y Est	3540.223
R Squared	0.951321
No. of Observations	10
Degrees of Freedom	8
X Coefficient(s)	-377280
Std Err of Coef.	30173.38

AT11

V	Io	It	EBt	DNAt	EBb	PORt	r	r/c
30	0.041	0.415	2.1E-06	4.45E-06	7.17E-07	6.71E-07	0.16128	76854.05
40	0.061	0.495	2.78E-06	4.43E-06	8.33E-07	6.68E-07	0.188076	67548.3
50	0.078	0.564	3.46E-06	4.4E-06	9.32E-07	6.64E-07	0.211642	61108.04
60	0.091	0.61	4.14E-06	4.38E-06	9.96E-07	6.61E-07	0.227116	54912.97
70	0.107	0.65	4.8E-06	4.36E-06	1.04E-06	6.58E-07	0.238772	49724.09
80	0.119	0.685	5.46E-06	4.34E-06	1.09E-06	6.55E-07	0.250088	45790.72
90	0.137	0.719	6.11E-06	4.32E-06	1.12E-06	6.52E-07	0.258394	42256.88
100	0.153	0.744	6.76E-06	4.3E-06	1.13E-06	6.49E-07	0.263645	38989.75
110	0.166	0.774	7.4E-06	4.28E-06	1.17E-06	6.45E-07	0.27252	36812.91
120	0.18	0.793	8.04E-06	4.26E-06	1.18E-06	6.42E-07	0.276064	34345.93

Regression Output:

Constant	137830.7
Std Err of Y Est	1092.746
R Squared	0.994656
No. of Observations	10
Degrees of Freedom	8
X Coefficient(s)	-370576
Std Err of Coef.	9603.481

V	Io	It	EBt	DNAt	EBb	PORt	r	r/c
30	0.041	0.36	2.1E-06	4.45E-06	6.12E-07	7.83E-07	0.137562	65551.99
40	0.061	0.432	2.78E-06	4.43E-06	7.12E-07	7.79E-07	0.160774	57742.9
50	0.078	0.489	3.46E-06	4.4E-06	7.88E-07	7.75E-07	0.178982	51677.78
60	0.091	0.534	4.14E-06	4.38E-06	8.5E-07	7.71E-07	0.193858	46871.76
70	0.107	0.573	4.8E-06	4.36E-06	8.94E-07	7.68E-07	0.204913	42672.97
80	0.119	0.604	5.46E-06	4.34E-06	9.3E-07	7.64E-07	0.214298	39237.63
90	0.137	0.641	6.11E-06	4.32E-06	9.67E-07	7.6E-07	0.223764	36593.58
100	0.153	0.67	6.76E-06	4.3E-06	9.92E-07	7.57E-07	0.230634	34107.78
110	0.166	0.696	7.4E-06	4.28E-06	1.02E-06	7.53E-07	0.237559	32090.2
120	0.18	0.72	8.04E-06	4.26E-06	1.04E-06	7.5E-07	0.243188	30255.8

Regression Output:

Constant	111766.2
Std Err of Y Est	243.7505
R Squared	0.999613
No. of Observations	10
Degrees of Freedom	8
X Coefficient(s)	-336139
Std Err of Coef.	2339.11

V	Io	It	EBt	DNAt	EBb	PORt	r	r/c
30	0.031	0.331	2.1E-06	4.45E-06	9.03E-07	8.95E-07	0.203045	96756.21
40	0.041	0.399	2.78E-06	4.43E-06	1.08E-06	8.9E-07	0.243494	87452.08
50	0.051	0.451	3.46E-06	4.4E-06	1.2E-06	8.86E-07	0.273394	78937.7
60	0.062	0.494	4.14E-06	4.38E-06	1.3E-06	8.82E-07	0.296706	71738.73
70	0.072	0.526	4.8E-06	4.36E-06	1.37E-06	8.77E-07	0.31333	65250.72
80	0.08	0.557	5.46E-06	4.34E-06	1.44E-06	8.73E-07	0.330793	60567.8
90	0.09	0.576	6.11E-06	4.32E-06	1.46E-06	8.69E-07	0.338655	55382.57
100	0.099	0.594	6.76E-06	4.3E-06	1.49E-06	8.65E-07	0.346577	51254.33
110	0.109	0.615	7.4E-06	4.28E-06	1.52E-06	8.61E-07	0.355966	48084.99
120	0.119	0.633	8.04E-06	4.26E-06	1.55E-06	8.57E-07	0.363307	45200.2

Regression Output:

Constant		166798.1
Std Err of Y Est		2239.638
R Squared		0.985248
No. of Observations		10
Degrees of Freedom		8
X Coefficient(s)	-328636	
Std Err of Coef.	14217.29	

AT14

V	Io	It	EBt	DNAt	EBb	PORt	r	r
30	0.017	0.14	2.13E-06	4.44E-06	1.03E-06	2.19E-07	0.232385	1091
40	0.023	0.166	2.82E-06	4.42E-06	1.2E-06	2.18E-07	0.271502	9615
50	0.029	0.189	3.51E-06	4.4E-06	1.34E-06	2.17E-07	0.305267	8691
60	0.035	0.21	4.19E-06	4.37E-06	1.47E-06	2.16E-07	0.335515	7999
70	0.0405	0.228	4.87E-06	4.35E-06	1.57E-06	2.15E-07	0.361225	7418
80	0.046	0.245	5.54E-06	4.33E-06	1.67E-06	2.14E-07	0.385233	6955
90	0.051	0.257	6.2E-06	4.31E-06	1.73E-06	2.13E-07	0.400701	6461
100	0.0565	0.27	6.86E-06	4.29E-06	1.79E-06	2.12E-07	0.417276	6085
110	0.0615	0.28	7.51E-06	4.27E-06	1.83E-06	2.11E-07	0.429082	5715
120	0.066	0.29	8.15E-06	4.25E-06	1.88E-06	2.1E-07	0.441968	5422

Regression Output:

Constant	165809.9
Std Err of Y Est	1187.386
R Squared	0.996072
No. of Observations	10
Degrees of Freedom	8
X Coefficient(s)	-252850
Std Err of Coef.	5613.651

V	Io	It	EBt	DNAt	EBb	PORt	r	r/c
30	0.029	0.222	2.13E-06	4.44E-06	9.49E-07	3.29E-07	0.213732	100434.1
40	0.038	0.262	2.82E-06	4.42E-06	1.1E-06	3.27E-07	0.249284	88287.91
50	0.047	0.298	3.51E-06	4.4E-06	1.23E-06	3.26E-07	0.2807	79921.63
60	0.057	0.329	4.19E-06	4.37E-06	1.34E-06	3.24E-07	0.305669	72879.43
70	0.065	0.355	4.87E-06	4.35E-06	1.43E-06	3.22E-07	0.327479	67250.19
80	0.076	0.38	5.54E-06	4.33E-06	1.49E-06	3.21E-07	0.344947	62282.09
90	0.094	0.4	6.2E-06	4.31E-06	1.5E-06	3.19E-07	0.348886	56263.19
100	0.093	0.422	6.86E-06	4.29E-06	1.62E-06	3.18E-07	0.376904	54965.14
110	0.102	0.443	7.51E-06	4.27E-06	1.68E-06	3.16E-07	0.392511	52285.29
120	0.111	0.458	8.15E-06	4.25E-06	1.71E-06	3.15E-07	0.401311	49234.87

Regression Output:

Constant	148583.2
Std Err of Y Est	2367.625
R Squared	0.958313
No. of Observations	8
Degrees of Freedom	6
X Coefficient(s)	-249633
Std Err of Coef.	21255.75

GC10

V	Io	It	EBt	DNAt	EBb	PORt	r	r/c
30	0.036	0.256	2.13E-06	4.45E-06	8.72E-07	5.34E-07	0.196043	92122.11
40	0.047	0.31	2.82E-06	4.43E-06	1.04E-06	5.31E-07	0.235515	83411.6
50	0.059	0.355	3.51E-06	4.4E-06	1.17E-06	5.29E-07	0.266366	75840.26
60	0.069	0.394	4.19E-06	4.38E-06	1.29E-06	5.26E-07	0.293889	70070.78
70	0.08	0.428	4.87E-06	4.36E-06	1.38E-06	5.24E-07	0.316215	64937.01
80	0.091	0.461	5.54E-06	4.34E-06	1.47E-06	5.21E-07	0.33783	60997.04
90	0.103	0.488	6.2E-06	4.32E-06	1.53E-06	5.19E-07	0.353216	56961.47
100	0.114	0.512	6.86E-06	4.3E-06	1.58E-06	5.16E-07	0.366889	53504.71
110	0.121	0.53	7.51E-06	4.28E-06	1.62E-06	5.14E-07	0.378825	50462.17
120	0.135	0.553	8.15E-06	4.26E-06	1.66E-06	5.11E-07	0.388996	47724.03

Regression Output:

Constant	136808.3
Std Err of Y Est	483.0774
R Squared	0.999036
No. of Observations	10
Degrees of Freedom	8
X Coefficient(s)	-227218
Std Err of Coef.	2495.337

GC11

V	Io	It	EBt	DNAt	EBb	PORt	r	r/c
30	0.017	0.136	2.13E-06	4.44E-06	8.92E-07	6.58E-07	0.200874	94392.27
40	0.023	0.164	2.82E-06	4.42E-06	1.06E-06	6.54E-07	0.239183	84710.67
50	0.029	0.189	3.51E-06	4.4E-06	1.2E-06	6.51E-07	0.272744	77656.24
60	0.035	0.211	4.19E-06	4.37E-06	1.32E-06	6.48E-07	0.301482	71881.06
70	0.041	0.229	4.87E-06	4.35E-06	1.41E-06	6.45E-07	0.323601	66453.7
80	0.0475	0.246	5.54E-06	4.33E-06	1.49E-06	6.42E-07	0.343325	61989.17
90	0.054	0.262	6.2E-06	4.31E-06	1.56E-06	6.39E-07	0.361485	58295.1
100	0.059	0.277	6.86E-06	4.29E-06	1.63E-06	6.36E-07	0.380677	55515.43
110	0.066	0.291	7.51E-06	4.27E-06	1.69E-06	6.33E-07	0.394772	52586.39
120	0.072	0.304	8.15E-06	4.25E-06	1.74E-06	6.3E-07	0.408983	50176.12

Regression Output:

Constant	135772.5
Std Err of Y Est	834.1239
R Squared	0.997107
No. of Observations	10
Degrees of Freedom	8
X Coefficient(s)	-211975
Std Err of Coef.	4036.923

GC12

V	Io	It	EBt	DNAt	EBb	PORt	r	r/c
30	0.017	0.126	2.13E-06	4.44E-06	8.17E-07	7.67E-07	0.183994	86460.15
40	0.023	0.146	2.82E-06	4.42E-06	9.22E-07	7.63E-07	0.208649	73896.54
50	0.029	0.164	3.51E-06	4.4E-06	1.01E-06	7.6E-07	0.230128	65522.45
60	0.035	0.182	4.19E-06	4.37E-06	1.1E-06	7.56E-07	0.251806	60037.03
70	0.041	0.199	4.87E-06	4.35E-06	1.18E-06	7.52E-07	0.271962	55849.38
80	0.0475	0.2125	5.54E-06	4.33E-06	1.24E-06	7.49E-07	0.285383	51527.52
90	0.054	0.226	6.2E-06	4.31E-06	1.29E-06	7.45E-07	0.298921	48205.56
100	0.059	0.237	6.86E-06	4.29E-06	1.33E-06	7.42E-07	0.310828	45329.11
110	0.066	0.25	7.51E-06	4.27E-06	1.38E-06	7.38E-07	0.322836	43003.98
120	0.072	0.263	8.15E-06	4.25E-06	1.43E-06	7.35E-07	0.336706	41308.79

Regression Output:

Constant		119456
Std Err of Y Est		785.2363
R Squared		0.992791
No. of Observations		8
Degrees of Freedom		6
X Coefficient(s)	-236018	
Std Err of Coef.	8210.416	

GC13

V	Io	It	EBt	DNAt	EBb	PORt	r	r/c
30	0.017	0.114	2.13E-06	4.44E-06	8.13E-07	8.77E-07	0.183263	86116.56
40	0.023	0.129	2.82E-06	4.42E-06	8.89E-07	8.73E-07	0.201253	71277.15
50	0.029	0.153	3.51E-06	4.4E-06	1.04E-06	8.68E-07	0.236582	67360.23
60	0.035	0.168	4.19E-06	4.37E-06	1.12E-06	8.64E-07	0.254991	60796.55
70	0.0405	0.187	4.87E-06	4.35E-06	1.23E-06	8.6E-07	0.282237	57959.47
80	0.046	0.198	5.54E-06	4.33E-06	1.27E-06	8.56E-07	0.294248	53128.11
90	0.051	0.21	6.2E-06	4.31E-06	1.33E-06	8.52E-07	0.309279	49875.97
100	0.0565	0.221	6.86E-06	4.29E-06	1.38E-06	8.48E-07	0.321508	46886.59
110	0.0615	0.231	7.51E-06	4.27E-06	1.42E-06	8.44E-07	0.332858	44339.02
120	0.066	0.24	8.15E-06	4.25E-06	1.46E-06	8.4E-07	0.343314	42119.56

Regression Output:

Constant	116118
Std Err of Y Est	1362.549
R Squared	0.984437
No. of Observations	9
Degrees of Freedom	7
X Coefficient(s)	-213999
Std Err of Coef.	10169.81

V	Io	It	EBt	DNAt	EBb	PORt	r	r/c
30	0.131	0.835	2.13E-06	4.45E-06	6.1E-07	2.6E-07	0.137193	64467.86
40	0.172	0.97	2.82E-06	4.43E-06	6.92E-07	2.58E-07	0.156277	55348.14
50	0.218	1.1	3.51E-06	4.4E-06	7.65E-07	2.57E-07	0.173574	49420.38
60	0.264	1.21	4.19E-06	4.38E-06	8.2E-07	2.56E-07	0.187077	44604.03
70	0.3	1.29	4.87E-06	4.36E-06	8.58E-07	2.55E-07	0.196729	40399.65
80	0.345	1.375	5.54E-06	4.34E-06	8.93E-07	2.53E-07	0.205666	37134.17
90	0.387	1.45	6.2E-06	4.32E-06	9.21E-07	2.52E-07	0.213276	34394.03
100	0.425	1.53	6.86E-06	4.3E-06	9.58E-07	2.51E-07	0.222763	32486.33
110	0.465	1.58	7.51E-06	4.28E-06	9.67E-07	2.5E-07	0.22585	30084.78
120	0.507	1.64	8.15E-06	4.26E-06	9.82E-07	2.49E-07	0.230583	28289.17

Regression Output:

Constant		114927.7
Std Err of Y Est		740.0403
R Squared		0.99649
No. of Observations		10
Degrees of Freedom		8
X Coefficient(s)	-375912	
Std Err of Coef.	7887.804	

CT7

V	Io	It	EBt	DNAt	EBb	PORt	r	r/c
30	0.035	0.195	2.11E-06	4.45E-06	5.13E-07	5.59E-07	0.115421	54616.55
40	0.047	0.234	2.8E-06	4.43E-06	6E-07	5.57E-07	0.135563	48347.66
50	0.057	0.261	3.49E-06	4.4E-06	6.55E-07	5.54E-07	0.148612	42609
60	0.069	0.292	4.17E-06	4.38E-06	7.16E-07	5.51E-07	0.163246	39194.17
70	0.08	0.314	4.84E-06	4.36E-06	7.51E-07	5.49E-07	0.17213	35595.24
80	0.092	0.333	5.5E-06	4.34E-06	7.73E-07	5.46E-07	0.178135	32388.23
90	0.102	0.355	6.16E-06	4.32E-06	8.12E-07	5.43E-07	0.187904	30514.35
100	0.113	0.37	6.81E-06	4.3E-06	8.25E-07	5.41E-07	0.191788	28164.7
110	0.124	0.388	7.45E-06	4.28E-06	8.47E-07	5.38E-07	0.19795	26552.76
120	0.134	0.4	8.09E-06	4.26E-06	8.54E-07	5.36E-07	0.200395	24757.43

Regression Output:

Constant	94899.63
Std Err of Y Est	663.2401
R Squared	0.995967
No. of Observations	10
Degrees of Freedom	8
X Coefficient(s)	-346662
Std Err of Coef.	7799.557

CT8

V	Io	It	EBt	DNAt	EBb	PORt	r	r/c
30	0.149	0.81	2.13E-06	4.45E-06	4.83E-07	1.06E-06	0.108579	51022.23
40	0.216	0.94	2.82E-06	4.43E-06	5.29E-07	1.06E-06	0.119514	42327.84
50	0.261	1.08	3.51E-06	4.4E-06	5.98E-07	1.05E-06	0.135859	38681.99
60	0.31	1.19	4.19E-06	4.38E-06	6.43E-07	1.05E-06	0.14669	34974.62
70	0.36	1.31	4.87E-06	4.36E-06	6.94E-07	1.04E-06	0.159127	32677.85
80	0.41	1.4	5.54E-06	4.34E-06	7.23E-07	1.04E-06	0.166628	30085.63
90	0.461	1.49	6.2E-06	4.32E-06	7.52E-07	1.03E-06	0.174025	28064.2
100	0.509	1.58	6.86E-06	4.3E-06	7.83E-07	1.03E-06	0.181995	26540.88
110	0.555	1.66	7.51E-06	4.28E-06	8.07E-07	1.02E-06	0.188666	25131.69
120	0.599	1.75	8.15E-06	4.26E-06	8.41E-07	1.02E-06	0.197452	24224.4

Regression Output:

Constant		77955.27
Std Err of Y Est		1814.417
R Squared		0.960108
No. of Observations		10
Degrees of Freedom		8
X Coefficient(s)	-282427	
Std Err of Coef.	20353.79	

CT9

V	Io	It	EBt	DNAt	EBb	PORt	r	r/c
30	0.1995	1.02	2.13E-06	4.45E-06	4.6E-07	1.18E-06	0.103343	48561.79
40	0.2755	1.24	2.82E-06	4.43E-06	5.4E-07	1.17E-06	0.122079	43236.23
50	0.338	1.41	3.51E-06	4.4E-06	6.01E-07	1.17E-06	0.13635	38821.99
60	0.4	1.555	4.19E-06	4.38E-06	6.47E-07	1.16E-06	0.147624	35197.39
70	0.465	1.68	4.87E-06	4.36E-06	6.81E-07	1.16E-06	0.156047	32045.29
80	0.5275	1.79	5.54E-06	4.34E-06	7.07E-07	1.15E-06	0.162931	29418.01
90	0.5955	1.92	6.2E-06	4.32E-06	7.42E-07	1.15E-06	0.171754	27697.93
100	0.6485	2.02	6.86E-06	4.3E-06	7.68E-07	1.14E-06	0.178699	26060.31
110	0.7175	2.115	7.51E-06	4.28E-06	7.83E-07	1.14E-06	0.182954	24370.77
120	0.7745	2.2	8.15E-06	4.26E-06	7.99E-07	1.13E-06	0.187504	23003.98

Regression Output:

Constant	80554.54
Std Err of Y Est	482.9673
R Squared	0.995649
No. of Observations	9
Degrees of Freedom	7
X Coefficient(s)	-307854
Std Err of Coef.	7692.395

CT10

V	Io	It	EBt	DNAt	EBb	PORt	r	r/c
30	0.1995	1.17	2.13E-06	4.45E-06	5.44E-07	1.3E-06	0.122236	57439.63
40	0.2755	1.34	2.82E-06	4.43E-06	5.96E-07	1.29E-06	0.134736	47718.99
50	0.338	1.5	3.51E-06	4.4E-06	6.51E-07	1.29E-06	0.147798	42081.29
60	0.4	1.66	4.19E-06	4.38E-06	7.06E-07	1.28E-06	0.161044	38397.15
70	0.465	1.78	4.87E-06	4.36E-06	7.37E-07	1.27E-06	0.16889	34682.76
80	0.5275	1.91	5.54E-06	4.34E-06	7.75E-07	1.27E-06	0.178417	32214.18
90	0.5955	2.015	6.2E-06	4.32E-06	7.95E-07	1.26E-06	0.184073	29684.57
100	0.6845	2.12	6.86E-06	4.3E-06	8.04E-07	1.25E-06	0.187038	27276.4
110	0.7175	2.215	7.51E-06	4.28E-06	8.39E-07	1.25E-06	0.196046	26114.65
120	0.7745	2.315	8.15E-06	4.26E-06	8.63E-07	1.24E-06	0.202631	24859.79

Regression Output:

Constant		91190.81
Std Err of Y Est		910.8346
R Squared		0.981076
No. of Observations		8
Degrees of Freedom		6
X Coefficient(s)	-332564	
Std Err of Coef.	18856.4	

CT11

V	Io	It	EBt	DNAt	EBb	PORt	r	r/c
30	0.018	0.109	2.13E-06	4.45E-06	5.75E-07	8.33E-07	0.129287	60752.78
40	0.024	0.126	2.82E-06	4.43E-06	6.45E-07	8.29E-07	0.145629	51576.81
50	0.031	0.137	3.51E-06	4.4E-06	6.7E-07	8.25E-07	0.152081	43300.96
60	0.037	0.153	4.19E-06	4.38E-06	7.33E-07	8.21E-07	0.167241	39874.49
70	0.043	0.165	4.87E-06	4.36E-06	7.71E-07	8.17E-07	0.176745	36295.81
80	0.048	0.174	5.54E-06	4.34E-06	7.96E-07	8.13E-07	0.183422	33117.78
90	0.054	0.184	6.2E-06	4.32E-06	8.22E-07	8.09E-07	0.190154	30665.31
100	0.059	0.194	6.86E-06	4.3E-06	8.53E-07	8.05E-07	0.198413	28935.19
110	0.064	0.2	7.51E-06	4.28E-06	8.59E-07	8.01E-07	0.200834	26752.55
120	0.07	0.206	8.15E-06	4.26E-06	8.59E-07	7.97E-07	0.201786	24756.16

Regression Output:

Constant	96004.92
Std Err of Y Est	788.8003
R Squared	0.985613
No. of Observations	7
Degrees of Freedom	5
X Coefficient(s)	-341316
Std Err of Coef.	18441.86

CT12

Bibliography
Chapter One

(1) Raner, G., Ward, B. and Dabrowiak, J.; Journal of Coordination Chemistry,1988, Vol. 19, p. 17.

(2) Van Den Bergh, H.; Chemische Berichte 1986, Vol. 22, p. 430.

(3) Robinson, G., Alavi, A., Vaum, R. and Staum, M.; Journal of Nuclear Medicine 1986, Vol. 26, p. 239.

(4) Fiel, R., Howard, J., Mark, E. and Datta-Gupta, N.; Nucleic Acids Research, 1979, Vol. 6, p. 3093.

(5) Pasternack, R., Gibbs, E. and Villafranca, J.; Biochemistry, 1983, Vol. 22, p.2406.

(6) Ward, B., Skorobogaty, A. and Dabrowiak, J.; Biochemistry 1986, Vol. 25, p. 6875.

(7) Ward, B., Skorobogaty, A. and Dabrowiak, J.; Biochemistry 1986, Vol. 25, p. 7827.

(8) Lavallee, D.; Inorganic Chemistry 1976, Vol. 15, p. 691.

(9) Lavallee, D. and Kuila, D.; Inorganic Chemistry 1984, Vol. 23, p. 3987.

(10) Kuila, D. and Lavallee D.; Inorganic Chemistry 1983, Vol. 22, p. 1095.

(11) Xu, Z.; Dissertation, City University of New York (1989), pp. 135-137.

(12) Kelly, J., Murphy, M., McConnell D. and OhUigin, C.; Nucleic Acids Research 1985, Vol. 13, no. 1, p. 167.

(13) Sari, M., Battioni, J., Mansuy, D. and Lepecq, J.; Biochemical and Biophysical Research Communications 1986, Vol. 141, p. 643.

(14) Bromley, S., Ward, B. and Dabrowiak, J.; Nucleic Acids Research 1986, Vol. 14, p. 9133.

(15) Scheidt, W.; Journal of the American Chemical Society 1974, Vol. 96, p. 84.

(16) Lavery, R. and Pullman B.; Journal of Biomolecular

Structure and Dynamics 1985, Vol. 2, p. 1021.

(17) Robic, N., Bied-Charreton, C., Perré-Fauvet, M., Verchère-Béaur, C., Salmon, L., Gaudemer, A. and Pasternack, R.; Tetrahedron Letters 1990, Vol. 31, p. 4739.

(18) Acheson, R.M., Acridines, 2nd Edition, Vol. 9, Interscience Publishers (A division of John Wiley and sons), New York, 1973.

(19) Wirth, M., Buchardt, O., Koch, T., Nielsen, P. and Norden, B.; Journal of the American Chemical Society 1988, Vol. 110, p. 932.

(20) Norden, B. and Tjerneld, F.; Biopolymers 1982, Vo. 21, p. 1713.

(21) Journal of the American Chemical Society 1985, Vol. 107, p. 2067.

Bibliography
Chapter Two

(1) Robic, N., Bied-Charreton, C., Perrée-Fauvet, M., Verchère-Beaur, C., Salmon, L., Gaudemer, A. and Pasternack, R.; Tetrahedron Letters 1991, Vol. 31, p. 4739.

(2) Petrova, R., Berezin, B., Potapova, T., Toropova, E.; Izvestiya Vysshikh Vchebnykh Zavedenii Khimiya i khimicheskaya Tekhnologiya 1986, Vol. 9, p. 55.

(3) Dugas, H. and Penney, C.; Bioorganic Chemistry, Springer-Verlag Publishing Co., New York, 1981, p. 71-73.

(4) Adler, A., Longo, F., Finarelli, J., Goldmacher, J., Assour, J. and Korsakoff, L.; Journal of Organic Chemistry 1967, Vol. 32, p. 476.

(5) Gaudry, R.; The Canadian Journal of Chemistry 1985, Vol. 31, p. 1060.

(6) Pouchert, C.; The Aldrich Library of NMR Spectra, Edition II, Aldrich Chemical Company (publishers), Vol. 2, nos. 379A-381C.

(7) Smith, K.; Porphyrins and Metalloporphyrins, 1st Edition, Elsevier Scientific Publishing Co., New York, 1976, p. 837.

(8) Xu, Z.; Dissertation, City University of New York, 1989, p. 71.

(9) Vogel, A.; A Textbook of Practical Organic Chemistry Including Qualitative Organic Analysis, 4th Edition, Lowe and Brydone Publishing Company, London, 1978, p. 1126.

(10) Dupré, D. and Robinson, F.; Journal of the American Chemical Society 1945, Vol. 1945, p. 549.

(11) Smith, K.; Porphyrins and Metalloporphyrins, 1st Edition, Elsevier Publishing Co., New York, 1976, pp. 399-524.

(12) Badger, G., Jones, R. and Laslett, R.; The Australian Journal of Chemistry 1964, Vol. 17, p. 1028.

(13) Little, R.; Journal of Heterocyclic Chemistry 1978, Vol. 15, p. 203.

(14) Pouchert, C.; The Aldrich library of NMR Spectra, Edition II, Vol. 1, nos. 59A, 59C and 59D.

(15) Dyer, J.; Applications of Absorption Spectroscopy of Organic Compounds, Prentice-Hall, Inc.; Englewood Cliffs, N.J.; 1981, p. 95.

(16) ibid; pp. 95-96.

(17) ibid; p 95.

Bibliography
Chapter Three

(1) Fiel, R., Carvlin, M., Byrnes, R. and Mark, E. The Molecular Basis of Cancer, Proc. Conf., 1984, Part B. 1985, p. 215.

(2) Fiel, R., Howard, J., Mark, E. and Datta Gupta, N.; Nucleic Acids Research 1979, Vol. 6, p. 3093.

(3) Carvlin, M., Mark, E., Fiel, R. and Howard, J.; Nucleic Acids Research 1983, Vol. 11, p. 6141.

(4) Carvlin, M.; Dissertation, State University of New York at Buffalo 1984, University Microfilms International, Ann Arbor, Michigan; p. 1.

(5) Carvlin, M. and Fiel, R.; Nucleic Acids Research 1983, Vol. 11, p. 6121.

(6) Carvlin, M., Datta-Gupta, N. and Fiel, R.; Biochemistry Research Communications 1982, Vol. 108, p. 66.

(7) Pasternack, R., Gibbs, E. and Villafranca, J.; Biochemistry 1983, Vol. 22, p. 2406.

(8) Gibbs, E., Muriel, C., Zhang, J., Reiff, W., Hill, D., Malicka-Blaszkiewicz, M., McKinnie, R., Lui, H-Q. and Pasternack, R.; Journal of Inorganic Biochemistry 1988, Vol. 32, p. 1988.

(9) Pasternack, R., Gibbs, E. and Villafranca, J.; Biochemistry 1983, Vol. 22, p. 5406.

(10) Pasternack, R., Garrity, P., Erhlich, B., Davis, C., Gibbs, E., Orloff, G., Giartoso, A. and Turano, C.; Nucleic Acids Research 1986, Vol. 14, p. 5919.

(11) Olmstead, J., Kearns, D.; Biochemistry 1977, Vol. 16, p. 3647.

(12) Schreiber, J. and Daune, M.; Journal of Molecular Biology 1984, Vol. 83, p. 487.

(13) Lober, G.; Journal of Luminescence 1981, Vol. 22, p. 221.

(14) Lober, G. and Kittler, L.; Biophysical Studies (Berlin) 1973, Vol. 73, p. 25.

(15) Kell, J., Murphy, M., McConnell, D. and OhUigin, C.; Nucleic Acids Research 1985, Vol. 13, p. 167.

(16) Skoog, D. and West, D.; Principles of Elemental Analysis, 2nd Edition, Springer-Verlag, 1980, pp. 279-289.

(17) Schmechel, D. and Crothers, D.; Biopolymers 1971, Vol. 10, p. 465.

(18) Muller, W. and Crothers, D.; Journal of Molecular Biology 1968, Vol. 35, p. 251.

(19) Wells, R., Larson, R., Grant, R., Shortle, B. and Cantor, C.; Journal of Molecular Biology 1970, Vol. 54, p. 465.

Bibliography
Chapter Four

(1) Pasternack, R., Gibbs, E. and Villafranca, J.; Biochemistry 1983, Vol. 22, p. 2406.

(2) Strickland, J., Marzilli, L. and Wilson, W.; Biopolymers (in press).

(3) Fiel, R., Howard, J., Mark, E. and Datta Gupta, N.; Nucleic Acids Research 1979, Vol. 6, p.3093.

(4) Gibbs, E.J., Maurer, M., Zhang, J., Reiff, W., Hill, D., Malicka-Blaszkiewicz, McKinnie, R., Liu, H. and Pasternack, R.; Journal of Inorganic Biochemistry 1988, Vol. 32, p. 39.

(5) Gibbs, E., Tinoco, I, Maestre, M., Ellinas, P. and Pasternack, R.; Biochemical and Biophysical Research Communications 1988, Vol. 157, p. 350.

(6) Strickland, J., Banville, D., Wilson, W and Marzilli, L.; Biochemistry 1987, Vol. 27, p. 8870.

(7) Strickland, J., Marzilli, L., Gay, K. and Wilson, W., Biochemistry 1988, Vol. 27, p. 8870.

(8) Lepecq, J. and Paoletti, C.; Journal of Molecular Biology 1967, Vol. 27, p. 87.

(9) Scatchard, G.; Annals of the New York Academy of Sciences 1949, Vol. 51, p. 660.

(10) Constant, J., Laugaa, P., Roques, B. and Lhome, J.; Biochemistry 1988, Vol. 27, p. 3997.

(11) Xu, Z.; Disertation, City University of New York, 1989, p. 135.

(12) Sari, M., Battioni, J., Mansuy, D. and Lepecq, J.; Biochemical and Biophysical Research Communications 1986, Vol. 141, p. 643.

(13) Sari, M., Battioni, J., Dupre, J., Mansuy, D. and Lepecq, J.; Biochemistry 1990, Vol. 29, p. 4205.

(14) Fiel, R., Howard, J., Mark, E. and Datta-Gupta, N.; Nucleic Acids Research 1979, Vol. 6, p. 3093.

(15) Dougherty, G. and Pilbrow, J.; International Journal of Biochemistry 1985, Vol. 24, p. 1179.

(16) Wirth, M., Buchardt, O., Koch, T., Nielsen, P. and Norden, B.; Journal of the American Chemical Society 1988, Vol. 110, p. 932.

(17) Baguley, B.; Anticancer Drug Design 1991, Vol. 1, p. 1.

(18) Lown, J., Sondhi, S. and Ong, C., Skorobogaty, A., Kishikawa, H. and Dabrowiak, J.; Biochemistry 1986, Vol. 25, p. 5111.

(19) Denny, W., Roos, I. and Wakelin, L.; Anticancer Drug Design 1986, Vol. 1, p. 141.